NORTHWESTERN UNIVERSITY

Characterization of Rare Genetic Variation in Polycystic Ovary Syndrome.

A DISSERTATION

SUBMITTED TO THE GRADUATE SCHOOL

IN PARTIAL FULFILLMENT OF THE REQUIREMENTS

for the degree

DOCTOR OF PHILOSOPHY

Field of Driskill Graduate Program in Life Sciences (DGP)

By

Lidija Kristina Gorsic

EVANSTON, ILLINOIS

June 2018

ABSTRACT

Characterization of Rare Genetic Variation in Polycystic Ovary Syndrome.

Lidija Kristina Gorsic

Polycystic ovary syndrome (PCOS) is a common endocrine disorder affecting approximately 1 in 10 reproductive-age women and remains the leading cause of female factor infertility among women of childbearing age. PCOS presents with features of hyperandrogenism, irregular menses and polycystic ovaries. Twin and family studies have demonstrated high heritability estimates for PCOS. Consequently, a number of common genetic PCOS susceptibility loci have been reproducibly mapped using family-based association tests or GWAS. However, taken together, these loci only account for a small fraction of PCOS heritability, analogous to findings in other complex traits/diseases. One hypothesis for the observed deficit in heritability is that uncommon or rare genetic variants with greater phenotypic effects contribute to disease pathogenesis. We tested this hypothesis using an unbiased whole genome sequencing (WGS) approach followed by targeted resequencing of a gene panel including 11 PCOS candidates in a case/control cohort. Subsequent *in silico* analyses yielded PCOS-associated rare genetic variants, both in coding and noncoding regions of the genome.

Two of the 11 panel genes included anti-Müllerian hormone (*AMH*) and its specific type II receptor (*AMHR2*). Women affected with PCOS often have elevated levels of AMH. In the ovary AMH inhibits follicle maturation, thus the elevated AMH levels seen in women with PCOS are consistent with the observed arrested folliculogenesis. Paradoxically, AMH also

inhibits androgen production through transcriptional repression of *CYP17*, a rate-limiting enzyme in steroidogenesis. This suggests a loss of AMH function in PCOS, a phenotype of androgen excess. Identified coding and select noncoding variants of *AMH* and *AMHR2* were studied to determine their functional impact on signaling ability. Using dual luciferase reporter assays and quantitative real-time PCR, we identified a total of 37 PCOS-specific variants in *AMH* and *AMHR2* that displayed a significant reduction in activity. Collectively, 45 PCOS cases harbored functionally validated pathogenic variants, equating to 6.4% (45/700) of our case cohort. None of the variants observed in control women had impaired signaling activity. Our findings are the first to identify and functionally validate rare genetic variants associated with a common PCOS phenotype and suggest a previously unrecognized mechanism for the role of AMH in PCOS: decreased AMH bioactivity.

Given that PCOS is a complex disorder with a heterogeneous presentation, several genes and pathways likely lead to various PCOS phenotypes. Analyses of targeted resequencing data also identified predicted deleterious missense variants, specific to PCOS cases, mapping to the *LMNA* and *INSR* genes that encode the lamin A/C and insulin receptor, respectively. Mutations in these genes cause disorders associated with extreme phenotypes of PCOS. Our results indicate that rare variants in *LMNA* and *INSR* also account for a subgroup of PCOS-affected women.

ACKNOWLEDGEMENTS

I would like to extend my deepest gratitude to my advisor, Dr. Margrit Urbanek, for the opportunity to complete my thesis in her laboratory. Throughout this adventure Margrit has been a true role model for me, both in science and in life. Over these years at Northwestern, I have been riding the science research roller coaster experiencing the excitement in the climb, the drops that make you sick and now the end where you can't help but love the ride, and if I had to do it again I could not imagine a more supportive, intelligent and kind mentor by my side! Most importantly, Margrit allowed me to grow as a scientist while prioritizing my family. She taught me so much in maintaining a work-life balance in order to produce my best quality work. I will greatly miss our conversations of genetics, PCOS and our children who seem to grow up too quickly. I would also like to thank current/previous members of Margrit's lab and collaborators: Dr. Antonia Navarro, Elona Liko-Hazizi, Elizabeth Nachtwey, Jan Stevens, Alexandra Fontaine, Ryan Sisk and Matthew Dapas. This journey would have been much more stressful and lonesome without them. Thank you to my committee members and mentors: Dr. Julie Kim, Dr. Geoffrey Hayes and Dr. Jose Teixeira, who were always available to offer their expertise and guidance. Furthermore, I would like to thank the NRSA-supported Northwestern University Program in Diabetes, Endocrinology and Hormone Action (NUPEDHA) for their training support (T32 DK007169).

I would also like to share my overwhelming appreciation for my parents, who have cared for my children and given their support throughout this entire experience. This achievement would have been impossible for me without their efforts and love! I am also grateful to my father, Dr. Joseph Gorsic, for teaching me to value the mysteries and beauty of our world and

inspired my scientific curiosity from a very young age! I would also like to thank my husband, John, who was there to provide a boost of confidence when I needed it most and never stopped believing in me. Big thanks to my genetic progeny, Troy and Lana, who continuously motivate me and keep me smiling and laughing everyday. They bring pure joy to all aspects of my life! I want to thank my family and friends, especially Fr. Gregor Gorsic and Shannon Breen, who have always been strong supporting sources of encouragement and helpful advice. Thank you to all my previous mentors at Elmhurst College and University of Chicago, Dr. Tamara Marsh, Dr. Stacey Raimondi, Dr. Eileen Dolan, Dr. Amy Stark and Shannon Delaney, for playing an enormous role in helping me become the scientist that I am today. It's been quite the adventure and I am so blessed to have these people and others play a significant part in this accomplishment; I am truly grateful to all!

LIST OF ABBREVIATIONS

17-OHPE	17-hydroxypregnenolone
AMH	anti-Müllerian hormone
AMHR2	anti-Müllerian hormone receptor type 2
ASRM	American Society for Reproductive Medicine
BH	Benjamini-Hochberg
BMI	body mass index
BMP	bone morphogenetic protein
bp	base pairs
BRE	BMP response element
CADD	Combined Annotation Dependent Depletion
cAMP	cyclic adenosine monophosphate
CCDC6	coiled-coil domain containing 6
CD/CV	common-disease common-variants
CD/RV	common-disease rare-variants
CGI	Complete Genomics
CHO-K1	ovarian Chinese hamster (*Cricetulus griseus*) epithelial-like cell line
chr	chromosome
CIDR	Center for Inherited Disease Research
c-MAF	MAF bZIP transcription factor
COS7	African green monkey kidney fibroblast-like cell line
CYP17A1	cytochrome P450 family 17 subfamily A member 1

DHEA	dehydroepiandrosterone
DHEAS	dehydroepiandrosterone sulfate
DLR	dual luciferase reporter
DNA	deoxyribonucleic acid
dNTPs	deoxyribonucleotide triphosphates
EBF1	early B cell factor 1
ELISA	enzyme-linked immunosorbent assay
ESHRE	European Society of Human Reproduction and Embryology
FATHMM-MKL	Functional Analysis through Hidden Markov Models - Multiple Kernel Learning
FBN3	fibrillin 3
FPL	familial partial lipodystrophy
FSH	follicle-stimulating hormone
GnRH	gonadotropin-releasing hormone
GWAS	genome-wide association study
indels	insertion-deletions
INSR	insulin receptor
IR	insulin resistance
IVF	in vitro fertilization
IVM	in vitro maturation
kb	kilobases
KLD	Kinase, Ligase & DpnI
LH	luteinizing hormone

LMNA	lamin A/C
MAF	minor allele frequency
MIS	Müllerian inhibiting substance
MISRII	Müllerian inhibiting substance receptor type II
MYC	MYC proto-oncogene, bHLH transcription factor
NGS	next generation sequencing
NICHD	National Institute of Child Health and Human Development
NIH	National Institutes of Health
PCOM	polycystic ovarian morphology
PCOS	polycystic ovary syndrome
PCR	polymerase chain reaction
PMDS	persistent Müllerian duct syndrome
PWM	position weight matrices
qRT-PCR	quantitative real-time polymerase chain reaction
REF	reference
RPKM	reads per kilobase million
SHBG	sex hormone-binding globulin
SNP	single nucleotide polymorphism
SNV	single nucleotide variant
SP1	Sp1 transcription factor
T	testosterone
T2D	type 2 diabetes
TF	transcription factor

TGFβ	transforming growth factor beta
uT	bioavailable (unbound) testosterone
WES	whole exome sequencing
WGS	whole genome sequencing
WT	wild-type

TABLE OF CONTENTS

LIST OF TABLES

LIST OF FIGURES

CHAPTER 1

INTRODUCTION AND BACKGROUND

1.1 POLYCYSTIC OVARY SYNDROME (PCOS)

Polycystic ovary syndrome (PCOS) is a complex endocrine disorder affecting approximately 1 in 10 women of reproductive age (1-8). It is associated with substantially increased risk for infertility, prediabetes and type 2 diabetes (T2D) (2). PCOS is a highly heritable disorder with disease correlation of 71% in monozygotic twins, almost twice as large as that in dizygotic twins (38%) (9), suggesting a genetic susceptibility to the disorder. Furthermore, male as well as female first-degree relatives have metabolic and reproductive features of the syndrome, including increased T2D risk, consistent with a genetic contribution to these phenotypes (2).

PCOS has a prevalence of 5-18% in reproductive-age women depending on ethnic population and clinical criteria used to determine diagnosis (3-8). PCOS can be diagnosed using criteria defined by three groups. The Rotterdam (ESHRE/ASRM) consensus defines PCOS with having at minimum 2 of the 3 following symptoms: oligo-ovulation/anovulation, hyperandrogenism and polycystic ovaries through ultrasound confirmation (10). However, other groups have disagreed with the diagnosis of PCOS in the absence of hyperandrogenemia (11). Thus, the NIH/NICHD and Androgen Excess and PCOS Society require the presence of elevated androgen levels (12, 13).

In addition to reproductive symptoms, this complex disorder also involves metabolic and dermatological symptoms. Metabolic characteristics of PCOS may include insulin resistance (IR), hyperinsulinemia, dyslipidemia and obesity (14). Cutaneous manifestations of insulin resistance or hyperandrogenemia such as acanthosis nigricans, acne, alopecia and hirsutism (14, 15), as well as psychiatric effects of anxiety and depression (16) are also associated. Furthermore, PCOS is diagnosed through an elimination process of other potential conditions that have similar phenotypic indicators, such as androgen secreting tumors (17). Some have also

questioned whether subclinical hypothyroidism should also be an exclusion criterion for PCOS diagnosis (18). This variability in diagnostic qualifications for PCOS and the significant heterogeneity in patient symptoms create challenging obstacles in understanding the underlying biological processes involved in its pathogenesis. As a result, much of the etiology of PCOS still remains unknown.

1.2 SIGNIFICANCE

Chronic ovulation irregularities as well as IR put affected individuals at a greater risk for additional health complications. IR was found to be a frequently observed PCOS characteristic with 75% incidence in PCOS women with lean body mass index (BMI) and in 95% of overweight PCOS women (19). Yet, in general, women with PCOS have significant IR independent of obesity (20). Studies have further shown that Caucasian and South Asian women with PCOS and IR have a heightened risk for developing type 2 diabetes (T2D), particularly at younger stages in life (21-24). The prevalence of obesity in women with PCOS is estimated to be approximately 61% (25, 26). Even though BMI has been suggested to positively correlate with PCOS phenotype severity, risks of metabolic and cardiovascular diseases remain substantially increased independent of BMI (23, 27). For instance, a meta-analysis for PCOS-associated coronary heart disease established a 2-fold increased risk among patients with PCOS regardless of BMI status (27). Despite serious risk factors related to PCOS, preventative screening measures for women affected with this disorder continue to be neglected in today's clinical practices (28).

In addition, researchers have also uncovered an association between PCOS and endometrial cancer occurrence (29, 30). Due to ovulatory dysfunction, increased estrogen levels,

and lack of shedding endometrial cells through menstruation, it has been suggested that women with PCOS may have an increased risk for developing uterine diseases (31). Gottschau *et al*. confirmed this phenomenon in a Danish population, finding a 4-fold increase in endometrial cancer risk among PCOS patients (30). Collectively, not only does PCOS have immediate premenopausal health complications such as infertility and IR, it also substantially increases risk for severe metabolic, cardiovascular and tumorigenic problems throughout a woman's lifespan. Thus, PCOS has a significant impact on health and quality of life.

Given that the cause of PCOS has yet to be identified, treatment options are restricted to alleviating symptoms. Initial treatment recommendations typically focus on lifestyle changes with an increase in exercise and restrictive diet (32). In some circumstances, lowering BMI through lifestyle changes or bariatric surgery may improve IR and resume regular ovulation thus improving fertility (33-35); however, this approach is not always effective (15). Therefore, treatment for PCOS must be individualized depending on existing symptoms as well as specific interests of each patient, mainly whether or not their goal includes immediate and/or future pregnancy. Hormonal treatments during in vitro maturation (IVM) (36, 37) and in vitro fertilization (IVF) (38, 39) have shown successful pregnancy and live birth outcomes in women with PCOS. In circumstances where pregnancy is not the desired outcome, combined oral contraceptives (40) and/or insulin-sensitizing agents, such as metformin (41, 42), may be prescribed to regulate ovulation and IR. A meta-analysis evaluating toxic effects of routine PCOS intervention therapeutics found low associated risks with severe adverse events (43), however this study only included patients undergoing treatment for a span of one year. It is possible that cardiovascular, hepatic, or multisystem toxicities would accumulate past this window of observation. Ultimately, a greater understanding of the mechanistic underpinnings of

PCOS is paramount to developing distinguished diagnostic criteria, targeted treatment options and preventative measures for women of all ages.

1.3 GENOME WIDE ASSOCIATION STUDIES (GWAS) IDENTIFY LOCI FOR PCOS SUSCEPTIBILITY

In light of the strong heritability observed in PCOS twin studies and families, researchers have utilized candidate gene analyses and genome wide association studies (GWAS) to discover susceptibility loci in multiple ethnicities (44-50). These association studies have revealed several loci within genes significantly related to PCOS; namely mapping to, *C9orf3, DENND1A, ERBB4, FBN3, FSHB, FSHR, GATA4/NEIL2, HMGA2, INSR, KRR1, LHCGR, RAD50, RAB5B/SUOX, SUMO1P1, THADA, TOX3* and *YAP1* (44-51). Yet, some results have been contradictory and replication sets have not been able to validate certain loci (52).

Collectively, GWAS in Han Chinese and European PCOS cohorts have implicated gonadotropin secretion and action, ovarian androgen biosynthesis, insulin resistance, body weight and sex hormone binding globulin in the development of PCOS (53-55). However, as with other complex diseases (56), the susceptibility loci identified have modest effect sizes and thus account for only a small fraction of the estimated heritability of PCOS (44, 45, 54, 55, 57).

1.4 WHAT ACCOUNTS FOR MISSING HERITABILITY?

One hypothesis for this deficit in heritability is that low frequency or rare genetic variants with larger biologic effects play a more important role in complex disease pathogenesis than do variants that can be detected by GWAS (56). Over the years, the general consensus and approach for studying complex traits has largely been based on the common-disease common-

variants (CD/CV) hypothesis (58-62), which suggests that common complex diseases are due to common variants (minor allele frequencies (MAF)≥0.05). GWAS are designed to detect common genetic variation (MAF≥0.05) (56). These variants are expected to have modest phenotypic impact since they have not been subjected to strong selective pressure (63). However, in recent years and with the development of more advanced sequencing methods, researchers have begun to investigate whether common diseases are due to low frequency (MAF<0.05) or rare variants (MAF<0.01): the common-disease rare-variants (CD/RV) hypothesis (59-62). In contrast to common variants, rare variants often show extreme allelic heterogeneity (62) and result in greater biologic effects.

1.5 NEXT GENERATION SEQUENCING (NGS)

Next generation sequencing (NGS) technologies have allowed researchers to explore the CD/RV hypothesis, by providing a reliable and high-throughput method for the discovery of low frequency and rare genetic variation. With a greater number of research studies utilizing NGS strategies to study common complex disorders, our understanding of their allelic architecture will only continue to improve throughout the coming years (62).

Modes of sequencing DNA have come a long way since the Sanger chain termination method was developed in 1977 (64). Even though the Sanger method is still highly useful and reliable for sequencing validation purposes (65), it is not ideal for high-throughput studies of the genome. Short read, massively parallel sequencing of the "next generation" revolutionized sequencing capabilities.

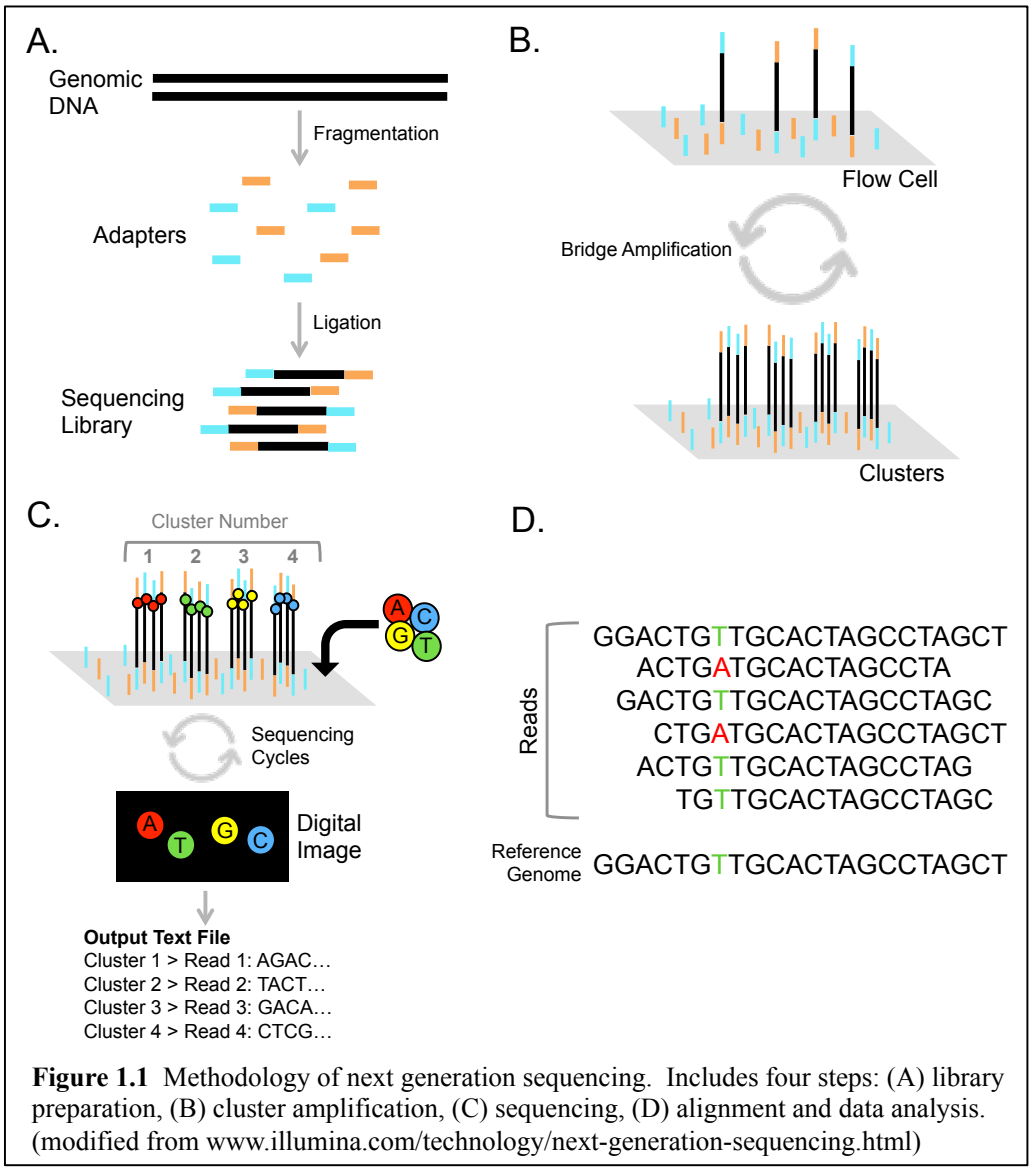

Figure 1.1 Methodology of next generation sequencing. Includes four steps: (A) library preparation, (B) cluster amplification, (C) sequencing, (D) alignment and data analysis. (modified from www.illumina.com/technology/next-generation-sequencing.html)

Generally, the process of sequencing on the Illumina HiSeq platform uses a DNA polymerase to catalyze the incorporation of fluorescently labeled deoxyribonucleotide triphosphates (dNTPs) into a DNA template strand through repeated cycles of DNA synthesis (65). The technology can be divided into four basic steps: library preparation, cluster generation, sequencing and data analysis (**Figure 1.1**). During library preparation DNA undergoes random fragmentation followed by adapter ligation on both the 5' and 3' ends (**Figure 1.1A**). PCR amplification is used to amplify adapter-ligated fragments, which are gel purified. The library is

then loaded into a flow cell, where adapters hybridize to complementary surface-bound oligos and bridge amplification creates separate clonal clusters (**Figure 1.1B**). Illumina sequencing by synthesis chemistry uses four reversible terminator-bound dNTPs that are incorporated, imaged and repeated during DNA synthesis of each cluster (**Figure 1.1C**). Data alignment, annotation and analysis can then identify genetic variations present in the DNA sequence including single nucleotide variants (SNVs) as well as insertion-deletions (indels) (**Figure 1.1D**). Furthermore, advancement in NGS technology has included the development of paired-end sequencing, where both ends of DNA fragments can be sequenced resulting in read pairs of forward and reverse reads. Paired-end sequencing allows for an increase in the number of reads, greater accuracy in read alignment and the capability of indel detection (www.illumina.com/technology/next-generation-sequencing.html).

Various sequencing approaches include whole genome sequencing (WGS), whole exome sequencing (WES) and custom targeted sequencing of selected gene regions (65, 66). WGS provides sequence information of coding and noncoding regions of the genome, while WES is focused on the ~1-2% of the genome that codes for proteins. Targeted sequencing can be performed on specific genes of interest and is a cost-effective option for candidate gene studies in larger cohorts and produces higher rates of coverage. For instance, WGS studies typically attain 30-50x coverage per genome; however, a targeted resequencing project can achieve target region coverage at 500-1000x or more (www.illumina.com).

NGS technologies have also given rise to a powerful medical tool for the discovery of causal variants underlying genetically inherited diseases, allowing for targeted therapies in the clinical setting (67, 68). WGS and WES have substantially decreased in cost over recent years and are potentially a faster and more cost-effective option compared to traditional diagnostic

modalities (67). Today, the Illumina HiSeqX system has the ability to perform high-quality sequencing of over 45 human genomes in a single day at approximately 1000 US dollars per genome (www.illumina.com). Even though applications of WGS and WES have not yet been widely adopted in the medical practice, their use in enabling diagnoses and influencing therapy has been demonstrated in several instances (69-73) and will only continue to grow across numerous clinical specialties.

1.6 RARE VARIATION IN COMPLEX TRAITS

In translational research, rare variants that cause larger biologic effects than common susceptibility variants have been found in other common, complex diseases. Particularly, targeted candidate gene resequencing has been successful in a number of examples, such as variants linking to obesity (74), T2D (75), Crohn's disease (76) and longevity (77). In T2D, rare, likely-to-be-deleterious variants were found in *MTNR1B*, which encodes melatonin receptor 1B (MT_2) (75). Only the rare *MTNR1B* variants that resulted in total or partial loss of MT_2 function increased T2D risk (75). Rare coding variants have also been found in *GCKR*, another T2D GWAS susceptibility gene encoding glucokinase regulatory protein, in subjects with higher circulating triglyceride levels (78). Collectively, these findings support the hypothesis that rare, functional coding variants can produce common, complex disease/trait phenotypes (56).

For complex traits like PCOS, disease burden attributable to a single gene is expected to be modest. A large-scale analysis of rare *PPARG* variants with reduced function in an adipocyte differentiation assay that substantially increased T2D risk, identified one such variant per 1000 individuals screened (0.1% carrier rate) (79).

1.7 FOLLICULOGENESIS AND STEROIDOGENESIS ALTERATIONS IN PCOS

Despite the remaining questions in the etiology of PCOS, a great deal of progress has been made throughout the years to better define the molecular changes in patients. In PCOS affected women, hypothalamic gonadotropin-releasing hormone (GnRH) pulses at a higher frequency (80). It has been theorized that increased GnRH pulses may be due to decreased progesterone and estradiol levels in women with PCOS (80). Normal triggering of anterior pituitary hormones, follicle-stimulating hormone (FSH) and luteinizing hormone (LH), are also disrupted resulting in LH hypersecretion. Increased LH levels as well as insulin stimulate androgen production in follicular theca cells (81). Elevated androgen levels propagate this cycle, preventing continued follicular development and dominant follicle selection, resulting in irregular menses or anovulation (81, 82). Current known consequences of increased androgen levels in PCOS etiology across the hypothalamic-pituitary-ovarian axis and certain related tissues are summarized in **Figure 1.2**.

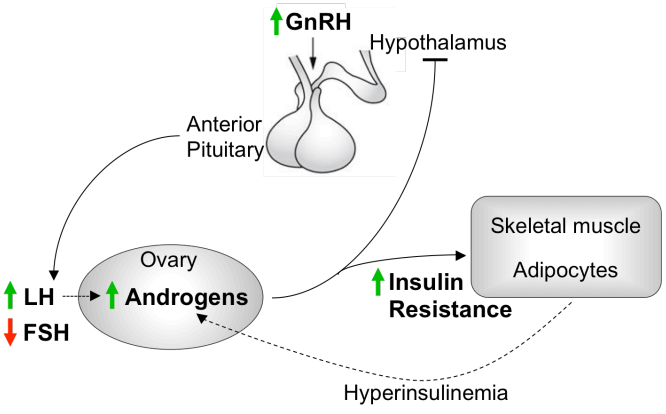

Figure 1.2 Hyperandrogenemia in PCOS pathogenesis. Increased hypothalamic GnRH pluses cause LH hypersecretion. LH stimulates testosterone production in theca cells within the ovary. Androgens inhibit negative progesterone feedback on GnRH pulse generator and amplify insulin resistance in fat and muscle cells. Hyperinsulinemia propagates androgen production within the ovary. (modified from Chang, *Nat Clin Pract Endocrinol Metab* 2007)

Disrupted processes of folliculogenesis found in PCOS women include a surplus of primordial follicles initially recruited for growth. Yet, their development is arrested when they reach early antral stages, causing the characteristic cystic morphology (81, 83) (**Figure 1.3**). Polycystic ovarian morphology (PCOM) is a key reproductive feature of PCOS (84, 85). PCOM is characterized by a distinctive 2- to 4-fold increase in early-stage follicles suggesting an alteration in gonadotropin-independent folliculogenesis (84). In females, anti-Müllerian hormone (AMH), or Müllerian inhibiting substance (MIS), is secreted by the granulosa cells of early primary stage to early antral stage follicles (84-87) and its expression is inversely correlated with follicle size (88).

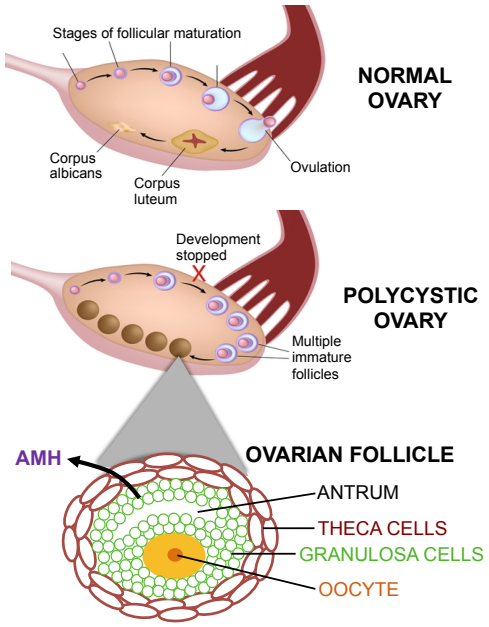

Figure 1.3 Developmentally arrested follicles in PCOS. In the normal ovary follicles undergo maturation toward ovulation; however, in the polycystic ovaries this development stops resulting in multiple immature follicles. Ovarian follicles consist of the oocyte, theca cells as well as granulosa cells, which produce AMH. (modified from © Alila Medical Media, Shutterstock)

1.8 ABNORMAL ANTI-MÜLLERIAN HORMONE (AMH) LEVELS IN PCOS

Levels of AMH are typically elevated in PCOS-affected women (85, 89-94), yet it remains unclear whether this is due to the follicle surplus observed in PCOS or a pathogenic effect. Serum AMH levels correlate with antral follicle counts in both reproductively normal women as well as in those with PCOS (85, 95). Accordingly, elevated AMH levels in women with PCOS have been considered to be a consequence of the increased number of early-stage follicles (85). Therefore, elevated AMH levels are proposed to be a marker for the distinctive alteration in folliculogenesis that is a cardinal feature of PCOM (85, 96, 97). Interestingly, elevated AMH levels have also been found in the sons, brothers and fathers of PCOS affected women (98), suggesting a possible defect in the AMH pathway in PCOS. While women with PCOS typically have distinctly high levels of AMH, a subgroup of women also experience normal or low levels (99).

1.9 ROLE OF AMH IN FOLLICULAR RECRUITMENT AND DEVELOPMENT

Once a follicle is recruited from the primordial pool it begins to increase layers of two main types of cells that surround the oocyte: granulosa and theca cells (**Figure 1.3**). Follicular maturation requires bi-directional communication between the theca and granulosa cells, and granulosa cells and oocyte (100). Ligands of the TGFβ superfamily, including AMH, are especially prominent in this dialogue (**Figure 1.4**). In the ovary, AMH has been shown to be a key regulator of follicular recruitment and folliculogenesis (101). AMH signaling involves both autocrine and paracrine actions within the follicle that regulate follicular development and production of steroid hormones (100).

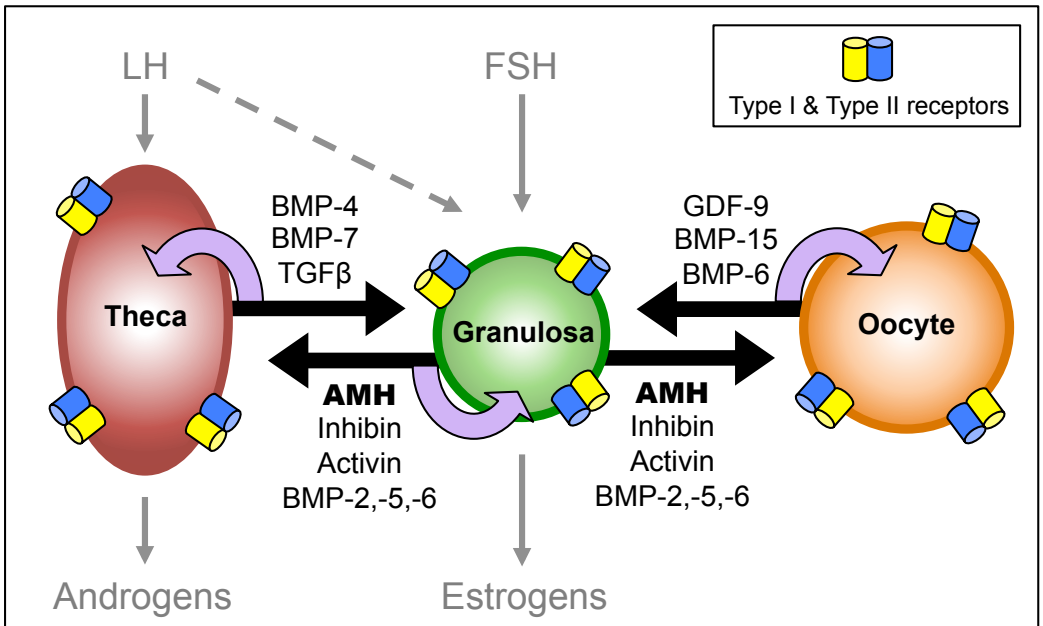

Figure 1.4 Action of TGFβ family members across follicular cell types. Follicular development involves bi-directional signal exchange between theca and granulosa cells, and granulosa cells and oocyte. Many signaling communication ligands belong to the TGFβ family. Both autocrine (purple arrows) and paracrine (black arrows) mechanisms are likely to occur, depending the the presence of type I and type II receptors at the cell membrane. (modified from Knight and Glister, *Repro* 2006)

In vitro and *in vivo* studies of the postnatal ovary have demonstrated two follicle selection points at which AMH plays a regulatory function during folliculogenesis (102). Firstly, AMH has been proposed to repress initial recruitment of follicles from the primordial pool (103, 104). Secondly, AMH has demonstrated an inhibitory role on early stage follicular growth by attenuating sensitivity to FSH (88). Studies in rodent as well as human granulosa and Sertoli cells have found AMH to inhibit FSH-induced adenylyl cyclase activation, aromatase expression, and estradiol production (88, 105, 106). Consequently, targeted disruption of AMH-induced primordial follicle recruitment and FSH-induced follicular growth in female mice resulted in premature ovarian failure (102), the opposite phenotype of PCOM (85). Further, the loss of one *AMH* allele in mice caused a significant enhancement of follicle recruitment followed by premature ovarian failure compared to control littermates suggesting a gene-dosage effect for

AMH in the rodent ovary (103). However, there have been conflicting reports on the role of AMH in primordial follicular recruitment (101, 107, 108). In contrast to findings in mice, knockdown of AMH bioactivity by active immunization with keyhole limpet hemocyanin conjugated AMH peptides in female sheep did not affect the rate of primordial follicle recruitment (108). These findings suggest that there are species differences in the ovarian actions of AMH.

1.10 AMH EFFECTS ON GONADAL STEROIDOGENESIS

AMH has also been shown to modulate gonadal steroidogenesis through its inhibition of *CYP17* in the normal testis (109, 110) (**Figure 1.5**). In transgenic male mice overexpressing AMH (111), as well as in isolated mouse Leydig cell cultures (109, 111), AMH inhibits testosterone production by downregulating transcription of *CYP17*, reducing both its 17α-hydroxylase and 17,20-lyase activities, which are rate-limiting for androgen biosynthesis. Amh has also been shown to inhibit androgen production and spermatogenesis in male adult zebrafish (112). In human boys, AMH levels decrease just prior to puberty and are inversely correlated with testosterone postnatally (111). The inhibitory role of AMH on steroidogenesis has also been observed in female models. For example, in female mice, intraperitoneal administration of recombinant AMH significantly lowers testosterone levels (113). Wild-type AMH is, thus, predicted to inhibit theca cell androgen production in the normal ovary analogous to its action in male Leydig cells (109) (**Figure 1.5**). However, the relationship between AMH and testosterone is complicated. While, on one hand, AMH has an inhibitory effect on testosterone production, testosterone has also been shown to inhibit AMH. For instance, testosterone treatment significantly decreased AMH mRNA and protein expression in bovine granulosa cells isolated

from early stage follicles (114). Likewise, testosterone-stimulated mouse preantral follicles exhibited down-regulated levels of Amh (115).

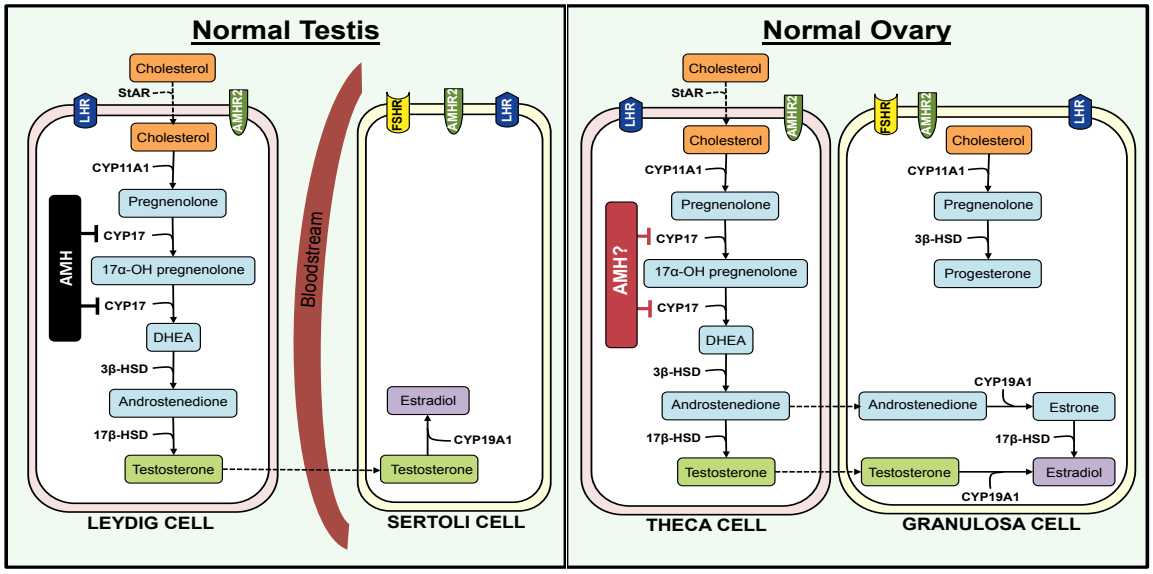

Figure 1.5 Gonadal steroid production and inhibitory role of AMH on CYP17. In the normal testis, AMH is produced by Sertoli cells and exerts an inhibitory effect on CYP17 transcription in Leydig cells. It is predicted that in the normal ovary, AMH would play the same role in female counterpart theca cells. (modified from Teixeira et al, *Endocrinology* 1999, and clinicalgate.com)

1.11 THE AMH AND TESTOSTERONE PARADOX IN PCOS

Given that AMH has an inhibitory role on testosterone production and visa versa, one would predict that conditions of high testosterone would result in decreased AMH levels. It is, therefore, paradoxical that women with hyperandrogenic PCOS also have high levels of AMH. This suggests possible defects in the AMH pathway and its inhibitory regulation on gonadal steroidogenesis in the development of hyperandrogenemia and PCOS.

1.12 AMH IN SEX DEVELOPMENT

The role of AMH was first described in prenatal male sex determination where AMH induces the regression of the Müllerian duct, which in females would develop into the fallopian tubes, uterus and upper vagina (116, 117) (**Figure 1.6**). In males, homozygous or compound heterozygous mutations in *AMH* and its receptor, *AMHR2*, account for roughly 85-88% of persistent Müllerian duct syndrome (PMDS) cases (118-120). PMDS is a rare autosomal recessive intersex disorder characterized by the presence of Müllerian duct structures in genotypic males with normally virilized external genitalia and occasional unilateral or bilateral cryptorchidism (118, 121). PMDS-affected males with *AMH* mutations have AMH levels that range from undetectable to normal (118); thus, indicating that AMH levels cannot be used as a surrogate for AMH activity. PMDS-associated *AMH* variants have showed impaired function due to defects in protein folding and/or stability (R194C (122), V12G(123)), impaired AMH secretion (H506Q (122)), and impaired AMH bioactivity (Q496H (122)). Unfortunately, phenotypic characteristics of female relatives of PMDS patients have not been reported. While AMH expression is specific to male Sertoli cells during prenatal development, female granulosa cells begin to express low levels of AMH during folliculogenesis after birth (124).

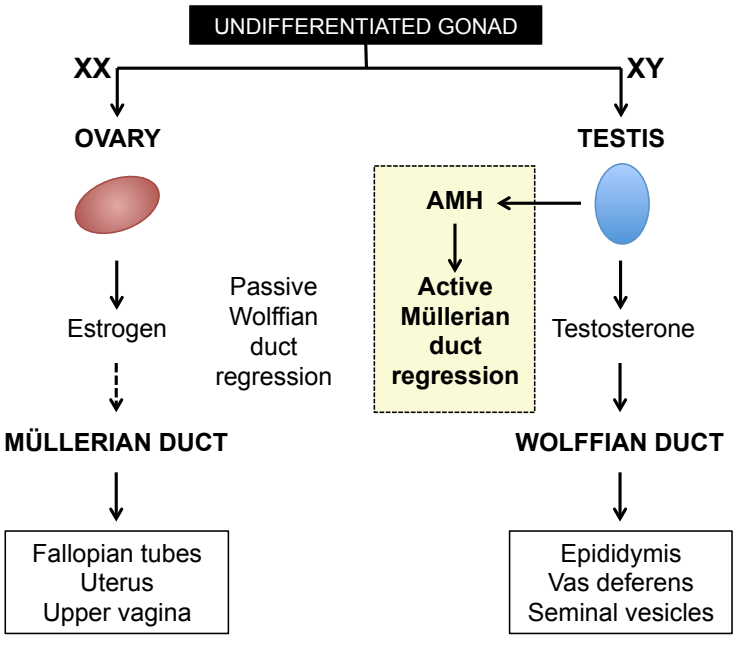

Figure 1.6 Role of AMH in male sex development. AMH induces the regression of the Mullerian duct, which in females would develop into the fallopian tubes, uterus and upper vagina. (Teixeira and Donahoe, *J Androl*. 1996, and modified from Hutson *et al*, *Nat Rev Endocrinol* 2014)

1.13 THE AMH GENE, PROTEIN AND SIGNALING PATHWAY

The AMH gene is encoded by 5 exons mapping to the p arm of chromosome 19 (**Figure 1.7**). The encoded AMH protein is a divergent member of the TGFβ superfamily, which includes the BMPs, activins, and inhibins (100). Similar to other protein members of this family, the furin protease post-translationally cleaves the AMH precursor into a 110-kDA N-terminal prodomain and 25-kDa C-terminal active mature domain, these remain in a noncovalent complex after cleavage (125). Through yet undefined mechanisms, the prodomain of AMH influences folding, secretion and biological activity of the active domain (126-130). However, given the sequence and structural variations of the prodomains of TGFβ family members, it is difficult to predict the function of the AMH prodomain on ligand activity as well as how genetic variants within this region impact function.

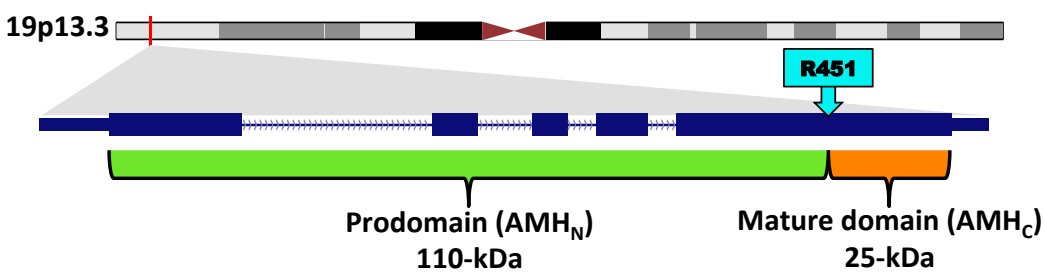

Figure 1.7 Gene map of *AMH*. Solid rectangles represent exons. Location of domains and cleavage site (teal) are shown. UCSC Genome Browser (https://genome.ucsc.edu/).

Family members of the TGFβ group trigger downstream signaling by binding type II serine-threonine receptors activating their latent kinase, which causes the recruitment and transactivation of type I receptors (131-133) (**Figure 1.8**). Thus far, 33 ligands have been defined within this family, while only 5 type II (TGFBR2, ACVR2B, ACVR2A, BMPR2 and AMHR2) and 7 type I (ALK1-7) receptors exist (131, 134, 135). Of the 33 ligands, AMH is

currently the only known member to bind its own specific type II receptor, AMHR2, while many other type II receptors can bind more than one ligand (134, 135).

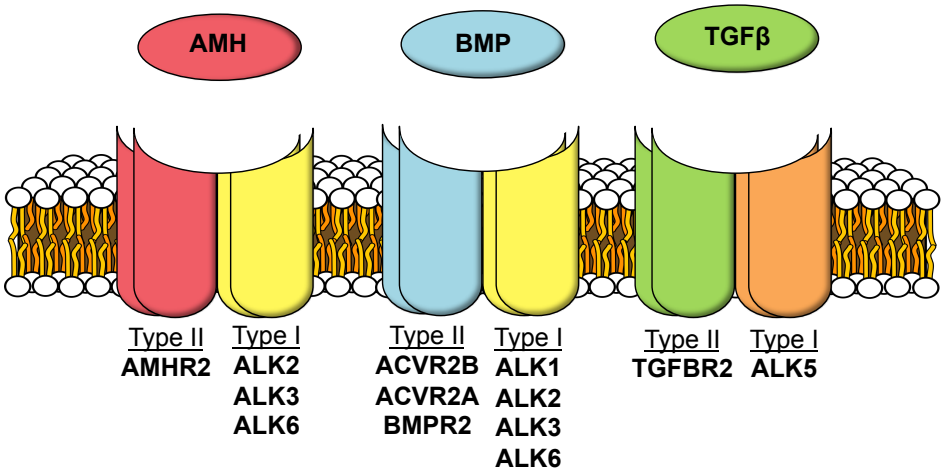

Figure 1.8 TGFβ family receptor ligand specificity. Members of the TGFβ family are subdivided based on which type I and type II receptor the ligand signals through. AMH signals through a unique type II receptor, AMHR2, and recruited type I receptors that are shared with BMP. (modified from Salazar *et al*, *Nat Rev Endocrinol* 2016)

Even though AMH is grouped within the TGFβ family, it only shares 20-25% sequence homology at the amino acid level. For instance, AMH lacks two surface-exposed tryptophan residues that are found in all other TGFβ ligands and are important for interactions with type I receptors (136). Furthermore, the type II receptor AMHR2 only shares 20% identity to the other type II receptors of the TGFβ family (134). This suggests that AMH has evolved unique interactions that are important for signaling and function compared with other members of its protein family. Signaling of AMH (**Figure 1.9**) is initiated by ligand binding to the AMH-specific type II receptor, AMHR2 (137-139). Once bound, the prodomain dissociates and type II receptors recruit and phosphorylate type I receptors (ALK2/3/6) (138, 140-142). Active type I receptors subsequently activate SMADs (1/5/8) triggering a signaling cascade that results in transcriptional regulation of target gene expression (143).

Importantly, AMH is secreted from cells as a disulfide-linked homodimer (125, 144). Moreover, the AMHR2 receptor also undergoes dimerization prior to ligand binding (137-139). Given that AMH and AMHR2 function as dimers, damaging variants resulting in a defective mutant product could have a dominant-negative effect on wild-type protein action. For example, wild-type AMH dimers would only account for 25% of total AMH in heterozygous individuals with AMH variants (144) (**Figure 1.10**).

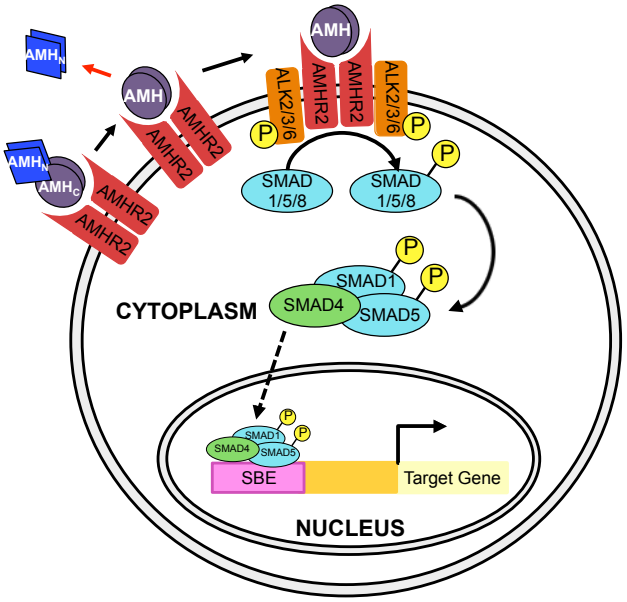

Figure 1.9 AMH signaling cascade via specific type 2 receptor, AMHR2. Signaling is initiated by binding AMH-specific dimer type II receptor (AMHR2). Once bound N dissociates and type II receptors recruit and activate type I receptors (ALK 2/3/6). Active type I receptors phosphorylate SMADs (1/5/8) facilitating complex formation between SMAD1, SMAD5 and SMAD4. Nuclear translocation of this complex stimulates target gene expression by binding to SMAD binding elements (SBE). (modified from Kristensen *et al*, *Mol Hum Reprod* 2014 and Rocha *et al*, *Biol Reprod* 2016)

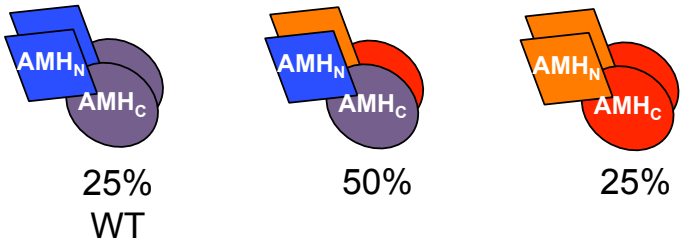

Figure 1.10 Potential dominant-negative interactions of variant AMH. In heterozygous individuals wild-type (WT) AMH dimer accounts for 25% of total AMH. (modified from Rocha *et al*, *Biol Reprod* 2016)

1.14 GENES OF THE AMH PATHWAY AND PCOS GENETICS

AMH is a plausible PCOS candidate gene given its role in folliculogenesis and steroidogenesis. *AMH*, itself, has not been identified as a PCOS susceptibility candidate in previous GWAS; however, a smaller scale case-control study found a polymorphism in *AMH* to be associated with androgen levels in Chinese PCOS women with insulin resistance (145). Furthermore, PCOS family based association testing has identified a susceptibility risk allele mapping to fibrillin-3 (*FBN3*, 19p13.2), a neighboring gene of *AMH* (146, 147). Additionally, while common variants in *AMHR2* were not associated with PCOS *per se* in PCOS subjects of Dutch ancestry, they were associated with AMH levels in women with PCOS (148, 149). In a Greek cohort, the common *AMHR2* variant, rs2002555, was associated with PCOS directly (150). Recently, a genetic association study from North India identified a significant association of -34 T>C polymorphism of *CYP17A1* with PCOS (151). Although these studies were limited to common variation they provide further evidence for a role of AMH signaling in PCOS.

1.15 ADDITIONAL PATHWAYS IMPLICATED IN PCOS

With more than 250 case-control studies of approximately 160 candidate genes (147), PCOS studies have revealed mechanisms of ovarian androgen biosynthesis, gonadotropin secretion and action, insulin resistance and body weight in PCOS pathogenesis (53-55). Therefore, the AMH pathway, and its role in ovarian androgen biosynthesis, falls under only one of the several mechanisms associated with the development of PCOS. Given that PCOS is a complex disorder with great heterogeneity among patients, it is likely that numerous genes and pathways contribute to PCOS phenotypes.

Several GWAS-identified loci (*LHCGR*, *FSHR*, *FSHB*, *DENND1A*, *THADA* and *INSR*) may predict additional pathways critical in PCOS etiology (147). PCOS-associated abnormalities in LH secretion magnify the *LHCGR* gene as a highly plausible candidate for PCOS (152, 153). Furthermore, observed defects in normal folliculogenesis also support the *FSHR* association with PCOS (154). LHCGR and FSHR are both responsible for modulating gonadotropin action, while FSHB regulates FSH secretion. DENND1A, similarly to AMH and FBN3, may regulate gonadal androgen production in theca cells, via augmentation of *CYP17A1* and *CYP11A1* expression (155). *THADA* and *INSR* are T2D susceptibility genes (156) and are candidates for the metabolic, insulin resistance phenotype of PCOS.

1.16 EXTREME PHENOTYPES OF PCOS

Rare variants identified in the insulin receptor (*INSR*) gene and in genes regulating adipogenesis, such as those encoding lamin A/C and peroxisome proliferating factor-γ, cause extreme phenotypes of PCOS: type A syndrome and familial partial lipodystrophies (FPL), respectively (157). Women with these disorders also present with elevated androgens, irregular menses and PCOM.

FPL is characterized by an abnormal distribution of subcutaneous adipose tissue and usually experienced in late childhood or early adulthood (158). Individuals affected with this disorder typically have loss of adipose tissue in lower and upper extremities; however, may accumulate excess fat around the face and neck (158). Lipoatrophy, however, is not the only concerning characteristic of FPL. Serious metabolic abnormalities also commonly associated include, IR, T2D and hypertriglyceridemia. Moreover, FPL patients may present with additional

PCOS-associated features such as hirsutism, polycystic ovaries and menstrual irregularities (159).

There is also a substantial amount of heterogeneity in lipodystrophy disorders, thus identifying a causal mutation has remained challenging for certain subtypes. However, through the use of family studies, researchers have been able to uncover mutations in genes that have elucidated impaired adipogenesis at the center of genetic lipodystrophy etiology (160). Specifically for FPL, variants have been most frequently found in lamin A/C (*LMNA*) or peroxisome proliferator-activated receptor-γ (*PPARG*) genes (160). *LMNA* encodes multiple protein isoforms and partakes in nuclear stability, chromatin structure, RNA processing, gene expression and is directly involved in adipocyte development (161-165).

Variants in the insulin receptor (*INSR*) gene are also involved in extreme PCOS phenotypes and are a cause of Mendelian disorders of insulin resistance, including type A syndrome, Donohue syndrome and Rabson-Mendenhall syndrome (166-170). Mutations that affect the tyrosine kinase domain of the INSR cause severe hyperinsulinemia and insulin resistance (171-173). In normal circumstances the insulin signaling pathway is activated by binding of insulin or other ligands to the INSR. Downstream functions of this pathway include the regulation of insulin metabolism, glucose transport as well as several other vital processes (174-176). Common SNPs mapping to the *INSR* gene have been found to be associated with PCOS in both individuals of Han Chinese and European ancestry (45, 177, 178). Thus, PCOS GWAS results have also provided evidence for the role of the INSR in phenotypes of PCOS, namely associated with insulin resistance.

CHAPTER 2

IDENTIFICATION OF RARE VARIATION IN POLYCYSTIC OVARY SYNDROME (PCOS) BY NEXT GENERATION SEQUENCING

2.1 OVERVIEW

Polycystic ovary syndrome (PCOS), a common endocrine condition, is the leading cause of female factor infertility. Given that common disease-susceptibility variants account for only a small percentage of the estimated PCOS heritability, we tested the hypothesis that rare variants contribute to this deficit in heritability. Whole genome sequencing (WGS) of 80 PCOS cases and 24 reproductively normal control women identified potentially deleterious variants in *AMH*, the gene encoding anti-Müllerian hormone (AMH). Targeted sequencing of *AMH* and 10 additional PCOS-associated genes or candidate genes was conducted in 643 PCOS cases and 153 controls. Subject cohorts, sequencing analyses and general approach discussed in Chapter 2 are summarized in **Figure 2.1A**. Subsequent Chapters 3 and 4 report on the methods outlined in **Figure 2.1B** and **Figure 2.1C**, respectively. Herein, we report the rare genetic variation identified in PCOS cases and reproductively normal phenotyped controls, specifically focusing on select target genes: *AMH*, *AMHR2*, *LMNA* and *INSR*.

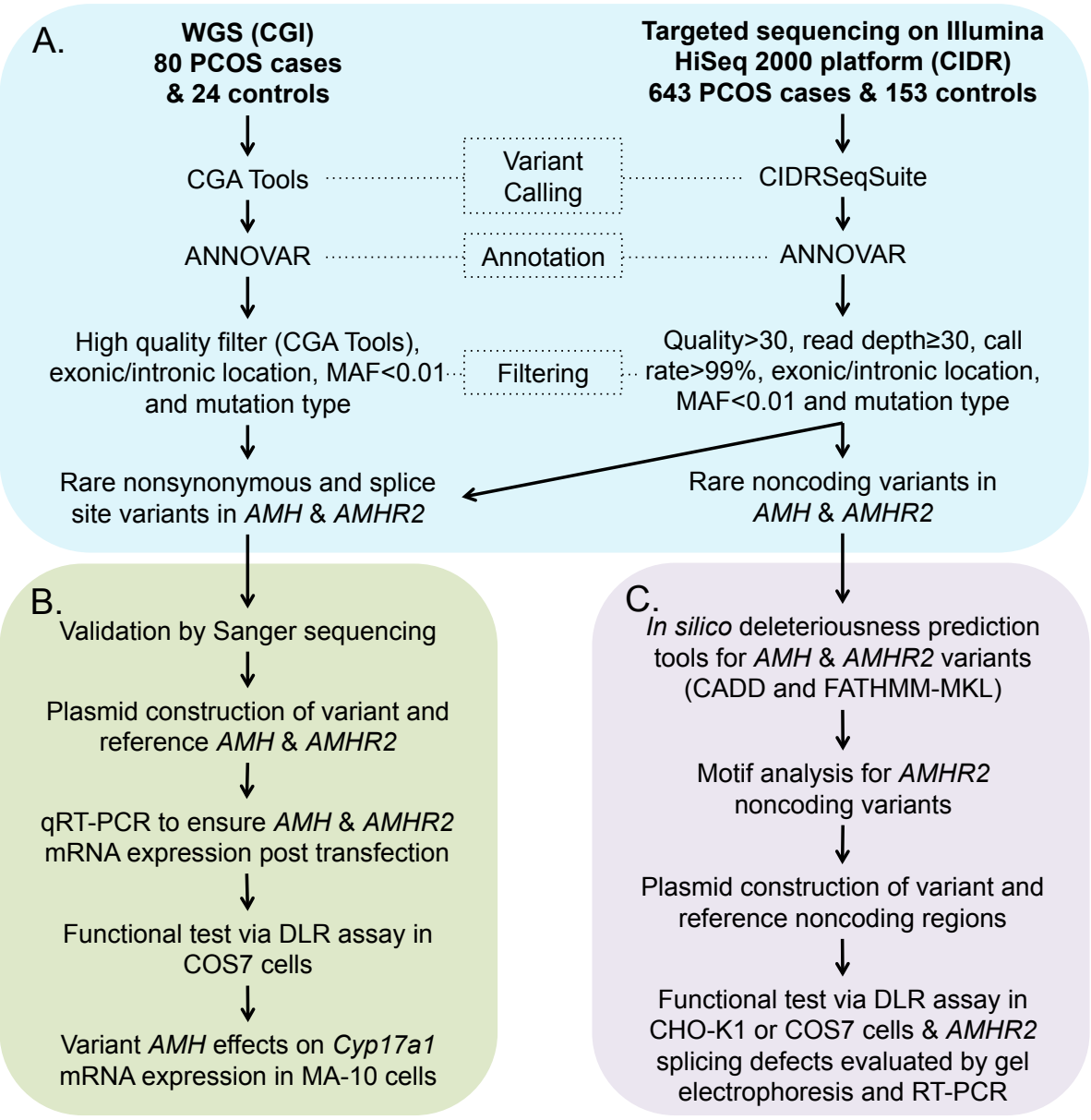

Figure 2.1 Pipeline of sequencing data analyses and functional assessment of variants. Figure denotes analytical steps applied to identify high quality rare (MAF<0.01) *AMH* and *AMHR2* variants from WGS and targeted resequencing data (A) as well as the molecular approach used to determine effects of *AMH* and *AMHR2* coding (B) and noncoding (C) variants on downstream signaling activity. Dual luciferase reporter (DLR) assay included one of the methods to evaluate variant changes in signaling ability compared to reference. Analogous analyses for targeted resequencing of *LMNA*, *INSR* and remaining 7 panel genes were also performed (not noted in figure).

2.2 STUDY PARTICIPANT CHARACTERISTICS

Characteristics of subjects included in this study are listed in **Table 2.1**. PCOS cases were significantly younger and heavier than controls. T, uT, DHEAS, LH, and AMH levels were significantly elevated in PCOS cases. SHBG levels were significantly decreased in PCOS cases compared to controls. These observations are consistent with the biochemical profile of PCOS (179). The results of these comparisons using other assays methodologies were similar to those reported in the tables. There were no significant differences in the clinical or biochemical features of the PCOS cases who underwent WGS compared to those who underwent targeted resequencing.

2.3 RARE VARIATION IN AMH

Analysis of WGS data in 80 PCOS cases and 24 controls (**Figure 2.1A**) identified three rare putative functional coding variants in *AMH,* the gene encoding AMH. These variants were found in 5 PCOS cases (T143I n=3, P270S n=1, Exon2/3 splice site n=1) and were confirmed by Sanger sequencing. No *AMH* coding variants were found in controls. AMH was the most plausible PCOS candidate gene, thus AMH was carried forward for further analysis.

We used a targeted resequencing approach to further evaluate genetic variation in *AMH* in a larger PCOS cohort (**Figure 2.1A**). Resequencing PCOS cases (n=643) and controls (n=153), including 22 PCOS and 12 controls from the WGS cohort, identified 21 additional rare (MAF<0.01) coding variants (**Table 2.2**). All subjects were heterozygous for variants and validated by Sanger sequencing. Furthermore, where parental DNA was available for sequencing, variants were inherited rather than generated *de novo*. The variants were dispersed

across all five exons of *AMH*, including one splice-site variant following the second exon (**Figure 2.2**).

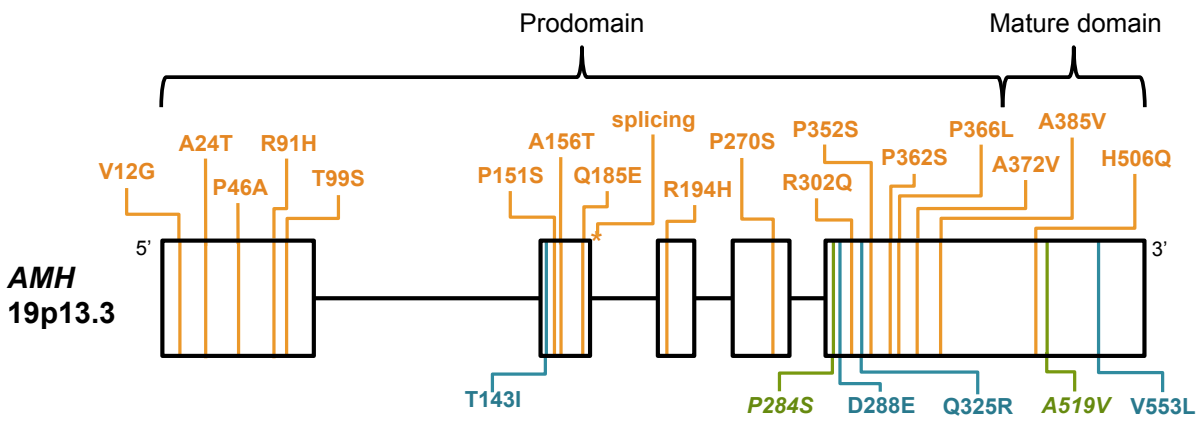

Figure 2.2 Rare coding and splice site variants identified in *AMH*. Rare variants at a MAF<0.01. PCOS-specific variants indicated in orange (n=18). Non-PCOS specific variants are shown in blue (n=4) and variants present in controls only in green (n=2).

Twenty-one variants were located in the prodomain region and three variants were located in the mature domain of the AMH protein. Eighteen of the variants were found only in PCOS cases (PCOS-specific variants). Fifteen out of the 18 variants were singletons (found only in one subject), while three variants occurred in multiple PCOS cases (V12G occurred in 6; T99S in 2; P352S in 3). One PCOS case had two missense variants, R194H and A385V mapping to the same copy of the gene (**Figure 2.3A**). Four variants were found in both PCOS cases and controls; two variants were found only in controls. One control woman was a compound heterozygote for variants D288E and V553L (**Figure 2.3B**). Five *AMH* variants (V12G, P151S, splicing (ex2/3), R302Q, and H506Q) found in 10 PCOS cases have also been identified in PMDS (118). None of the PMDS variants were found in controls.

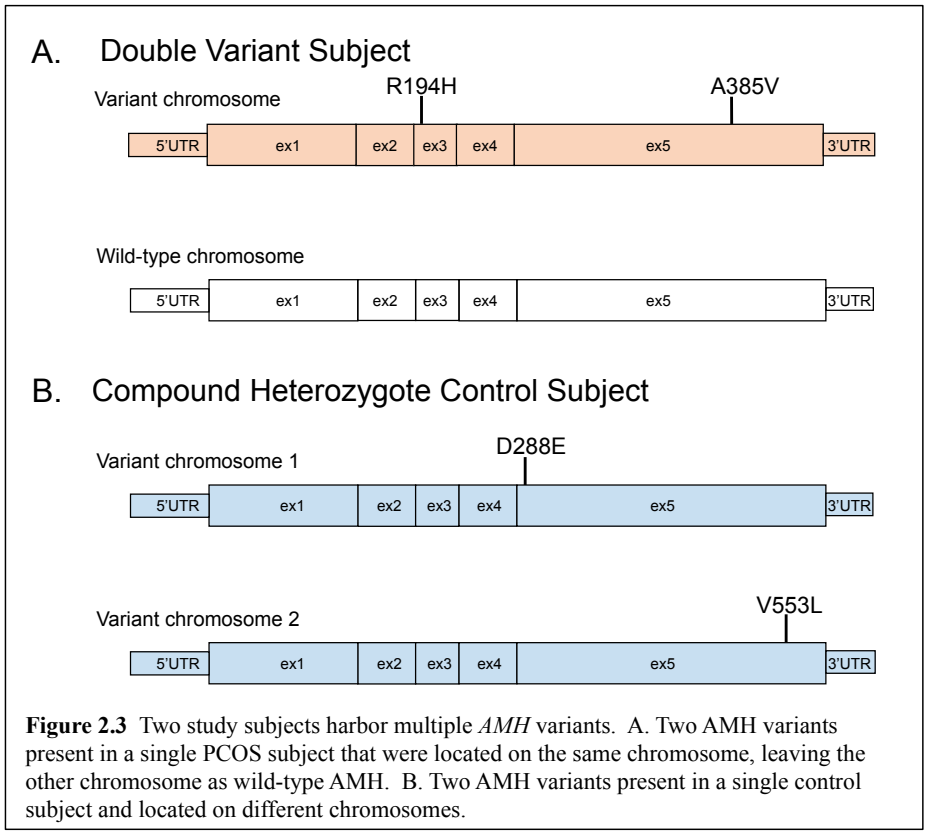

Figure 2.3 Two study subjects harbor multiple *AMH* variants. A. Two AMH variants present in a single PCOS subject that were located on the same chromosome, leaving the other chromosome as wild-type AMH. B. Two AMH variants present in a single control subject and located on different chromosomes.

Deleteriousness of *AMH* coding variants was evaluated using Combined Annotation Dependent Depletion (CADD) (180). The CADD scores were broadly distributed, and did not correspond well with known loss of function in PMDS variants (**Table 2.2**). Analogous analyses with Polyphen (181), SIFT (182), and GERP (183) were also inconsistent.

Noncoding variants also have the potential of altering protein activity through disruption of regulatory elements. Therefore, rare noncoding variation in and near *AMH* was also investigated to assess whether regulatory region impairment played a role in PCOS. We identified 12 variants specific to PCOS cases, 3 variants in cases and controls and 1 variant in a control subject (**Table 2.3**, **Figure 2.4**). All subjects were heterozygous for noncoding *AMH* variants, except for one subject who was homozygous for variant rs374418184. One of the 12

PCOS-specific noncoding *AMH* variants had an insertion of 1 base, while all other variants found were single nucleotide substitutions (**Table 2.3**).

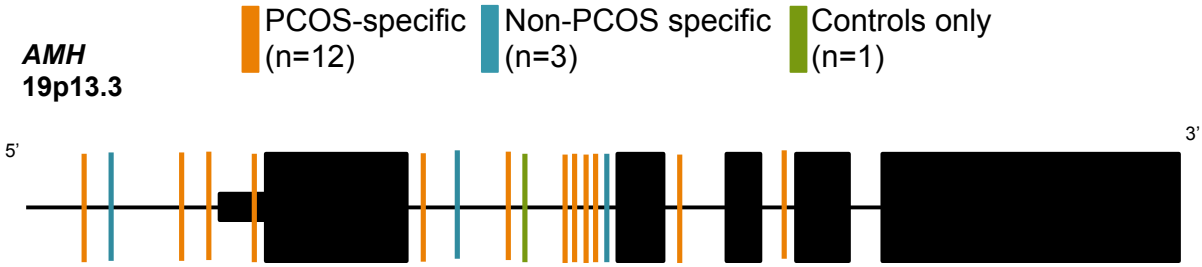

Figure 2.4 Rare noncoding variants identified in *AMH*. Rare variants at a MAF<0.01. PCOS-specific variants indicated in orange (n=12). Non-PCOS specific variants are shown in blue (n=3) and variants present in controls only in green (n=1). Black rectangles indicate exons of *AMH*.

2.4 RARE VARIATION IN AMHR2

The genomic region plus 5 kb upstream and downstream of *AMHR2* gene was sequenced in 643 PCOS women and 153 reproductively normal controls. We identified two missense variants in *AMHR2* at a MAF<0.01; one PCOS-specific (P30S) and one non-PCOS specific variant found in a single case and a single control (R548Q) (**Table 2.4, Figure 2.5**). All subjects were heterozygous for these missense variants.

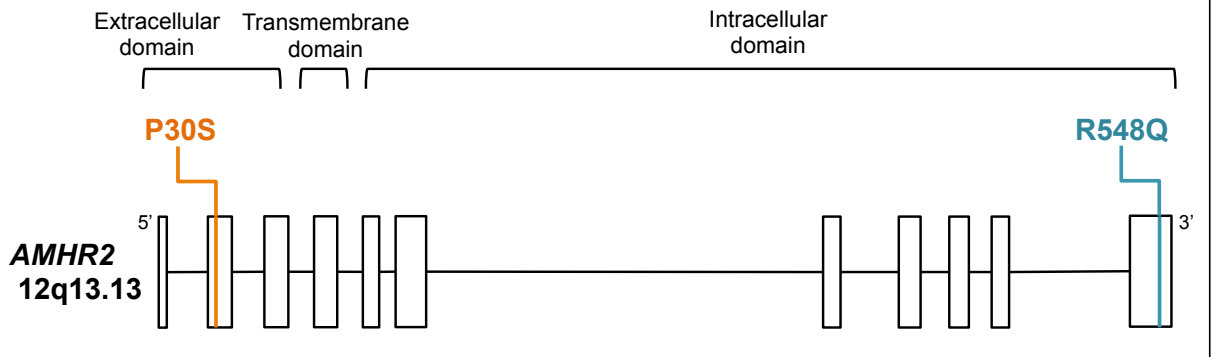

Figure 2.5 Rare coding variants identified in *AMHR2*. Rare variants at a MAF<0.01. PCOS-specific variants indicated in orange (n=1) and non-PCOS specific variants are shown in blue (n=1).

Additionally, 52 noncoding variants were identified upstream and within introns of *AMHR2*, while only 8 such variants were found in cases and controls (MAF<0.01, **Table 2.5, Figure 2.6**). Of the 52 PCOS-specific noncoding variants, 2 variants included 3-4 base deletions and another 2 variants created 1 and 6 base insertions (**Table 2.5**). Subjects presented with noncoding variants in the heterozygous state, except 3 PCOS cases were found to be homozygous for variant chr12:53820453 A>C. No noncoding *AMHR2* variants were identified solely in control subjects.

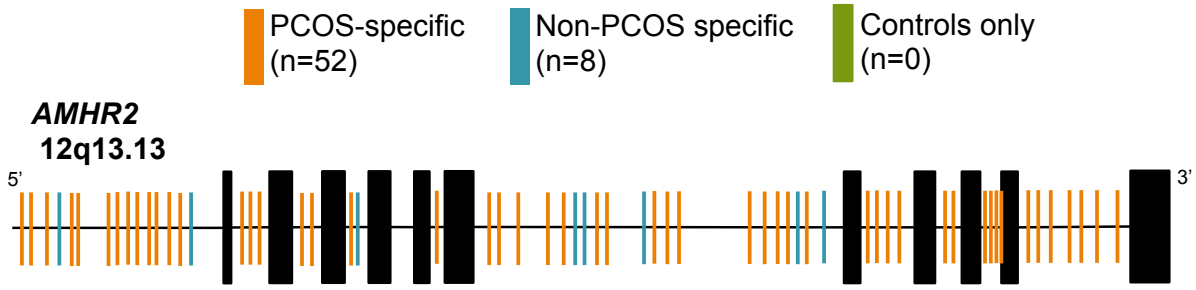

Figure 2.6 Rare noncoding variants identified in *AMHR2*. Rare variants at a MAF<0.01. PCOS-specific variants indicated in orange (n=52). Non-PCOS specific variants are shown in blue (n=8) and variants present in controls only in green (n=0). Black rectangles indicate exons.

2.5 RARE CODING VARIATION IN LMNA

The genomic region of *LMNA* gene was also included for custom targeted sequencing of 604 PCOS women and 125 reproductively normal controls. We identified 7 nonsynonymous variants with a MAF<0.01. Variants were found in a total of 9 PCOS subjects and 0 controls (**Table 2.6**). Combined Annotation Dependent Depletion (CADD) and Functional Analysis through Hidden Markov Models - Multiple Kernel Learning (FATHMM-MKL) analyses were completed to predict the deleteriousness of these variants (180, 184). These *in silico* tools can be used for scoring deleteriousness of variants based on multiple annotations integrated into one metric,

where a CADD score above 15 and a FATHMM-MKL *P*-value closer to 1 are generally considered deleterious. All variants were considered damaging according to CADD and FATHMM-MKL with C-scores above 15 and *P*-values near 1, respectively. All subjects were heterozygous for these variants. Mutations in the *LMNA* gene can lead to several different diseases (185, 186): such as types of muscular dystrophy (187, 188), familial partial lipodystrophy (189), dilated cardiomyopathy (190), Charcot-Marie-Tooth disease (191), and Hutchinson-Gilford progeria syndrome (192, 193). Three of the variants in our cohort have been previously associated with these disorders (**Table 2.7**). This data provides supporting evidence that mutations in genes that cause Mendelian disorders with PCOS symptoms, account for a subgroup of PCOS patients.

2.6 RARE CODING VARIATION IN INSR

The *INSR* gene was also included in our custom targeted resequencing panel. In our cohort of PCOS cases and reproductively normal controls we identified 11 nonsynonymous variants at a MAF<0.05 (**Table 2.8**). Variants were found in a total of 23 subjects, and more specifically 22 PCOS cases and 1 control subject. Ten out of the 11 variants in *INSR* were specific to PCOS cases. One variant was found in a case and control. CADD and FATHMM-MKL analyses were conducted to predict the deleteriousness of these variants on protein function. Nine out of 10 PCOS-specific variants were deemed deleterious (C-score>15, **Table 2.8**). One subject heterozygous for deleterious *INSR* variant, rs146588336, also harbored a predicted harmful variant in *LMNA* gene, rs777841827.

2.7 RARE VARIATION IN ADDITIONAL PCOS CANDIDATE GENES

Eleven genes (*AMH, AMHR2, LMNA, INSR, LHB, FSHB, CPEB2, EIF2AK4, ENTPD5, SLC22A1, AKAP17A*) were included in our targeted custom sequencing array. These genes were chosen based on previously published candidate genes as well as our whole genome sequencing screen of 80 PCOS cases and 24 controls by Complete Genomics (CGI). **Table 2.9** shows the frequency of subjects (cases or controls) with nonysynonymous variants in each sequenced gene with MAF<0.01 and 0.05. For several of the genes sequenced, the number of variants was similar regardless of MAF<0.01 and 0.05. Therefore, many variants found in our cohort are extremely rare. We discovered a number of genes from our panel with an increased frequency of nonsynonymous variants in PCOS cases compared to controls. Variants identified in *FSHB* are also of interest for future follow-up studies.

2.8 MATERIALS AND METHODS

Subjects

This study was approved by the Institutional Review Boards of Northwestern University Feinberg School of Medicine, Pennsylvania State University College of Medicine and Brigham and Women's Hospital. Written informed consent was obtained from the study participants. All subjects were self-reported Caucasians of European ancestry, ages 16-48 years old and in good general health. The subjects had participated in our previous studies of PCOS (47, 54) and the details of the assessment of study subjects and their clinical and biochemical features at enrollment have been reported (54, 179, 194).

In brief, women were not taking any medications known to alter reproductive or metabolic hormone levels for at least one month prior to study; contraceptive steroids were

discontinued three or more months prior to study. All PCOS cases had the so-called "classic" or National Institutes of Health (NIH) phenotype of PCOS with elevated total testosterone (T) or non-sex hormone binding globulin bound T (uT) levels as well as chronic oligomenorrhea (eight or fewer menses per year) (195). Control women had regular 27-35 day menstrual cycles and no history of reproductive disorders. They had Ferriman and Gallwey hirsutism scores less than eight and circulating T, uT and dehydroepiandrosterone sulfate (DHEAS) levels within the normal range we previously established in healthy, non-hirsute, premenopausal women with 27-35 day menstrual cycles (54, 179). Disorders of the ovary, adrenal and pituitary that can present similarly to PCOS were excluded by appropriate tests (179). Ovarian morphology was not assessed since this finding is not a criterion for the diagnosis of the NIH PCOS phenotype. AMH levels were measured in subjects for whom serum stored at -80°C was available (194).

Hormone Assays

T, uT, DHEAS, sex hormone-binding globulin (SHBG), luteinizing hormone (LH) and follicle-stimulating hormone (FSH) levels were determined as previously reported (12, 194, 196). Thirty-one PCOS cases were diagnosed based on their medical records, including laboratory results, documenting elevated total or free/bioavailable T and/or DHEAS levels. The assay methodology changed for DHEAS, SHBG, LH and FSH. The results for 70 DHEAS, 104 SHBG, 168 uT, 123 LH and 123 FSH measurements in PCOS and 75 DHEAS, 99 SHBG, 100 uT, 94 LH and 94 FSH measurements in controls were not included in the end point analyses due to the difference in assay methods (**Table 2.10**). Results were missing for technical reasons for uT in 4 PCOS; SHBG in 3 PCOS and 1 control; DHEAS in 4 PCOS; and LH and FSH in 28

PCOS cases and 12 controls. AMH was measured by ELISA (Ansh Labs (194)) on 259 PCOS cases and 126 controls in whom serum was available.

Next Generation Sequencing

Whole genome sequencing was performed on DNA from 80 PCOS cases and 24 controls by Complete Genomics (CGI, Mountain View, CA, USA). Targeted resequencing of *AMH* was performed in DNA from in 643 PCOS cases and 153 controls at the Center for Inherited Disease Research (CIDR, Johns Hopkins University, MD, USA). Twenty-three PCOS cases and 12 controls were sequenced on both platforms. Genomic sequence data was thus available for analysis for a total of 700 PCOS cases and 165 controls. For targeted resequencing, DNA capture kits (Agilent SureselectXT or NimbleGenSeqCap EZ Choice Library) were used to generate custom DNA libraries of targeted gene regions (based on GRCh37/hg19 genome build: *AMH* chr19:2244000-2258000; *AMHR2* chr12:53813000-53831000; *LMNA* chr1:156047000-156055000, chr1:156059000-156062000, chr1:156080000-156115000; *INSR* chr19:7107000-7188000, chr19:7266000-7269000, chr19:7292000-7299000; *LHB* chr19:49514000-49525000; *FSHB* chr11:30247000-30261000; *CPEB2* chr4:14999000-15020000, chr4:15033238-15078000; *EIF2AK4* chr15:40221347-40333000; *ENTPD5* chr14:74418000-744910000; *SLC22A1* chr6:160537863-160565500, chr6:160574800-160584000; *AKAP17A* chrX:1705486-1724196). Sequencing was carried out using Illumina HiSeq2000 platform.

Bioinformatic Pipeline

The whole genome sequence alignment and quality control were implemented using CGI's proprietary software (Assembly Pipeline version 2.0 (197)). Variant calling was accomplished

using CGA Tools workflow version 1.7.1 in conjunction with the Galaxy analysis platform for filtering of variants subsequently annotated using ANNOVAR (198) (**Figure 2.1A**). For targeted resequencing, alignment to reference genome build 37 and variant calling were completed using the CIDRSeqSuite pipeline. Annotation of called SNPs and indels was executed using ANNOVAR (198) and 1000Genomes (1000g2014sep_eur) MAF was included. Annotated variants were filtered based on phred quality score >30, read depth ≥30, call rate >99%, exonic/intronic location, MAF<0.01 and mutation type (predicted missense, nonsense, frameshift, and splice site variants) (**Figure 2.1A**). Population-based allele frequencies for each rare variant noted in table footnotes were obtained from one of the following databases: Genome Aggregation Database (gnomAD, Eurpean Non-Finnish cohort frequency when available) (http://gnomad.broadinstitute.org/), ExAc Aggregated Populations cohort (http://exac.broadinstitute.org), or 1000Genomes European ancestry cohorts (http://www.1000genomes.org). Deleteriousness of each variant was assessed using CADD (180), FATHMM-MKL (184), PolyPhen-2 (181), SIFT (182), and GERP (183). Further discussion of these variant scoring tools and results is addressed in subsequent chapters.

Statistical Analysis

Statistical tests were implemented using IBM SPSS statistics (SPSS Inc., Chicago, IL). Normality of hormonal and demographic endpoints were evaluated by the Kolmogorov-Smirnov test. Alpha levels of less than 0.05 were considered statistically significant. Nonparametric tests (Mann-Whitney U tests) were used to compare groups with non-normally distribution traits. Analysis of covariance using age and BMI as covariates was applied for traits (FSH and AMH)

with significant evidence correlation with age and BMI ($p<0.05$). All tests were two-tailed. Pearson's Chi-Square test was used to evaluate significance of genetic associations.

Variant Validation

Annotated variants surviving the filters for *AMH* and *AMHR2* were verified using PCR amplification of genomic DNA and Sanger sequencing. Sanger sequencing results were analyzed with SeqMan Sequencing Software (DNAstar, Inc., Madison, WI). Variant validation by Sanger sequencing is critical to eliminate the inclusion of sequencing errors in the functional analysis.

2.9 CONCLUSIONS

Custom targeted NGS has proven to be a reliable and accurate tool in evaluating the contribution of rare genetic variation, both coding and noncoding, in our PCOS/control patient cohort. Filtered variants were of high quality, and those resequenced by Sanger method all validated. We discovered multiple genes within our panel of PCOS candidates to harbor predicted deleterious variants (*AMH*, *AMHR2*, *LMNA* and *INSR*). Additional analyses can be performed to investigate the association of variants within the other genes of our panel and PCOS. Here, we have successfully identified rare (MAF<0.01) coding and splice site variants within *AMH*: 18 variants specific to PCOS cases, 4 variants in cases and controls, and 2 variants solely in control subjects. Furthermore, 2 rare variants were found in coding regions of *AMHR2*: 1 PCOS-specific and 1 in a case and control. Seeing as a PCOS phenotype is often observed in cases of familial partial lipodystrophies and syndromes of insulin resistance, we also investigated whether rare variation in genes that cause these disorders account for a subgroup of our PCOS cohort.

Predicted pathogenic rare (MAF<0.01) coding variants were, in fact, identified in both *LMNA* and *INSR*. Seven PCOS-specific variants were found in the *LMNA* gene and 11 variants in the *INSR* gene, 10 of which were specific to PCOS cases. While association of *LMNA* variants with PCOS in our cohort of 604 PCOS women and 125 controls did not reach significance ($\chi = 3.429$; $p = 0.064$; OR = 1.89), evidence for association between *LMNA* variants and PCOS was highly significant using a larger Genome Aggregation Database (gnomAD) control cohort ($\chi = 60$; $p < 10^{-8}$; OR = 9.56). Association of *INSR* variants with PCOS was neither significant with our control cohort ($\chi = 2.7$; $p = 0.1$) nor a larger population-based control cohort ($\chi = 1.16$; $p = 0.281$).

While coding variants are generally assumed to cause a greater impact on protein function, variants in noncoding regions can just as likely alter gene regulation and function by disrupting vital regulatory elements and other processes still unknown. Given that roughly 98-99% of the human genome is noncoding, we have only begun to scratch the surface of understanding the mechanisms that lie and interact within these regions. Therefore, we also evaluated the extent of rare (MAF<0.01) noncoding variation in/near *AMH* and *AMHR2* in our PCOS case/control cohort. Filtering analyses for noncoding *AMH* regions yielded 12 PCOS-specific variants, 3 variants in cases and controls, and 1 variant in a single control subject. Interestingly, a larger number of rare noncoding variants were found in *AMHR2* with 52 variants specific to PCOS women and 8 variants in both cases and controls. Technical advancements and cost effectiveness of next generation sequencing have enabled the first findings for the contribution of rare genetic variation in a common PCOS phenotype.

CHAPTER 3

FUNCTIONAL CODING VARIANTS IN MEMBERS OF THE ANTI-MÜLLERIAN HORMONE (AMH) PATHWAY

3.1 OVERVIEW

The overarching goal of the following studies was to differentiate between functional and therefore putatively causal variants versus rare polymorphisms. Using NGS, we identified rare variants in members of the AMH pathway, *AMH* and *AMHR2*. Dual luciferase reporter (DLR) assays measured the impact of the *AMH* and *AMHR2* coding variants on AMH signaling (**Figure 2.1B**). We found 24 rare (MAF<0.01) *AMH* variants in PCOS cases and controls; 18 variants were specific to PCOS cases. Seventeen of 18 (94%) PCOS-specific variants significantly reduced AMH signaling, while 0 out 6 *AMH* variants observed in controls showed significant defects in signaling. Furthermore, 1 PCOS-specific rare nonsynonymous variant was found in *AMHR2* and showed significant decrease in signaling compared to reference *AMHR2*. Thus, in a subset of PCOS cases, we have identified rare *AMH* and *AMHR2* coding variants that reduced AMH mediated signaling *in vitro*. This study is the first to identify rare genetic variants that are associated with a common PCOS phenotype. AMH has been previously shown to inhibit *CYP17* transcription in cells of the testis, a rate-limiting enzyme for androgen biosynthesis. All 17 of the PCOS-specific functional *AMH* variants also failed to inhibit *CYP17* expression in mouse Leydig MA-10 cells compared to reference *AMH*. Our findings suggest a novel mechanism for the pathogenesis of PCOS, where decreased AMH signaling in the PCOS ovary is predicted to result in increased *CYP17* transcription and testosterone production.

3.2 PCOS-SPECIFIC AMH VARIANTS SIGNIFICANTLY REDUCE SIGNALING ACTIVITY

Dual luciferase reporter assays demonstrated a significant reduction of AMH-mediated BRE induction in 17 of the 18 PCOS-specific variants (**Figure 3.1A**, **Table 3.1**) in COS7 cells

cotransfected with AMHR2 and variant AMH constructs. In contrast, none of the variants that were found in both PCOS cases and controls (n=4) or controls only (n=2) showed a significant reduction in signaling compared to reference *AMH* (**Figure 3.1A**, **Table 3.1**). Quantitative real-time PCR (qRT-PCR) of RNA isolated from COS7 cells transfected with *AMH* variants found in cases and controls demonstrated that all variant *AMH* transcripts were similarly expressed to reference *AMH* transcripts 48 hours after transfection (**Figure 3.1B**), thus the signaling impairment observed in the functional variants was not simply due to a defect in variant expression but is due to a reduction in signaling capacity.

Sixteen of the 17 functional PCOS-specific variants were located in the prodomain region of AMH. Upon proteolytic cleavage, the prodomain remains non-covalently associated with the mature domain and has been shown to influence mature domain activity (199, 200), thus variants in the prodomain are likely to have an effect on mature protein processing and/or bioactivity.

Approximately 3% (24/700) of our European ancestry PCOS cohort had functional *AMH* protein coding variants. The PCOS cases were younger and heavier than the controls, a common finding in studies of PCOS (54), accordingly the analyses were adjusted for age and BMI. There were no significant phenotypic differences between PCOS cases with functional *AMH* variants and those with wild-type *AMH* genotypes. The serum AMH levels in cases with mutations were within the range of AMH levels observed in PCOS (1) and significantly higher than those observed in controls (**Table 3.2**). There were no significant differences in clinical and biochemical features between PCOS cases with *AMH* functional variants and PCOS cases without coding variants.

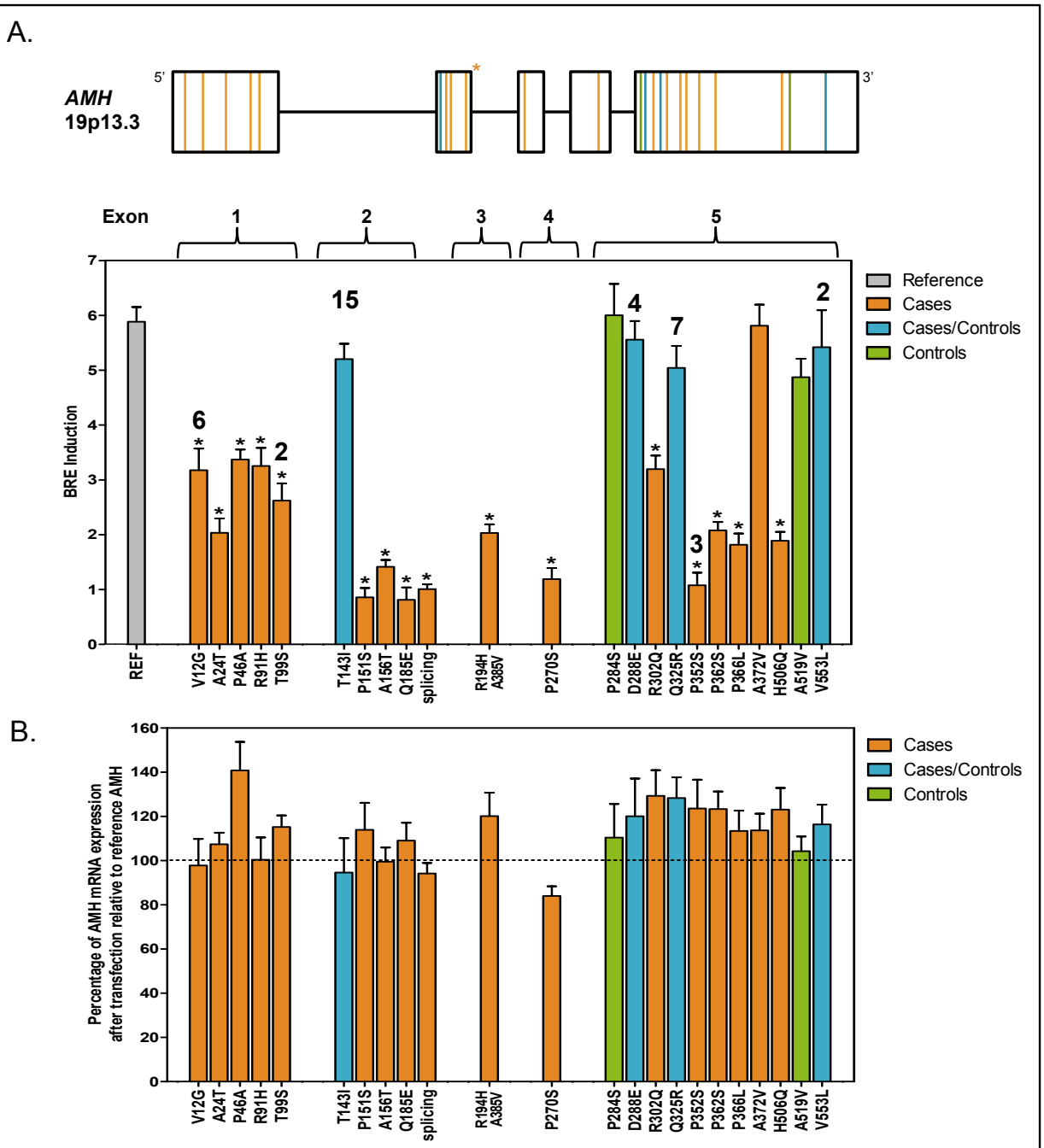

Figure 3.1 Effect of *AMH* variants on signaling ability. A. Average induction of BRE-firefly luciferase normalized to *Renilla* reporter and empty vector control in COS7 cells transfected with reference (REF) or variant *AMH* constructs. Results represent three independent experiments done in triplicate with SEM. Asterisks indicate significantly reduced BRE induction. The number of subjects (>1) is indicated above BRE induction bar. B. Percentage of *AMH* mRNA expression for each variant following transfection relative to reference *AMH*. Results represent three independent experiments with qRT-PCR run in duplicate with SEM.

As expected PCOS women with functional *AMH* variants have markedly elevated testosterone levels compared to control women, and while median testosterone levels in women with *AMH* mutations are nominally higher than what is observed in women without *AMH* variants this observation is not statistically significant. Given that PCOS is a complex, multifactorial trait, it is our hypothesis that the underlying cause of hyperandrogenemia in PCOS is due to multiple distinct mechanisms. In a subset of women with PCOS, hyperandrogenemia is due to mutations in *AMH* or other members of the AMH signaling pathway, while in other women with PCOS, as predicted by the GWAS findings, hyperandrogenemia is due to alternative pathways (53-55). Further evaluation of these pathways will elucidate the relative impact of a given PCOS sub-phenotype in individual PCOS subjects.

3.3 PCOS-SPECIFIC AMH VARIANTS SHOW DOMINANT-NEGATIVE EFFECT

DLR assays of COS7 cells co-transfected with equal amounts of PCOS-specific variant and reference constructs (i.e. heterozygous state) displayed 25.05% (±3.45%) greater signaling capacity than PCOS-specific variant constructs alone (i.e. homozygous variant state), averaged across 3 example PCOS-specific variants (**Figure 3.2**). If no impairment of activity was due to a dominant-negative interaction between wild type and variant peptides, then the expected signaling increase would be 50%-75%. Splicing variant displayed a 46% signaling increase consistent with the notion that the splicing variant would not produce viable AMH protein and thus not have a dominant-negative effect (**Figure 3.2**). Variant P284S, which was identified only in control women, showed wild-type signaling in homozygous and heterozygous states (**Figure 3.2**). **Figure 3.3** illustrates a dominant-negative assessment for all variants, which showed an average of 21.9% (±6.37%) signaling increase across the 16 functional *AMH* variants.

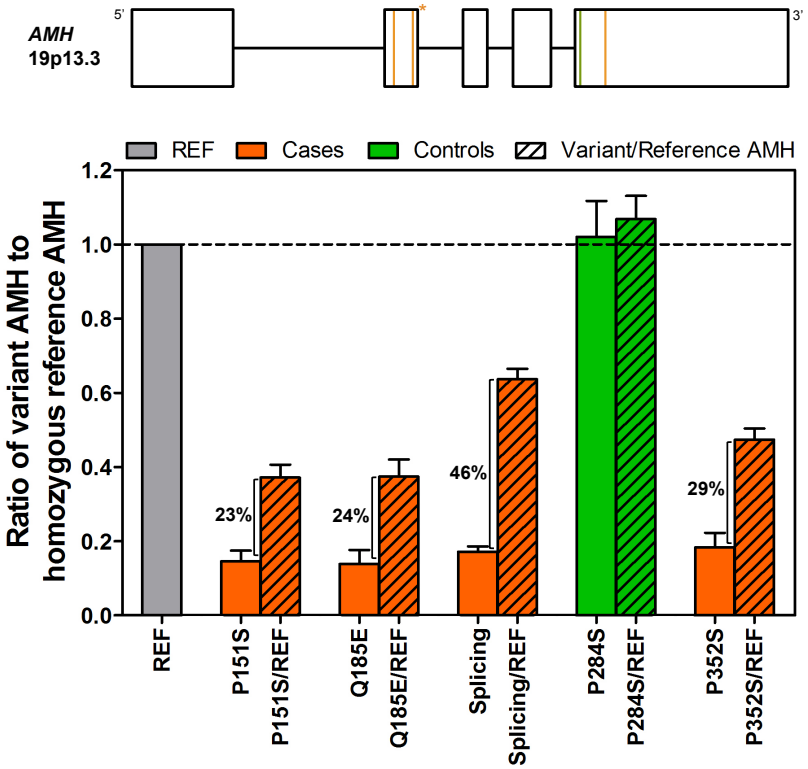

Figure 3.2 Dominant-negative effect of PCOS-specific *AMH* variants on signaling. Average BRE-firefly luciferase induction normalized to *Renilla* reporter and empty vector control in COS7 cells transfected with reference (REF) and/or variant *AMH* constructs. PCOS-specific *AMH* variants are shown in orange, and *AMH* variant present only in controls is shown in green. Solid colors indicate homozygous state, while diagonal line pattern indicates heterozygous state. Results represent three independent experiments done in triplicate with SEM.

All of the subjects were heterozygous for these variants. Given that AMH functions as a homodimer (200), *AMH* variants in the heterozygous state were hypothesized to have a phenotypic impact via a dominant-negative interaction between a wild-type and variant AMH peptide (200). Specifically, wild-type AMH dimers would only account for a quarter of total AMH in individuals heterozygous for *AMH* variants (**Figure 1.10**). In support of a dominant-negative interaction model, COS7 cells expressing *AMH* variants in the heterozygous state generated ~25% greater signaling capacity than *AMH* variants in the homozygous variant state exactly as predicted under a completely dominant-negative model. These results suggest that only the 25% of wild-type AMH dimers were able to achieve signaling capability *in vitro*.

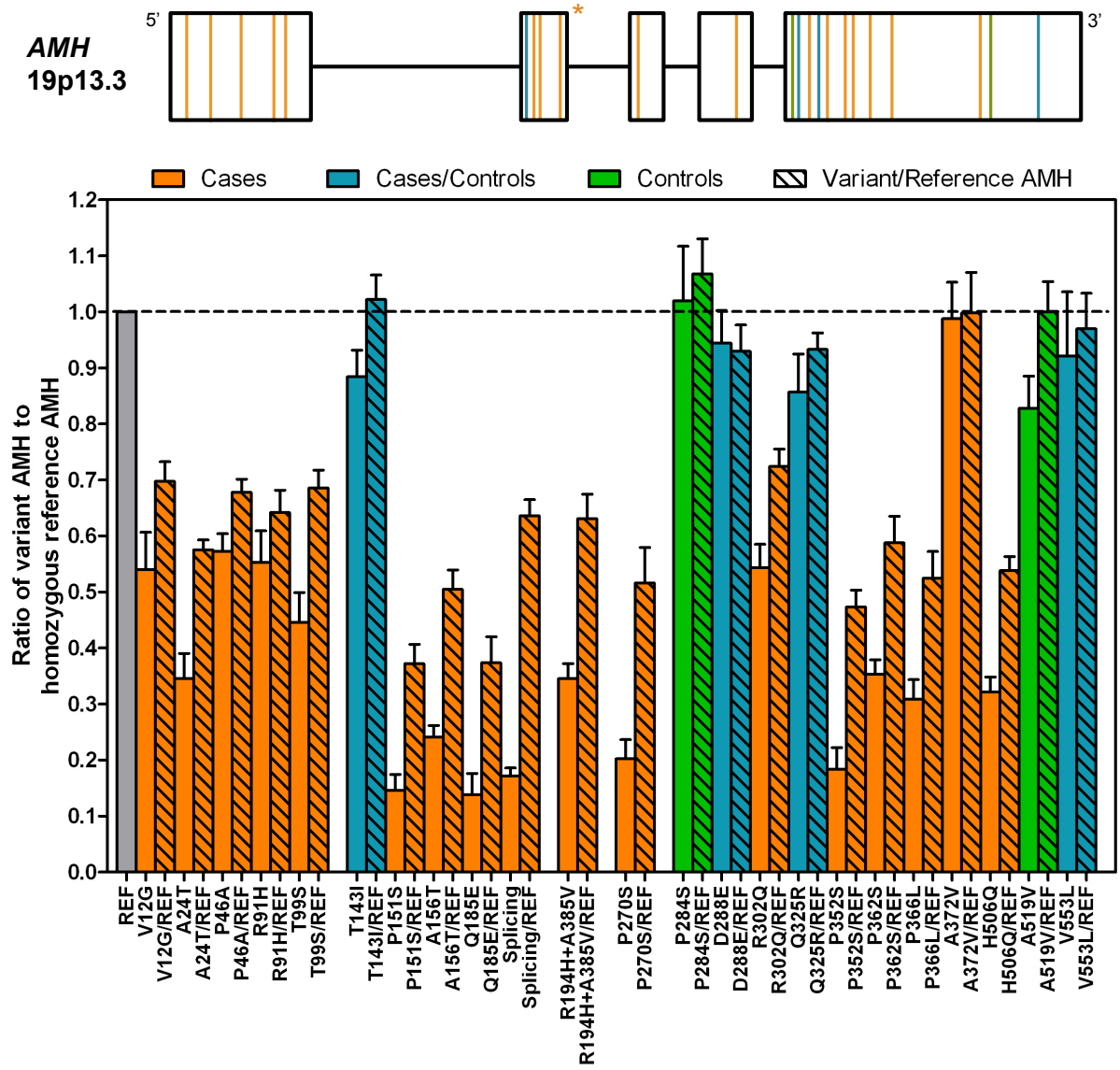

Figure 3.3 Dominant-negative effect across all *AMH* variants. Average BRE-firefly luciferase induction normalized to *Renilla* reporter and empty vector control in COS7 cells transfected with reference (REF) and/or variant *AMH* constructs. PCOS-specific *AMH* variants are shown in orange, and *AMH* variant present only in controls is shown in green. Solid colors indicate homozygous state, while diagonal line pattern indicates heterozygous state. Results represent three independent experiments done in triplicate with SEM.

3.4 SIGNIFICANT ASSOCIATION OF FUNCTIONAL AMH VARIANTS WITH PCOS

We tested for association between functional *AMH* variants and PCOS using two independent control groups: the 165 reproductively normal control women who were sequenced in this study

and population-based controls (men and women) from the ExAc Aggregated Populations cohort (n >100,000; http://exac.broadinstitute.org) or 1000Genomes European ancestry (n = 1006; http://www.1000genomes.org) cohorts, when no data was available in ExAc Aggregated Populations. The functional *AMH* variants were significantly associated with PCOS in our cohort of 700 women with PCOS and 165 controls ($\chi = 10.55$; $p = 0.0012$). Furthermore, evidence for association between functional *AMH* variants and PCOS was highly significant with the population-based control cohort ($\chi = 154$; $p < 10^{-8}$). Age, BMI, T, uT, DHEAS, SHBG, FSH, and LH levels did not differ significantly between PCOS cases with functional *AMH* variants compared to PCOS cases without *AMH* coding variants (**Table 3.2**). The functional *AMH* variants were significantly associated with PCOS relative to reproductively normal women (i.e. our phenotyped controls; n=165) and highly significant relative to a much larger population-based control cohort (in ExAc Aggregated Populations; n~120,000).

3.5 FREQUENCY OF PERSISTENT MÜLLERIAN DUCT SYNDROME (PMDS) MUTATIONS IN PCOS AND THE GENERAL POPULATION

Five of the *AMH* variants identified in our cohort of PCOS cases (V12G, P151S, splicing (ex2/3), R302Q, and H506Q) have also been identified in PMDS males (118). Of the women harboring PCOS associated *AMH* variants that reduced signaling, 42% (10/24) are PMDS associated *AMH* variants with documented loss of AMH activity in PMDS (118). The phenotypic features of females in PMDS families with *AMH* variants have not been reported, but based on our findings, one would predict that female carriers of *AMH* variants have PCOS. Males with PMDS and *AMH* variants have circulating AMH levels ranging from undetectable to normal (118). These findings are consistent with our observation that circulating AMH levels

are not correlated with AMH signaling capacity and suggest that AMH levels may not be an accurate measure of AMH signaling activity in PCOS.

The prevalence of PMDS within the population is unknown. To address this question, we used the population frequency of PMDS variants to calculate the frequency of PMDS cases (homozygote and compound heterozygote carriers of *AMH* and/or *AMHR2* PMDS mutations) and the frequency of heterozygous carriers of these mutations from the allele frequency of known PMDS variants (model of PCOS). We assembled a comprehensive list of PMDS mutations identified in *AMH* and *AMHR2* from the literature (120, 123, 201-230) and mapped those variants onto known genetic variants in dbSNP, a central public repository of genetic variation consisting of 324+ million human variants (https://www.ncbi.nlm.nih.gov/SNP/). Expected frequencies of homozygotes and compound heterozygotes (model of PMDS) and of heterozygote carriers (model of PCOS) of *AMH* and/or *AMHR2* functional variants were calculated from allele frequencies of PMDS mutations in dbSNP. We identified 133 PMDS mutations (69 *AMH*; 64 *AMHR2*) in 217 PMDS cases (108 *AMH*, 109 *AMHR2*) and were able to assign dbSNP identifiers to 57 of these mutations (26 *AMH*; 30 *AMHR2*) accounting for 57% of PMDS cases. Population based allele frequencies from the 57 informative PMDS variants predict a homozygote/compound heterozygote frequency, in *AMH* and/or *AMHR2* (PMDS model), of 1.63×10^{-5} or 5,312 individuals (2,656 males) in the U.S. (estimated 2017 population = 325,719,178). The frequency of heterozygote carriers (PCOS model) of PMDS variants was much higher (frequency =0.0101; 1,255,169 women in the U.S.) illustrating how causal variants of even very rare recessive disorders can be very prevalent in the heterozygous state. These estimates are likely to be 2-4 fold underestimates of the true frequency of PMDS since 1) we only surveyed published PMDS mutations and therefore did not count undiagnosed and/or

uncharacterized cases of PMDS, 2) we were not able to find dbSNP identifiers for approximately 50% of PMDS mutations, and 3) we do not account for the ~15% of PMDS cases without *AMH* or *AMHR2* variants. Using population frequencies of known PMDS mutations, we estimate the incidence of PMDS in the U.S. to be 2,600-10,000 and for *AMH*/*AMHR2* mutations to impact 1-4% of women in the U.S.

3.6 PATHOGENIC PCOS-SPECIFIC AMH VARIANTS CAUSE LOSS OF CYP17 INHIBITION

Inhibitory action of AMH on *Cyp17* expression in cAMP-stimulated MA-10 mouse Leydig cells has been previously observed (231). Using qRT-PCR, we assessed the downstream inhibitory effects of variant AMH on *Cyp17a1* expression in cAMP-treated MA-10 cells in comparison to wild-type AMH. Reference sequence AMH inhibited *Cyp17a1* expression by an average of 80% relative to cAMP-treated vector only control (**Figure 3.4**). Inhibition levels of *Cyp17a1* expression with previously found AMH mutants with wild-type function (T143I, P284S, D288E, Q325R, A372V, A519V and V553L) were not significantly different from reference AMH (**Figure 3.4**). However, the 17 *AMH* variants that previously reduced AMH signaling in the dual luciferase reporter assay, including the 5 known PMDS variants, showed an average of only 21.3% (±15.9%) decrease in *Cyp17a1* expression normalized to housekeeping gene, *Gapdh*, and relative to vector control (**Figure 3.4**). Variant *AMH* expression levels were not significantly different from reference *AMH*. These results provide further evidence that previously identified functional *AMH* signaling variants also display a loss of inhibition on *Cyp17a1* expression compared to reference *AMH*, *in vitro*.

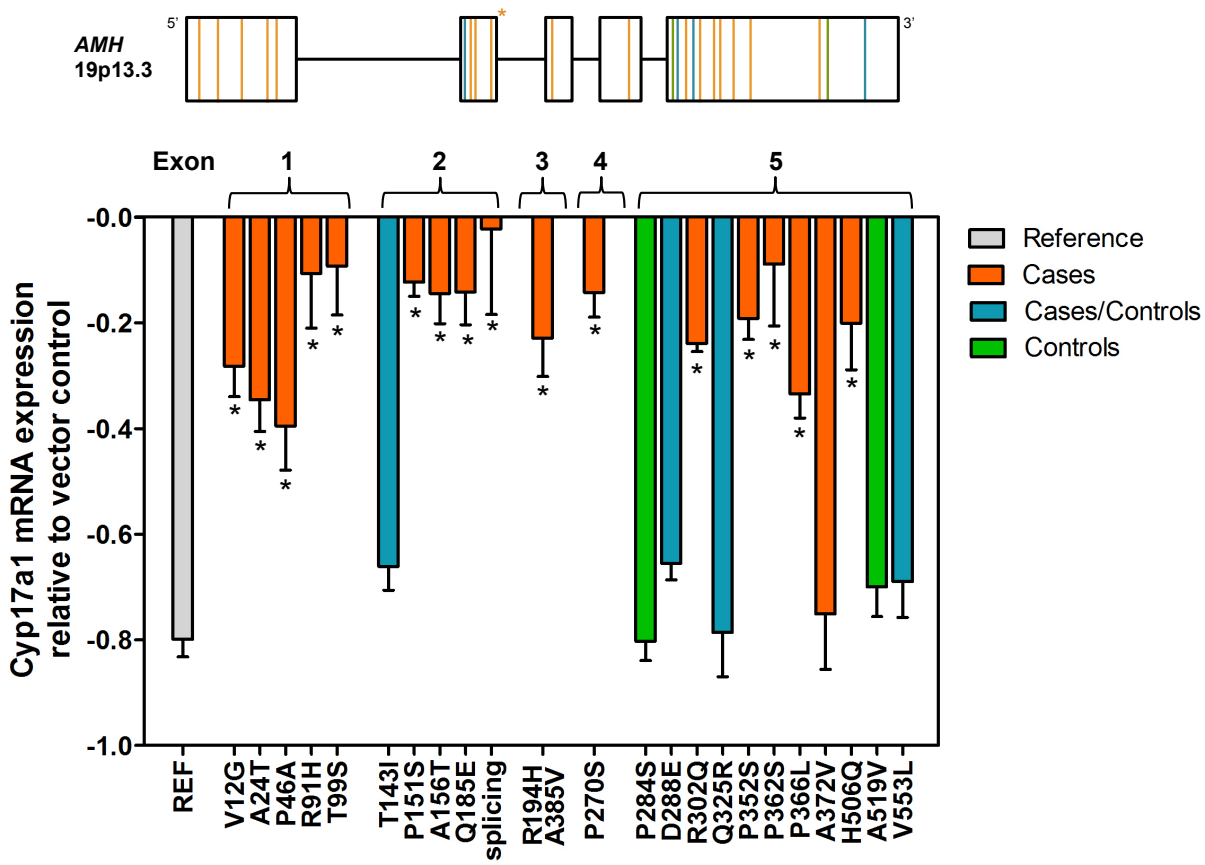

Figure 3.4 *AMH* variants cause loss of *Cyp17a1* expression *in vitro*. Application of qRT-PCR shows mutant AMH impact on *Cyp17a1* mRNA expression in cAMP-stimulated MA-10 cells relative to reference AMH. Asterisks indicate significantly reduced *Cyp17a1* inhibition compared to REF. Results represent three independent experiments with SEM.

A plausible mechanism by which reduced AMH signaling could contribute to the pathogenesis of PCOS would be by decreased inhibition of ovarian testosterone production. Accordingly, *AMH* mutations with reduced bioactivity are predicted to increase theca cell androgen production due to loss of *CYP17* inhibition by AMH in the PCOS ovary (**Figure 3.5**). In support of this hypothesis, Nelson and colleagues (232) observed an increase in *CYP17* mRNA in theca interna cells of women with PCOS compared to that in reproductively normal control women.

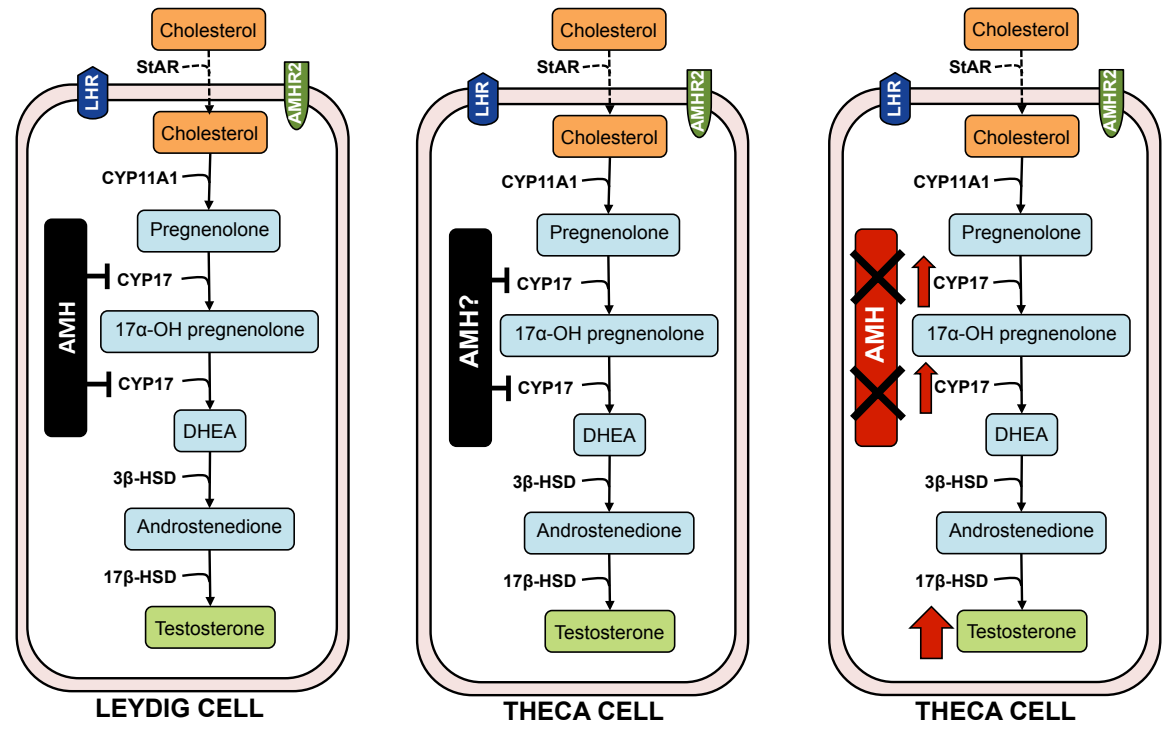

Figure 3.5 Model of AMH role in gonadal steroidogenesis. A. AMH inhibition of testosterone synthesis in normal male testis via downregulation of CYP17 transcription observed in rodent Leydig cells. B. Model of AMH inhibition of testosterone production in normal female ovarian theca cells via inhibition of CYP17 transcription. C. Impact of AMH inactivating mutation on testosterone production in PCOS theca cells. Gorsic *et al*, *J Clin Endocrinol Metab* 2017.

3.7 PCOS-SPECIFIC AMHR2 VARIANT SIGNIFICANTLY REDUCES SIGNALING ACTIVITY

To determine whether missense variants found in *AMHR2* affected downstream signaling, we employed the same signaling assay used for *AMH* variant studies. *AMHR2* mutant constructs were created and tested for signaling ability. *AMHR2* variant P30S found in 1 PCOS case showed significant impaired AMH signaling, while R548Q retained wild-type signaling (**Figure 3.6A**). Functional results were consistent with CADD and FATHMM-MKL prediction tools, where only *AMHR2* sequence variant c.C88T (p.P30S) was deemed deleterious (**Table 2.4**).

Quantitative RT-PCR confirmed that *AMHR2* mRNA expression levels were consistent between variants and reference control (**Figure 3.6B**). The first 3 exons of *AMHR2* comprise the extracellular domain of the receptor protein (233). Missense mutation P30S is located in exon 2 and, thus, likely affects ligand binding.

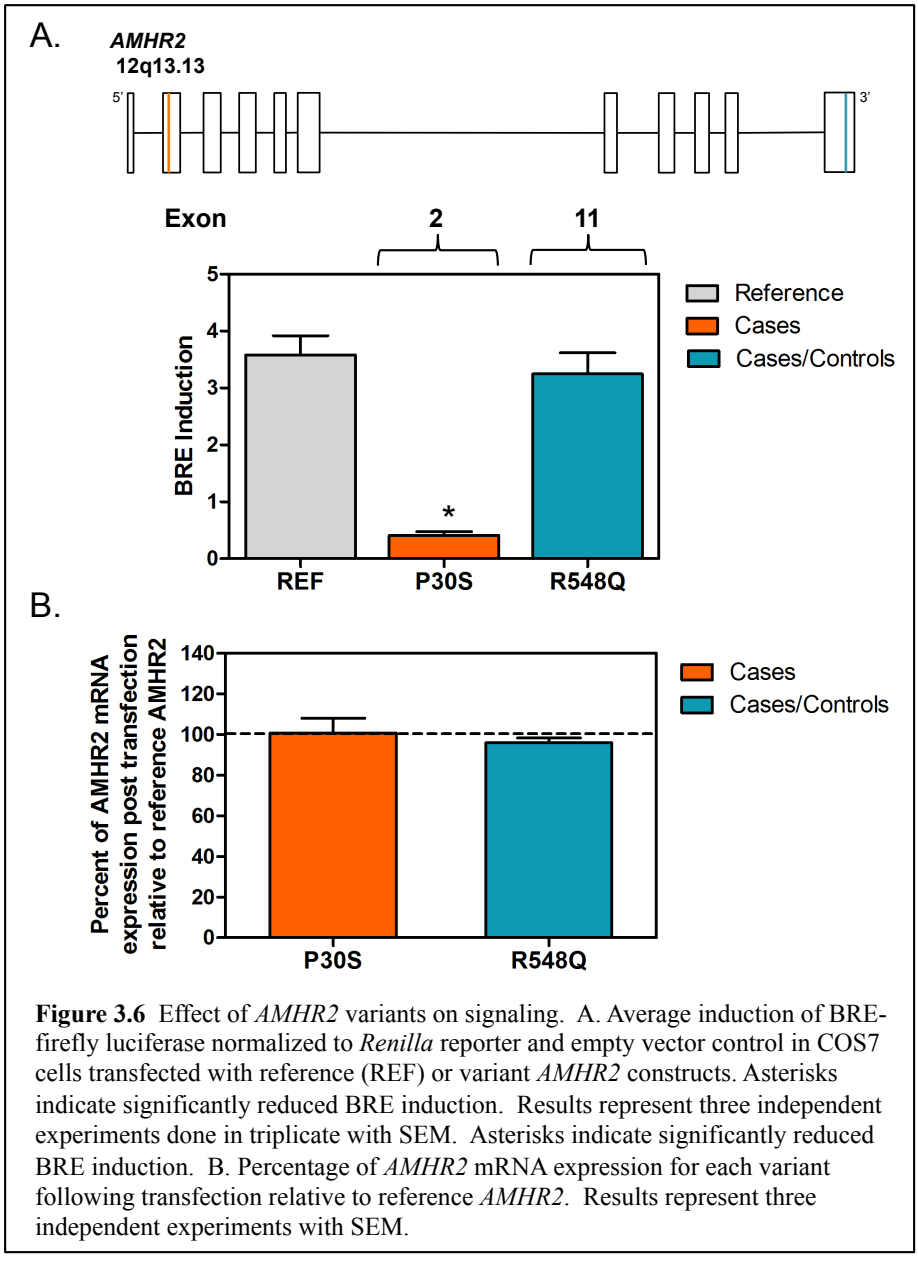

Figure 3.6 Effect of *AMHR2* variants on signaling. A. Average induction of BRE-firefly luciferase normalized to *Renilla* reporter and empty vector control in COS7 cells transfected with reference (REF) or variant *AMHR2* constructs. Asterisks indicate significantly reduced BRE induction. Results represent three independent experiments done in triplicate with SEM. Asterisks indicate significantly reduced BRE induction. B. Percentage of *AMHR2* mRNA expression for each variant following transfection relative to reference *AMHR2*. Results represent three independent experiments with SEM.

Given that *AMHR2* requires dimerization for proper signaling, we also tested whether variant P30S had a dominant-negative interaction with wild-type AMHR2. In transfection of reference *AMHR2* alongside variant P30S *AMHR2*, we observed an average increase of 45% signaling ability compared to P30S homozygous state (**Figure 3.7**). Therefore, our findings do not indicate a dominant-negative interaction between AMHR2 P30S mutant and wild-type AMHR2 *in vitro*.

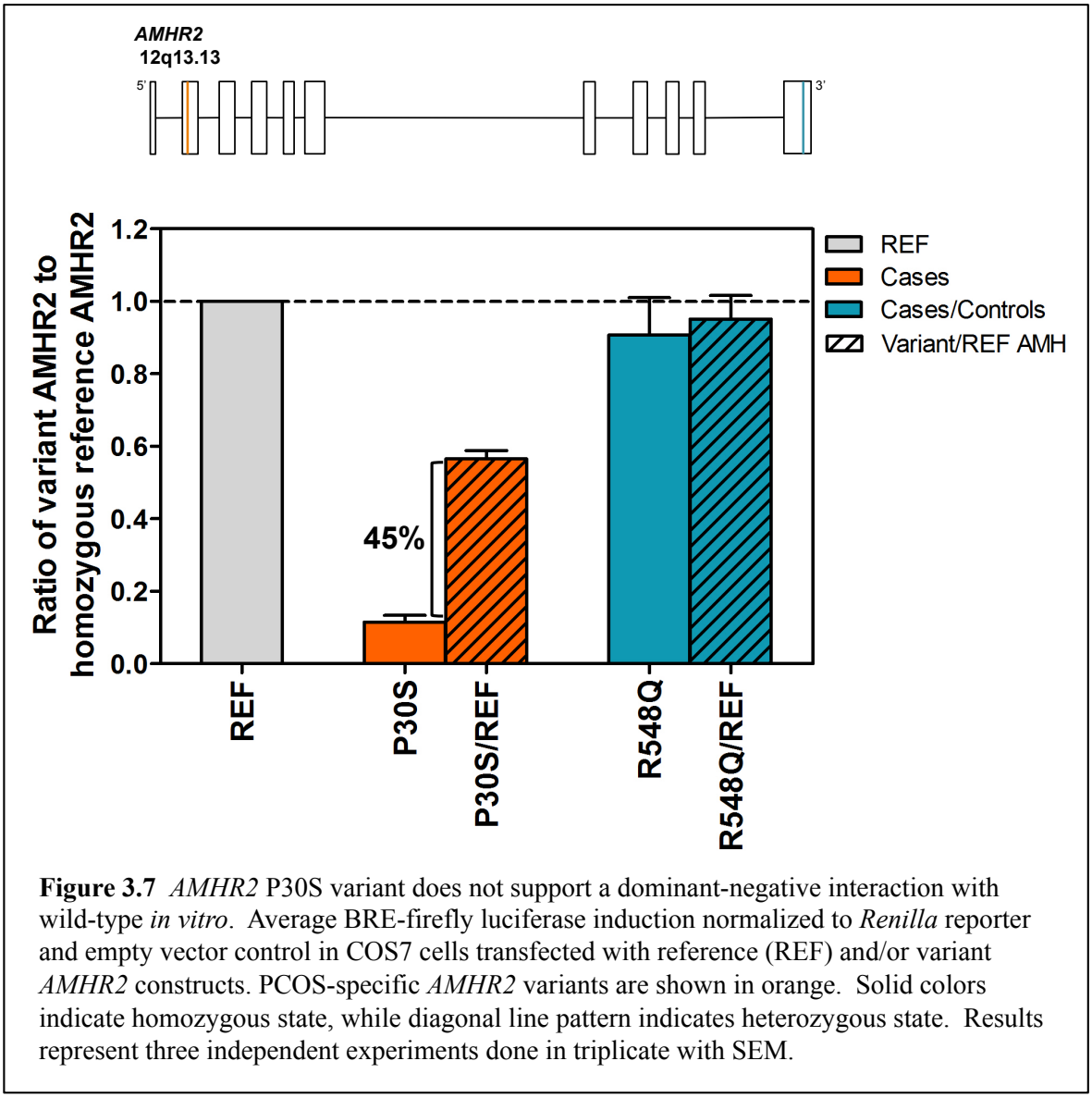

Figure 3.7 *AMHR2* P30S variant does not support a dominant-negative interaction with wild-type *in vitro*. Average BRE-firefly luciferase induction normalized to *Renilla* reporter and empty vector control in COS7 cells transfected with reference (REF) and/or variant *AMHR2* constructs. PCOS-specific *AMHR2* variants are shown in orange. Solid colors indicate homozygous state, while diagonal line pattern indicates heterozygous state. Results represent three independent experiments done in triplicate with SEM.

3.8 MATERIALS AND METHODS

Cell Culture

COS7 (African green monkey kidney fibroblast-like cell line, ATCC) cells were maintained in DMEM, high glucose + GlutaMAX (Thermo Fisher Scientific, Waltham, MA) containing 10% fetal bovine serum (Hyclone, Logan, UT) and stored in a 37°C incubator with 5% CO_2. MA-10 Leydig mouse cell line was maintained in DMEM:F12, 20 mM HEPES and 15% horse serum (Thermo Fisher Scientific Inc.). Plasticware used for culturing was coated with 0.1% gelatin (Attachment Factor Protein, Thermo Fisher Scientific) and incubated for 30 min in a 37°C incubator. Excess gelatin solution was aspirated prior to seeding cells.

AMH Plasmid Constructs

AMH coding region was PCR amplified from carriers of *AMH* variants using AmpliTaq Gold 360 Master Mix (Thermo Fisher Scientific Inc.) and forward and reverse primers, 5'-CACCATGCGGGACCTGCCTCT-3' and 5'-GTCACCGGCAGCCACACT-3' (Integrated DNA Technologies, Inc., Coralville, IA) respectively. PCR products were subcloned into pcDNA 3.1. The reference *AMH* (build GRCh37/hg19) construct (**Figure 3.8A**) was generated in parallel to variant constructs. Vector phRL-CMV (**Figure 3.8B**) was purchased and used as a co-transfected *Renilla* control vector (Promega Corporation, Milwaukee, WI). Each variant construct was verified using Sanger sequencing (**Figure 3.9**).

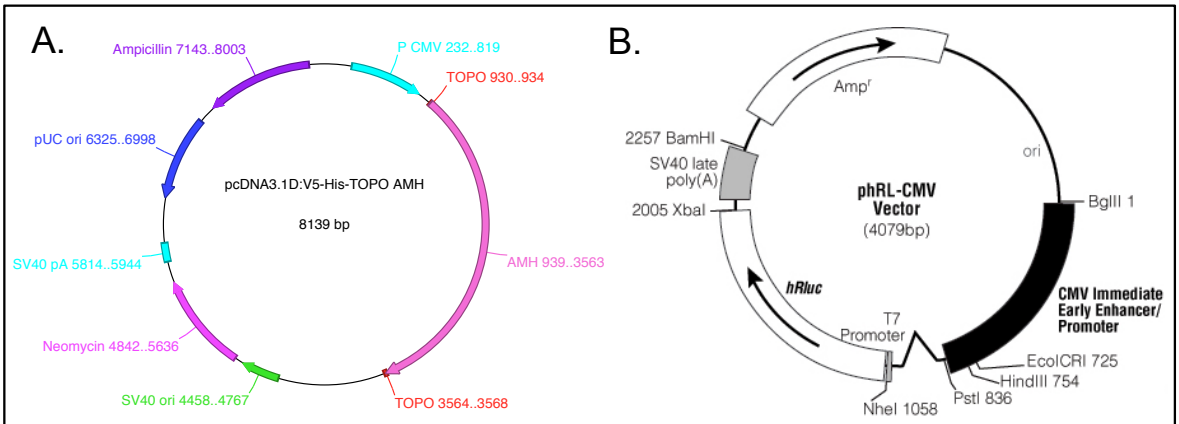

Figure 3.8 Plasmids used in dual luciferase reporter assay for coding variants. A. Reference and variant *AMH* sequences from subject genomic DNA were subcloned into pcDNA3.1D:V5-His-TOPO vector. B. Promega phRL-CMV co-transfected Renilla control vector. Promega Corporation (www.promega.com).

AMHR2 Plasmid Site-Directed Mutagenesis

To assess the functional impact of *AMHR2* coding variants, we used a human *AMHR2* cDNA expression construct (Sino Biological, Beijing, China). Reference sequence *AMHR2* cDNA construct was utilized in creating *AMHR2* variants P30S and R548Q. Q5 Site-Directed Mutagenesis (New England BioLabs, Ipswich, MA) was performed according to the manufacturer's protocol. Briefly, mutagenesis primers were designed using the NEBaseChanger v.1.2.7 (https://nebasechanger.neb.com/). Reverse primers and mutation containing forward primers were used in PCR amplification of mutated plasmid DNA. Using the Kinase, Ligase & DpnI (KLD) treatment mixture, the template (non-mutated) DNA was degraded, while mutated plasmid DNA was ligated and subsequently transformed into competent cells. Sequence of both *AMHR2* variant constructs was verified using Sanger sequencing (**Figure 3.9**).

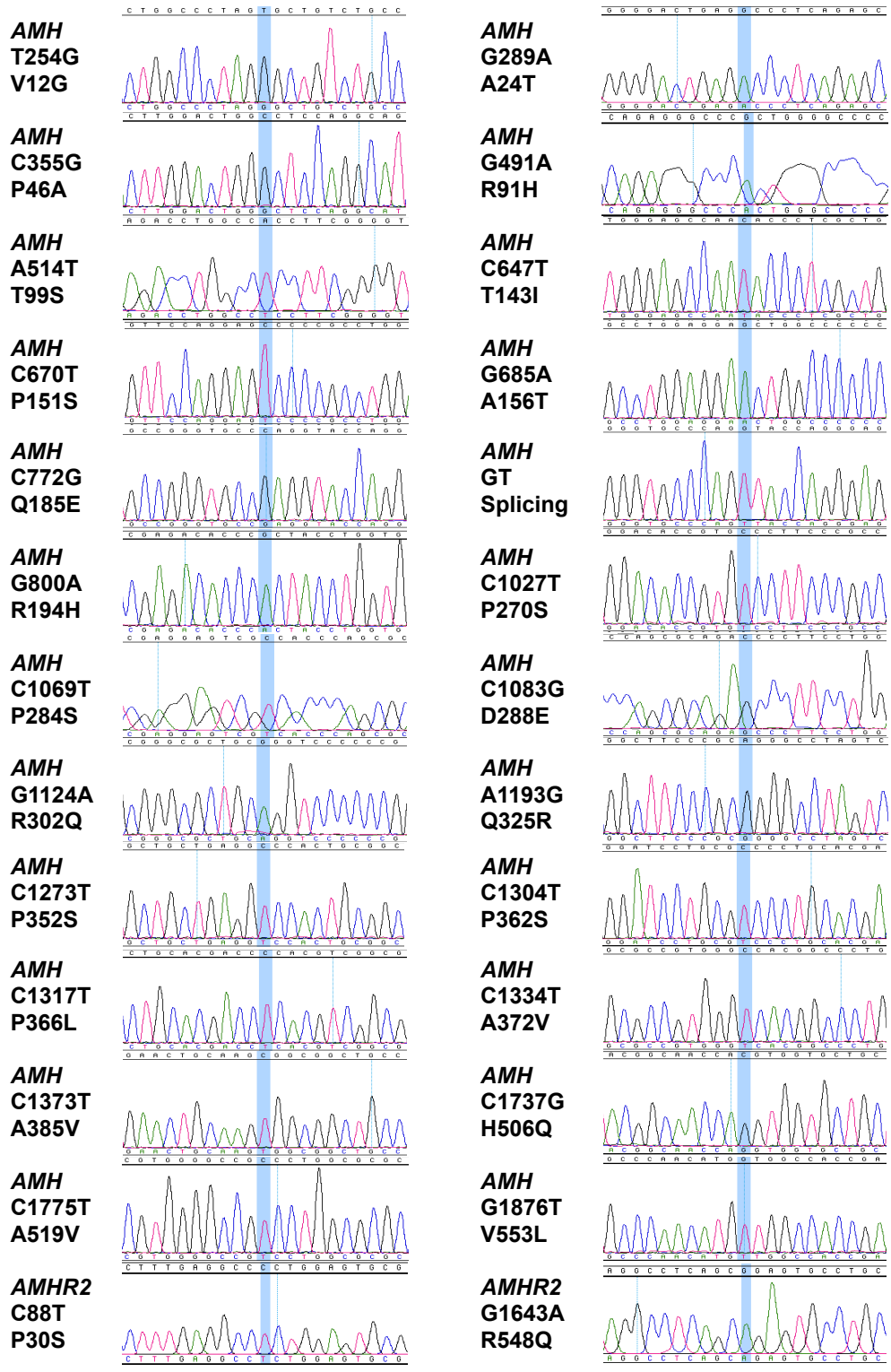

Figure 3.9 Sanger sequencing verification of *AMH* and *AMHR2* coding variant plasmids. Gene, mRNA and amino acid change are listed with each sequencing chromatogram. Variant location highlighted in blue. For mRNA base position, Nm_000479.3 was used for *AMH* and Nm_020547 for *AMHR2* transcript. See Tables 2.3 and 2.5 for additional variant information.

COS7 Cell Transfection and Dual Reporter Assay (Figure 3.10)

To quantify the signaling potential of *AMH* and *AMHR2* variants in their homozygous variant and heterozygous states relative to homozygous reference, we employed a dual luciferase reporter assay where binding to AMHR2 activates a firefly luciferase reporter (142). To test signaling potential of variants in a homozygous state, COS7 cells were transfected with each *AMH/AMHR2* variant or *AMH/AMHR2* reference sequence. To test variants in a heterozygous state for the possibility of a dominant-negative interaction, COS7 cells were transfected with equal concentration of reference and variant *AMH/AMHR2* constructs. COS7 cells were plated and transfected with *AMH* construct plus the rat *MISRII* cDNA expression construct (or human *AMHR2* cDNA expression construct), bone morphogenetic protein (BMP)-responsive element (BRE) firefly luciferase reporter and control *Renilla* luciferase reporter (phRL-CMV) (142). Cells were incubated for 48 h. Firefly and *Renilla* luciferase readings were obtained using the Dual-Luciferase Reporter Assay System (Promega Corporation, Milwaukee, WI) according to manufacturer's instructions and luminescence was measured with the Synergy 2 plate reader (BioTek, Winooski, VT). BRE induction of reference and variant *AMH/AMHR2* was calculated with emissions of firefly luciferase divided by *Renilla* luminescence and normalized to empty vector control. Two-tailed t-test was used on raw data to determine degree of significance between variant and reference activity. *P*-values<0.05 were noted as significant. Applied Biosystem TaqMan primers were used to quantify mRNA expression of *AMH* (Hs01006984_g1), *AMHR2* (Hs00179718_m1) and housekeeping gene *GAPDH* (Hs02758991_g1) to ensure the constructs were expressing variants comparable to reference.

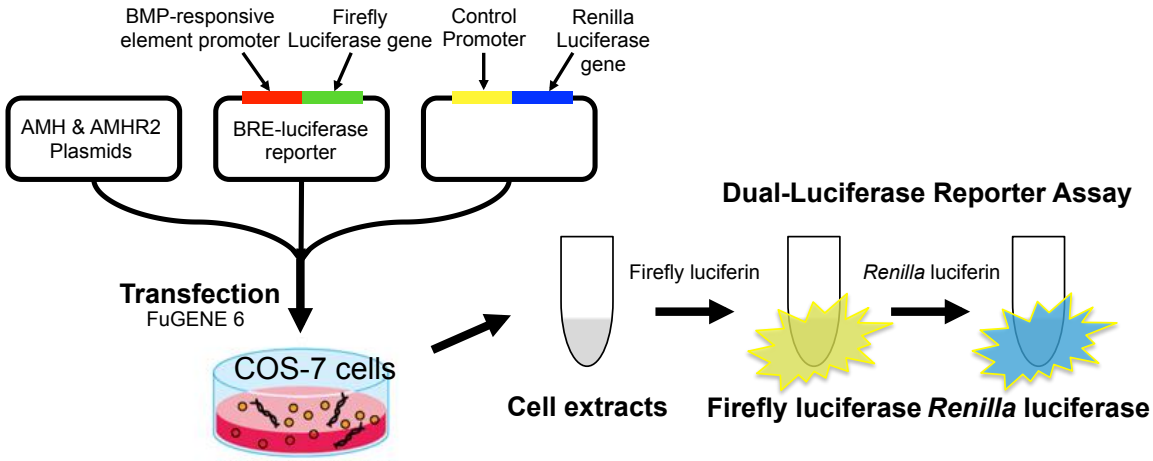

Figure 3.10 Procedure to test impact of *AMH* and *AMHR2* variants on signaling. (modified from http://photobiology.info/Ohmiya.html)

MA-10 Cell Transfection and Expression Analysis

AMH variants were also tested for their impact on *Cyp17a1* mRNA expression in the mouse Leydig cell line MA-10. Cells were plated at 200,000 cells per well in 12-well plates coated with 0.1% gelatin (Attachment Factor Protein, Thermo Fisher Scientific Inc.) and transfected 24 hours later with the vector only control, reference or variant *AMH* plasmids (constructs used in previous signaling studies). Transfection reagent Lipofectamine 2000 was used (Thermo Fisher Scientific Inc.). Cells were also stimulated with 50 µM cAMP (Sigma-Aldrich) at the time of transfection. 48 hours post transfection cells were collected, RNA isolated and reverse transcribed. RNA was extracted using the RNeasy Plus Mini kit (Qiagen) following the manufacturer's protocol. mRNA was then reverse transcribed to cDNA yielding final concentrations of 100 ng/µL using the High Capacity Reverse Transcription kit (Applied Biosystems). The cDNA was used to perform qRT-PCR using Taqman Fast Advanced Master Mix (Thermo Fisher Scientific Inc.) to measure *Cyp17a1* expression relative to *AMH* and

housekeeping gene *Gapdh*. Applied Biosystem TaqMan primers were used to quantify mRNA expression of *Cyp17a1* (Mm00484040_m1), *AMH* (Hs01006984_g1) and *Gapdh* (Mm99999915_g1).

Association Testing

To evaluate the significance of functional *AMH* variants in PCOS, we used a gene based burden test approach (234) and combined all functional *AMH* variants into one statistical test. We tested for association between functional *AMH* variants and PCOS using two independent control groups: the 165 control women that were sequenced in this study and population-based controls. Population-based allele frequencies for each rare variant were obtained from one of the following databases: Genome Aggregation Database (gnomAD, Eurpean Non-Finnish population frequency when available) (http://gnomad.broadinstitute.org/), ExAc Aggregated Populations cohort (http://exac.broadinstitute.org), or 1000Genomes European ancestry cohorts (http://www.1000genomes.org) as noted in each table. Evidence for genetic association was evaluated using Chi-Square statistic.

3.9 CONCLUSIONS

In summary, we identified 17 coding and splice site variants in *AMH* and 1 coding variant in *AMHR2* with reduced signaling potential in 25 women with PCOS. No such variants were observed in unaffected control women. Thus, rare genetic variants do contribute to the pathogenesis of PCOS and account for some of the heritability not explained by the common PCOS susceptibility variants identified in GWAS. Furthermore, no evidence for association with PCOS in the *AMH* genomic region was detected in GWAS studies of PCOS (53, 54)

underscoring the need of rare variant screens in parallel with GWAS to detect the full spectrum of PCOS associated genetic variation. It is our hypothesis that these *AMH* and *AMHR2* mutations lead to the PCOS phenotype by abrogating AMH's transcriptional inhibition of CYP17 role in androgen biosynthesis, resulting in hyperandrogenemia (**Figure 3.5**). In support of this, we found that 17 *AMH* variants were unable to inhibit *Cyp17a1* expression to the extent of reference *AMH* in an *in vitro* cell model. Our findings provide a novel mechanism for the characteristic increase in circulating AMH levels in PCOS, decreased bioactivity of the molecule. Further, they implicate the AMH signaling pathway in the pathogenesis of PCOS.

CHAPTER 4

FUNCTIONAL NONCODING VARIANTS IN MEMBERS OF THE ANTI-MÜLLERIAN HORMONE (AMH) PATHWAY

4.1 OVERVIEW

Genetic variants in *AMH* and *AMHR2* regulatory elements that decrease gene transcription are predicted to have a similar phenotypic effect as *AMH* and *AMHR2* coding variants that reduce AMH bioactivity. Here, we tested this hypothesis (**Figure 2.1C**) by filtering sequence data for quality, rare (MAF<0.01) noncoding variation in *AMH* and *AMHR2*. *In silico* methods, such as CADD, FATHMM-MKL and transcription factor motif analyses, where used to rank and prioritize variants for functional follow-up. For noncoding variants in or near *AMH*, variants in the proximal promoter region were of greatest interest based on deleteriousness scoring metrics. High priority noncoding variants in or near *AMHR2* were also upstream and in the proximal promoter region as well as the first intron. Five *AMHR2* high priority variants in these regions also caused a gain or loss of transcription factor binding motif. Intronic variants of *AMHR2* were also evaluated for alternative splicing. All 3 of the tested *AMH* noncoding PCOS-specific variants as well as 16 out of the 20 tested *AMHR2* noncoding PCOS-specific variants showed a significant reduction in signal compared to reference, measured by dual luciferase reporter assays. We have found that noncoding variation in members of the AMH pathway may also negatively impact AMH signaling by disrupting regulatory elements or canonical splicing.

4.2 FUNCTIONAL PCOS-SPECIFIC NONCODING VARIANTS UPSTREAM OF AMH

We performed CADD and FATHMM-MKL analyses to computationally predict the functional impact of *AMH* noncoding variants. Given that FATHMM-MKL has been reported to be more effective for predicting the functional consequences of noncoding variants compared to CADD C-scores (184), we decided to rank variants based on FATHMM-MKL *P*-values. The top ranked variants were PCOS-specific variants located in the proximal promoter of *AMH* (**Table 4.1**).

The top 3 variants (chr19:2249171 C>G, rs746807694, rs777832730) were chosen for functional follow-up as well as a non-PCOS specific variant (rs186422293) as a positive control. The 3 selected PCOS-specific variants were found in 1 case each and subjects were heterozygous for these variants. Non-PCOS specific variant rs186422293 was found in 7 PCOS cases and 2 controls and ranked less damaging in both FATHMM-MKL *P*-value and CADD C-scores (**Table 4.1**). The 3 tested PCOS-specific *AMH* noncoding variants all significantly reduced Firefly luciferase signal in ovary CHO-K1 cells compared to reference sequence control (chr19:2249171 C>G, P=2.44x10^{-10}; rs746807694, P=2.04x10^{-10}; rs777832730, P=2.42x10^{-10}), while the non-PCOS specific variant (rs186422293, P=0.34) showed no change (**Figure 4.1**).

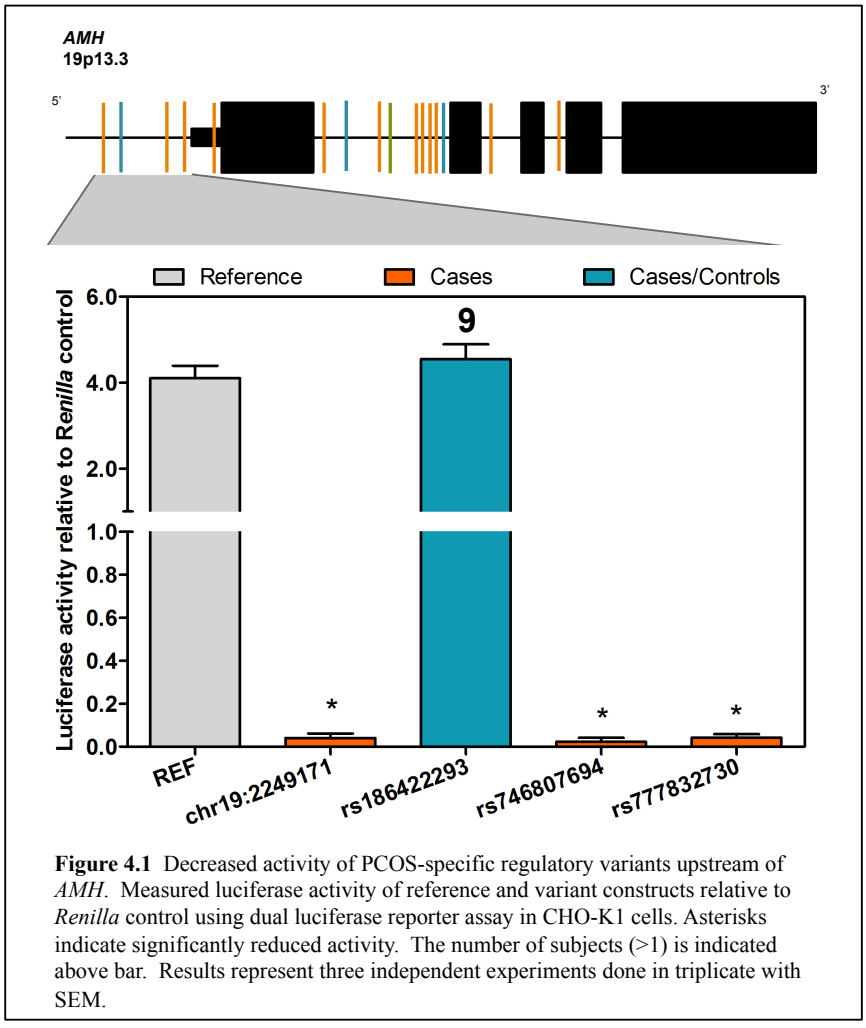

Figure 4.1 Decreased activity of PCOS-specific regulatory variants upstream of *AMH*. Measured luciferase activity of reference and variant constructs relative to *Renilla* control using dual luciferase reporter assay in CHO-K1 cells. Asterisks indicate significantly reduced activity. The number of subjects (>1) is indicated above bar. Results represent three independent experiments done in triplicate with SEM.

Reference and variant *AMH* constructs were also transfected into COS7 (African green monkey kidney fibroblast-like) cells during optimization stages. However, very low signal was seen with the use of this cell line even for reference *AMH*. Therefore, it is important to note that regulatory element activity is likely tissue specific and requires the presence of relevant transcription factors and machinery. CHO-K1 cells are ovarian derived and may have more of the relevant transcriptional machinery.

TFs that bind to the *AMH* promoter to influence activity in male Sertoli cells include SF-1, SOX9 and GATA4 (235, 236). Interactions of SF-1 and SOX8, SOX9, Wilms' tumor 1 (WT1), DAX-1, GATA4, and NF-κB in regulating the transcription of *AMH* in Sertoli cells during fetal development, has been relatively well-described (237-242). AMH has also been identified as a target gene of SF-1 in human granulosa cells (243). Additionally, transcriptional regulation of *AMH* by SF-1 involves the crucial role of FOXL2 as an essential factor (243). While variants that we identified in the proximal promoter of *AMH* did not directly impact known TF binding sites, they still demonstrated a significant functional impairment.

4.3 DELETERIOUS NONCODING AMHHR2 VARIANTS DISRUPT TRANSCRIPTION FACTOR BINDING MOTIFS

CADD and FATHMM-MKL analyses were also performed to predict the functional consequences of *AMHR2* noncoding variants. In parallel, we computationally predicted the regulatory impact of *AMHR2* noncoding variants by measuring differences in transcription factor (TF) binding affinities between alleles. Position weight matrices (PWMs) derived from ENCODE ChIP-Seq experiments (244, 245) were used to ascertain the statistical significance of single base changes on TF binding affinities, which thus suggested the relative regulatory impact

of each noncoding variant. TFs with known expression in ovarian tissues were utilized in the analyses. Congruently, noncoding variants were ranked by FATHMM-MKL *P*-values (184) and were comparable with their impact on TF binding motifs. The top 4 ranking FATHMM-MKL variants (**Table 4.2**) also disrupted TF binding motifs (**Figure 4.2**). PCOS-specific variant rs784894, located in intron 1 of *AMHR2*, resulted in the gain of CCDC6 binding motif (**Figure 4.2A**) and ranked as the most deleterious noncoding variant with FATHMM-MKL prediction (*P*-value=0.953, **Table 4.2**). Rs784894 was identified in 3 PCOS-affected cases. PCOS-specific variant rs777964297, mapping upstream of the *AMHR2* transcription start site, created a MYC binding site (**Figure 4.2B**) and was found in 1 PCOS subject (**Table 4.2**). Non-PCOS specific variant rs148189358, also upstream of *AMHR2*, caused the loss of SP1 binding site (**Figure 4.2C**). This particular variant was found in 7 PCOS cases and 3 control subjects (**Table 4.2**). Additionally, PCOS-specific variant rs777265708 was found to disrupt a c-MAF binding motif (**Figure 4.2D**) in intron 1 of *AMHR2* in a single PCOS case (**Table 4.2**).

Using UCSC genome browser (https://genome.ucsc.edu/), regions of *AMHR2* were also evaluated for chemical modifications and DNase hypersensitivity clusters that signify important areas of gene regulation and TF binding. A region upstream of the *AMHR2* transcription start site indicated marks of mono-methylation of lysine 4 of the H3 histone protein as well as a peak for acetylation of lysine 27 of the H3 histone protein (**Figure 4.3**). These marks have been associated with enhancer and insulator regions of gene regulation. Of the *AMHR2* noncoding variants identified in our cohort, 3 PCOS-specific variants and 1 non-PCOS specific variant mapped to this region (**Figure 4.3**). Furthermore, PCOS-specific variant rs866630130 resulted in the loss of an EBF1 binding site, which was also identified in the TF motif analyses (**Figure 4.4**).

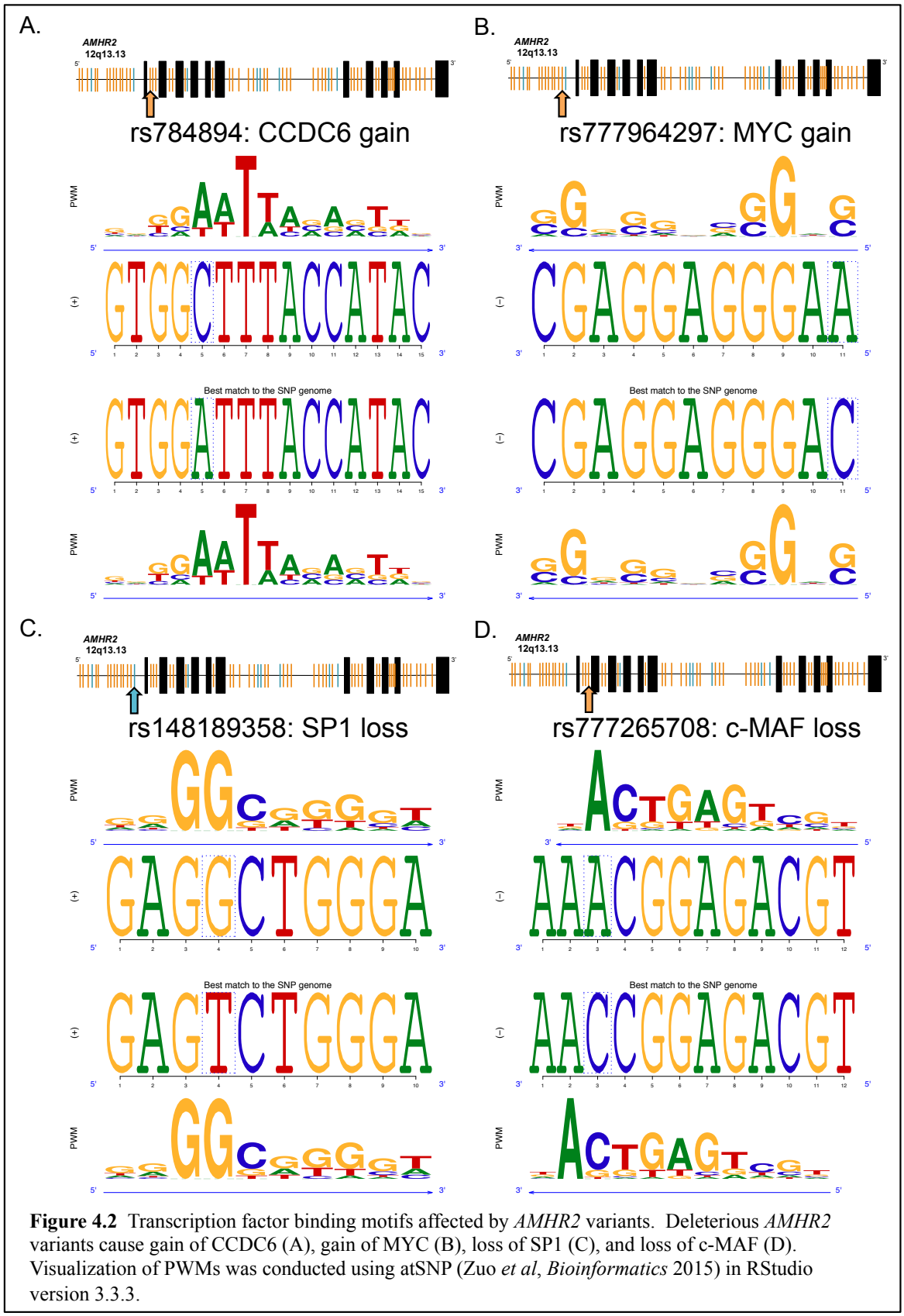

Figure 4.2 Transcription factor binding motifs affected by *AMHR2* variants. Deleterious *AMHR2* variants cause gain of CCDC6 (A), gain of MYC (B), loss of SP1 (C), and loss of c-MAF (D). Visualization of PWMs was conducted using atSNP (Zuo *et al*, *Bioinformatics* 2015) in RStudio version 3.3.3.

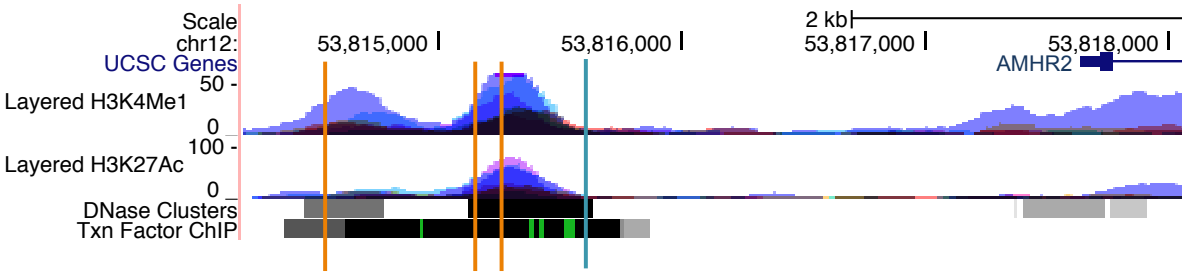

Figure 4.3 Variants in regions of chemical modifications upstream of *AMHR2*. Four PCOS-specific variants shown in orange (from left to right; chr12:53814515, chr12:53815129, rs866630130) and one non-PCOS specific variant shown in teal (rs181566505). UCSC Genome Browser (https://genome.ucsc.edu/).

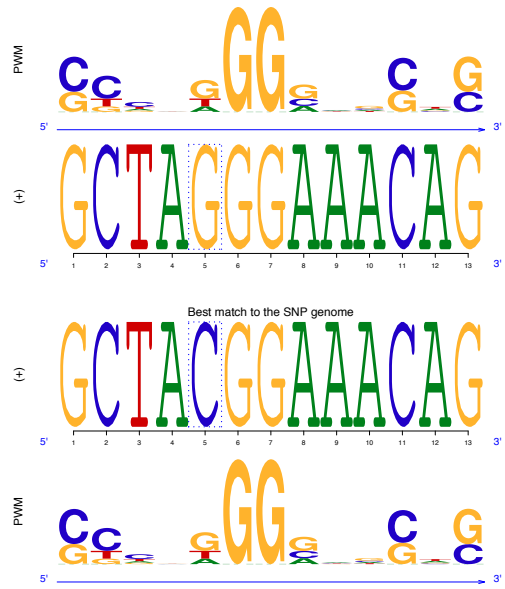

Figure 4.4 Variant rs866630130 causes loss of EBF1 transcription factor binding site. Visualization of PWMs was conducted using atSNP (Zuo *et al*, *Bioinformatics* 2015) in RStudio version 3.3.3.

4.4 FUNCTIONAL PCOS-SPECIFIC NONCODING VARIANTS OF AMHR2

The 6 top scoring variants by FATHMM-MKL were chosen for functional assessment via dual luciferase reporter assay. Additionally, given that the region upstream of *AMHR2* (**Figure 4.3**) may contain insulator and/or weak promoter regulation for *AMHR2* expression, we decided to also determine the functional impact of these variants despite having low priority FATHMM-MKL and CADD scores (**Table 4.2**). Therefore, we decided to functionally evaluate a total of 10 variants (8 PCOS-specific and 2 non-PCOS specific) based on predictive *in silico* tools and regions observed to be associated with chemical modifications.

Each regulatory region (of *AMHR2* reference and variant-containing sequence) was subcloned into a vector backbone containing a minimal promoter and Firefly luciferase gene. Constructs were transfected into mouse ovarian cells (CHO-K1). Firefly luciferase readings determined the relative activity of variant *AMHR2* region compared to reference *AMHR2* normalized to *Renilla* control. Three PCOS-specific variants upstream of *AMHR2*, that were located in regions of higher methylation and acetylation activity, showed a significant reduction in luminescence emissions compared to reference (chr12:53814515 A>T, P=1.32x10^{-7}; chr12:53815129 A>T, P=1.45x10^{-7}; rs866630130, P=1.56x10^{-7}), while non-PCOS specific variant, rs181566505, showed no significant change compared to reference (**Figure 4.5**). Three variants in the proximal promoter region of *AMHR2* were also tested for functional impact. PCOS-specific variant (chr12:53817187 A>G) was the only variant in this region to have significantly reduced signal (P=1.13x10^{-7}, **Figure 4.6**). Lastly, the 3 PCOS-specific *AMHR2* variants in intron 1 also significantly reduced signal compared to reference *AMHR2* (rs784894, P=3.31x10^{-5}; chr12:53817971 G>A, P=2.63x10^{-2}; rs777265708, P=3.06x10^{-5}, **Figure 4.7**).

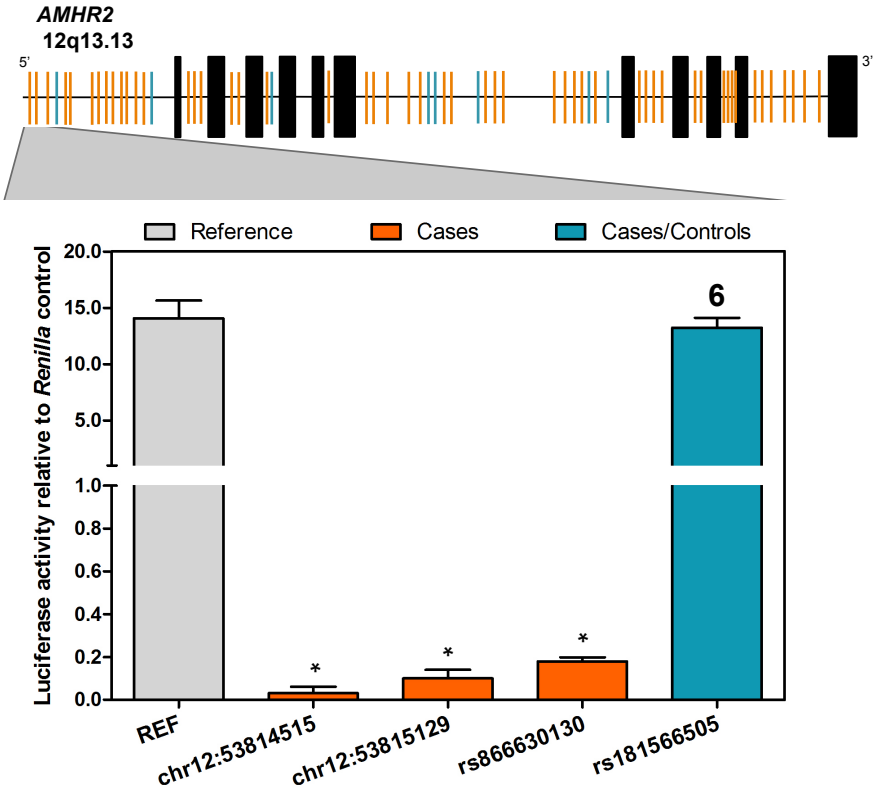

Figure 4.5 Decreased activity of PCOS-specific regulatory variants upstream of *AMHR2*. Measured luciferase activity of reference and variant constructs relative to *Renilla* control using dual luciferase reporter assay in CHO-K1 cells. Asterisks indicate significantly reduced activity. The number of subjects (>1) is indicated above bar. Results represent three independent experiments done in triplicate with SEM.

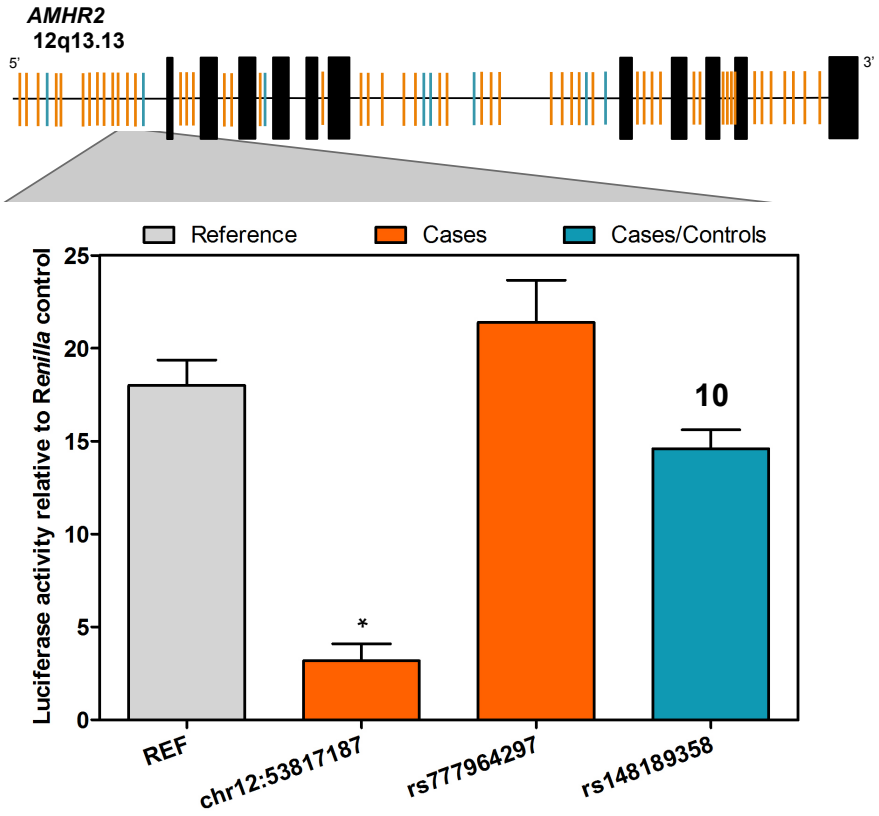

Figure 4.6 Activity of PCOS-specific regulatory variants near proximal promoter of *AMHR2*. Measured luciferase activity of reference and variant constructs relative to *Renilla* control using dual luciferase reporter assay in CHO-K1 cells. Asterisks indicate significantly reduced activity. The number of subjects (>1) is indicated above bar. Results represent three independent experiments done in triplicate with SEM.

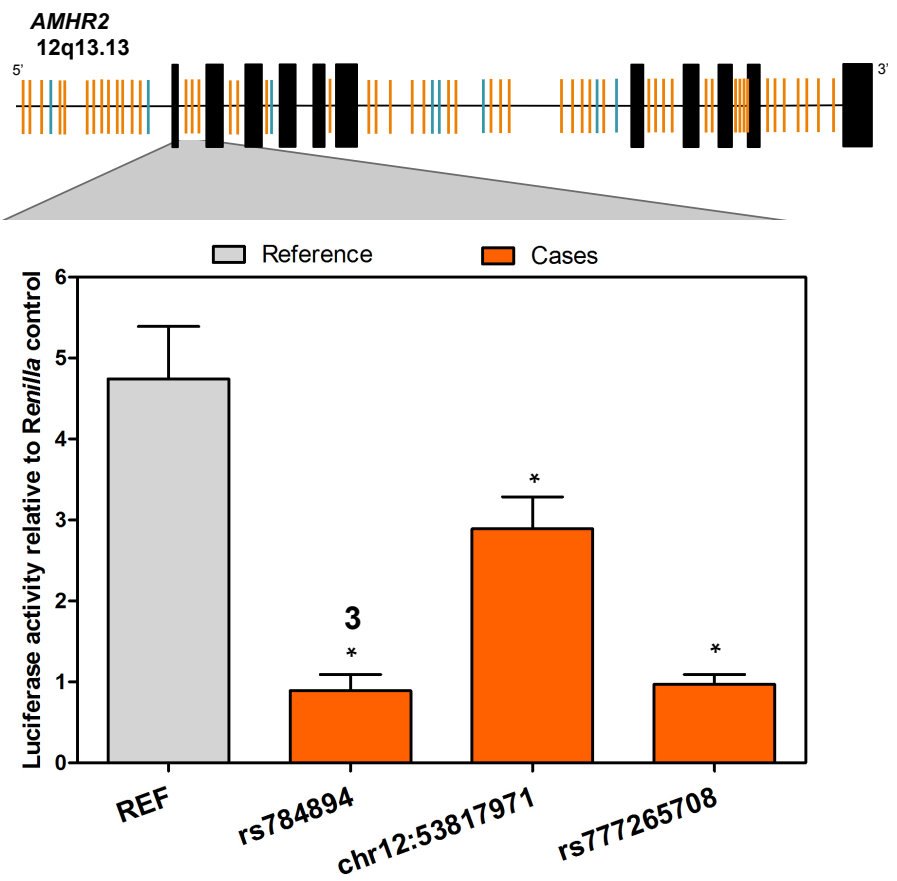

Figure 4.7 Decreased activity of PCOS-specific regulatory variants in intron 1 of *AMHR2*. Measured luciferase activity of reference and variant constructs relative to *Renilla* control using dual luciferase reporter assay in CHO-K1 cells. Asterisks indicate significantly reduced activity. The number of subjects (>1) is indicated above bar. Results represent three independent experiments done in triplicate with SEM.

Intriguingly, not all variants that showed a functional defect had a deleterious score from CADD and/or FATHMM-MKL analyses (chr12:53814515 A>T, chr12:53817971 G>A). Studies in clinical diagnostics have emphasized that pathogenicity ratings based on statistical online protein prediction programs must be used with caution in the absence of functional studies (246, 247). Even with extensive data on sequence conservation, protein structure, amino acid properties, etc. it remains a challenge to accurately predict whether coding and noncoding variants result in functional changes or if they are unremarkable polymorphisms (247). On the

flip side, not all variants with CADD C-scores>15 and FATHMM-MKL *P*-values>0.5 resulted in a functional impact (chr12:53815561 T>G, rs777964297, rs148189358), at least under tested conditions. It is possible that these variants may still have deleterious effects by means unable to be detected in our experimental system. Yet, it is also possible that although variants ranked as highly damaging they may, in fact, be benign. These varied results support what we previously observed with coding *AMH* variants, where even known PMDS-associated variants had low CADD and FATHMM-MKL scores. Prediction tools for variant deleteriousness are certainly beneficial in directing follow-up studies; however, our results also indicate that variants should be studied with molecular tests. Consequently, the accumulation of functional data for variants may help in refining algorithms and increase confidence levels in prediction tools.

Similarly, variants that result in TF binding motif changes may not necessarily have an impact on expression. For example, 5 of the 10 *AMHR2* variants tested were found to change specific TF binding sequences. No significant changes in signal were seen with the gain in TF MYC site (rs777964297) and loss of an SP1 site (rs148189358). *MYC* is a proto-oncogene and its encoded nuclear phosphoprotein is important in cell cycle progression, apoptosis and cellular transformation (248). Abnormal MYC expression is often seen in numerous human cancers (249). We observed a slight trend in increased activity compared to reference, however not enough to be significant. *SP1* encodes a zinc finger TF and is present in all mammalian cell types (250, 251). The loss of SP1 TF site had no affect on the activity of the promoter region of *AMHR2* in our assay, and thus may not be necessary for *AMHR2* gene regulation. Transcription factors shown to bind regions of the *AMHR2* promoter have thus far included SF-1 (252) and Wilms' tumor protein Wt1 (253). The absence of extensive *AMHR2* transcriptional regulation

studies in female cells has caused mechanisms and TFs of *AMHR2* regulation to remain poorly understood.

On the other hand, 3 PCOS-specific variants that caused a loss of EBF1 TF motif (rs866630130), gain of CCDC6 TF binding site (rs784894) and loss of c-MAF TF motif (rs777265708), showed significant reductions in luciferase expression in CHO-K1 cells. EBF1 activity plays an important role in the epigenetic and transcriptional events during B-cell programming (254), however little is known regarding additional regulatory functions of EBF1 within the ovary. *CCDC6* encodes a coiled-coil domain-containing protein, which functions as a tumor suppressor (255). The c-MAF protein is a DNA-binding, leucine zipper-containing TF (256) and has been implicated, with MAFB, in mouse gonadal morphogenesis (257). While specific functions of these TFs still remain unclear especially in cells of the ovary, their role or lack there of may be associated with altered *AMHR2* expression in PCOS women.

4.5 INTRONIC VARIANTS IN AMHR2 SHOW SPLICING DEFECTS

Given the evidence of multiple *AMHR2* mRNA transcripts and possible alternative splicing of exons 9 and 10 (258), we evaluated 12 PCOS-specific rare noncoding variants in introns 8, 9 and 10 for potential effect on canonical splicing patterns and AMH signaling (**Table 4.3**). Generated *AMHR2* constructs, with reference and variant sequence, were utilized in performing the previously described dual luciferase reporter (DLR) assay measuring BRE induction (**Figure 3.10**). We observed significantly decreased AMH signaling with 9 out of the 12 *AMHR2* variants (**Figure 4.8**, **Table 4.3**). Certain variants showed more drastic reduction than others, namely rs745713994, rs200284824, rs186948808, rs190814349 and chr12:53824544 G>T (**Figure 4.8**, **Table 4.3**).

We further wanted to assess whether the observed reduction in signaling activity was due to *AMHR2* splicing abnormalities. Following RNA isolation and reverse transcription, we performed RT-PCR to measure *AMHR2* expression. Primers that spanned various exon junctions of interest were used to determine defects in transcript splicing (**Figure 4.9A**). We found 4 variants (rs200284824, rs186948808, rs190814349 and chr12:53824544 G>T) to have no expression of *AMHR2* when using primers that spanned exons 8/9, 9/10 and 10/11 (**Figure 4.9A**). In parallel, cDNA was amplified by PCR using primers that spanned from *AMHR2* exon 7 to exon 11 to determine any changes in transcript size (**Figure 4.9B**). We found altered PCR amplicon size with the same 4 *AMHR2* variants (rs200284824, rs186948808, rs190814349 and chr12:53824544 G>T) compared to *AMHR2* reference (**Figure 4.9C**). These variants showed alternative splicing of *AMHR2* resulting in the deletion of exons 9 and 10 (**Figure 4.9B,C**). Similar splicing defects that cause Amhr2Δ9/10 in mice have also been shown to significantly reduce AMH signaling and, further, have demonstrated a dominant-negative impact on wild-type

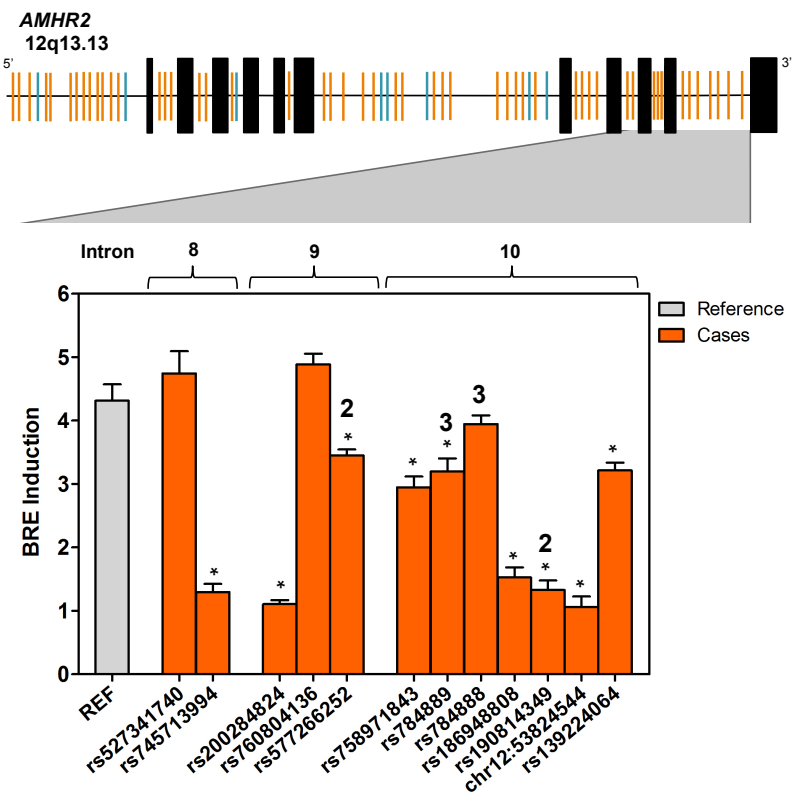

Figure 4.8 Effect of intronic *AMHR2* variants on signaling ability. Average induction of BRE-firefly luciferase normalized to *Renilla* reporter and empty vector control in COS7 cells transfected with reference (REF) or variant *AMHR2* constructs. Results represent three independent experiments done in triplicate with SEM. Asterisks indicate significantly reduced BRE induction. The number of subjects (>1) is indicated above BRE induction bar.

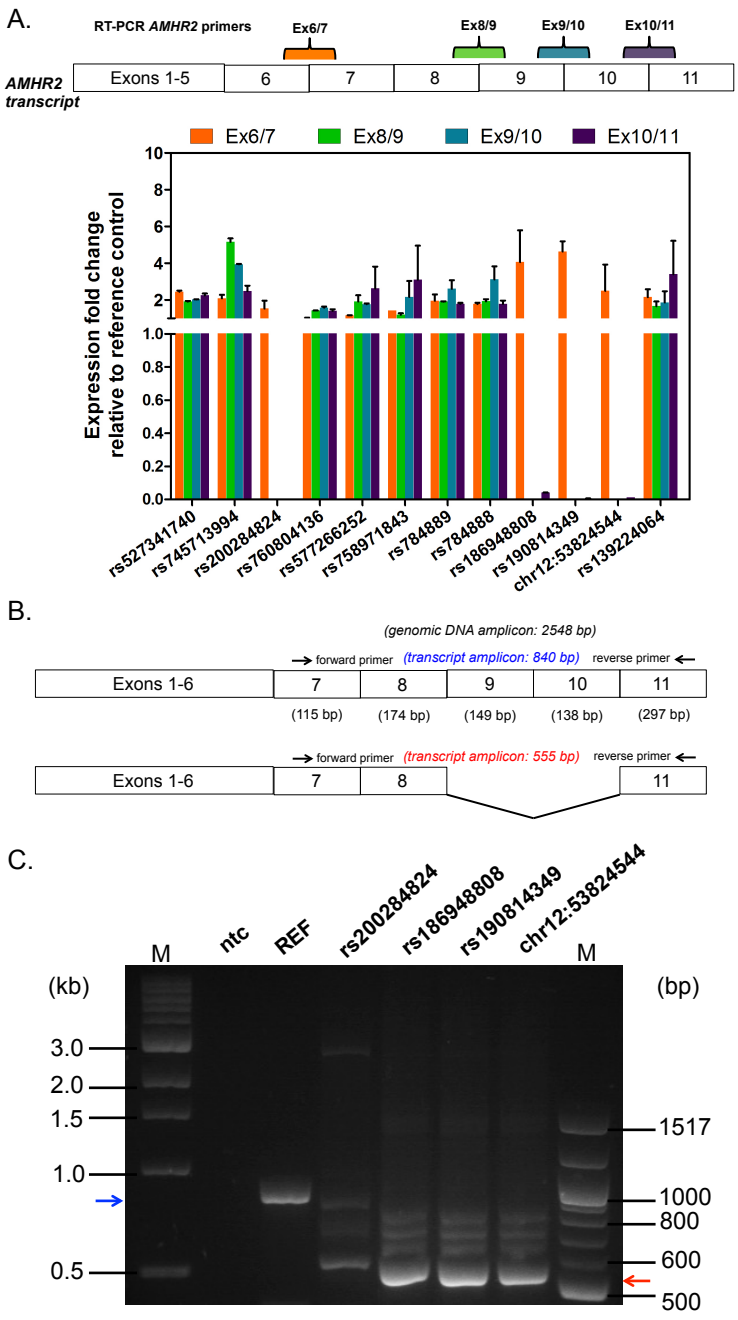

Figure 4.9 Intronic *AMHR2* variants affect canonical splicing patterns. A. Real-time PCR fold change expression (2^-ΔΔCt) of *AMHR2* variant expression compared to reference (reference=1). Taqman primers with 4 different *AMHR2* exon junctions were used to measure expression. Measurement of *AMHR2* exon junction 6/7 shown in orange, exon junction 8/9 in green, exon junction 9/10 in blue and exon junction 10/11 in purple. Diagram of exons not drawn to scale. Results show experiments run in duplicate with SEM. B. Graphic of transcript *AMHR2* exons showing number of base pairs (bp) plus forward and reverse primers for PCR amplification illustrated in C panel. Genomic DNA and transcript amplicon sizes indicated for normal *AMHR2* and alternatively spliced *AMHR2*. C. Gel electrophoresis of PCR amplicons from reference *AMHR2* (REF) and variant *AMHR2* (variants indicated above each lane). Negative no template control (ntc) is shown in first lane. Blue arrow indicates normal amplicon size of 840 bp. Red arrow indicates alternative spliced amplicon of 555 bp with exon 9 and 10 deletion. Marker (M) sizes are given in kilobases (kb) and base pairs (bp).

AMHR2 (258). Additionally, variant rs200284824 suggested splicing inefficiencies resulting in intron retention seen by the PCR amplicon band at ~2.5 kb (**Figure 4.9C**). The variant that did not display abnormalities in *AMHR2* splicing but substantially reduced AMH signaling in the DLR assay (rs745713994) likely affects *AMHR2* activity by other mechanisms that cause transcript instability. While DLR assay results for variants rs577266252, rs758971843, rs784889 and rs139224064 reached statistical significance with p-values below 0.05 (**Table 4.3**), their bioactivity is relatively similar to wild-type.

4.6 MATERIALS AND METHODS

Prediction and Prioritization of Variant Deleteriousness

Combined Annotation Dependent Depletion (CADD) (180) and Functional Analysis through Hidden Markov Models - Multiple Kernel Learning (FATHMM-MKL) (184) analyses are quantitative *in silico* prediction tools that can be used for scoring deleteriousness of variants based on multiple annotations/features integrated into one metric. A CADD C-score>15 and a FATHMM-MKL *P*-value >0.5 are generally considered deleterious. These analyses were performed for rare variants identified in our cohort of PCOS cases and reproductively normal controls. Both scores from CADD and FATHMM-MKL were considered in prioritizing variants, however we ranked and weighed FATHMM-MKL scores more heavily, since they have been suggested as more reliable for noncoding variant predictions (184).

Motif Analyses

For each *AMHR2* noncoding variant, we calculated TF predicted binding affinities for each subsequence overlapping the single nucleotide polymorphism (SNP) position in either strand within a ±20bp window. Binding affinity scores were computed from the ENCODE PWMs, which consist of the nucleotide frequencies observed at each position in different TF binding sites. Each binding affinity score equals the sum of the logged frequencies for a given sequence across a motif PWM. Each binding p-value was defined as the probability that a sequence sampled from a genomic background distribution has an affinity score ≥ largest affinity score produced from one of the tested subsequences. Genomic background sequences were generated using a first order Markov model (259). We also determined the significance of changes in binding affinity scores between reference and SNP alleles by assessing whether the differences

in binding affinity scores or relative rank between the two alleles was significantly different than what would be expected by chance (260, 261). P-values were adjusted to account for multiple testing using the Benjamini-Hochberg (BH) procedure (262).

Once binding affinities were calculated for each TF at each noncoding variant, additional filtering identified the most likely candidates for TF binding site disruption or generation. Only instances in which the predicted TF binding affinity score was ≥60% of the maximum affinity score for the given TF motif was considered (263). Variants in which both the reference and SNP alleles were predicted to bind a particular TF with statistical significance were removed from consideration. Furthermore, we only considered TFs that are expressed in the ovary with tissue-specific gene expression determined using GTEx data (264) (Reads Per Kilobase of transcript per Million mapped reads (RPKM) ≥0.1). In addition to enabling quantitative analyses, PWMs were used to visualize regulatory SNP affects using atSNP (261) in RStudio version 3.3.3 (**Figures 4.2 and 4.4**, http://www.rstudio.com/).

Cell culture

CHO-K1 cells (ovarian Chinese hamster (*Cricetulus griseus*) epithelial-like cell line, ATCC) were maintained in F-12K (Thermo Fisher Scientific Inc.) containing 10% fetal bovine serum (Hyclone, Logan, UT) and stored in a 37°C incubator with 5% CO_2. COS7 (African green monkey kidney fibroblast-like cell line, ATCC) cells were maintained in DMEM, high glucose + GlutaMAX (Thermo Fisher Scientific, Waltham, MA) containing 10% fetal bovine serum (Hyclone, Logan, UT) and stored in a 37°C incubator with 5% CO_2.

Noncoding AMH and AMHR2 Plasmids and Site-Directed Mutagenesis

To determine the functional impact of noncoding variants, noncoding sequences were synthesized and subcloned into a vector containing a minimal promoter. Custom gene synthesis was preformed by Biomatik (Cambridge, ON, Canada) for proximal promoter *AMH* (chr19:2249100-chr19:2249331), upstream *AMHR2* (chr12:53814453-chr12:53816008), proximal promoter *AMHR2* (chr12:53817150-chr12:53817599) and intron 1 of *AMHR2* (chr12:53817900-chr12:53818054). Positions based on GRCh37/hg19 genome build. Biomatik custom sequences were provided in a pBluescript II SK(+) cloning vector. 5' SacI and 3' EcoRV or XhoI restriction sites were incorporated into sequences for subcloning into pGL4.24[luc2P/minP] vector (Promega Corporation, **Figure 4.10A**). Reference sequence pGL4.24 constructs underwent mutagenesis to achieve genetic variants.

Q5 Site-Directed Mutagenesis (New England BioLabs, Ipswich, MA) was performed according to the manufacturer's protocol. Mutagenesis primers for each variant were designed using the NEBaseChanger v.1.2.7 (https://nebasechanger.neb.com/). Reverse primers and mutation containing forward primers were used in PCR amplification of mutated plasmid DNA. Using the Kinase, Ligase & DpnI (KLD) treatment mixture, the template (non-mutated) DNA was degraded, while mutated plasmid DNA was ligated and subsequently transformed into competent cells. Single colonies were picked and grown for DNA purification using PureLink Quick Plasmid Miniprep Kit (Invitrogen) and Plasmid Midi Kit (Qiagen). Correct sequence of variant constructs was verified using Sanger sequencing.

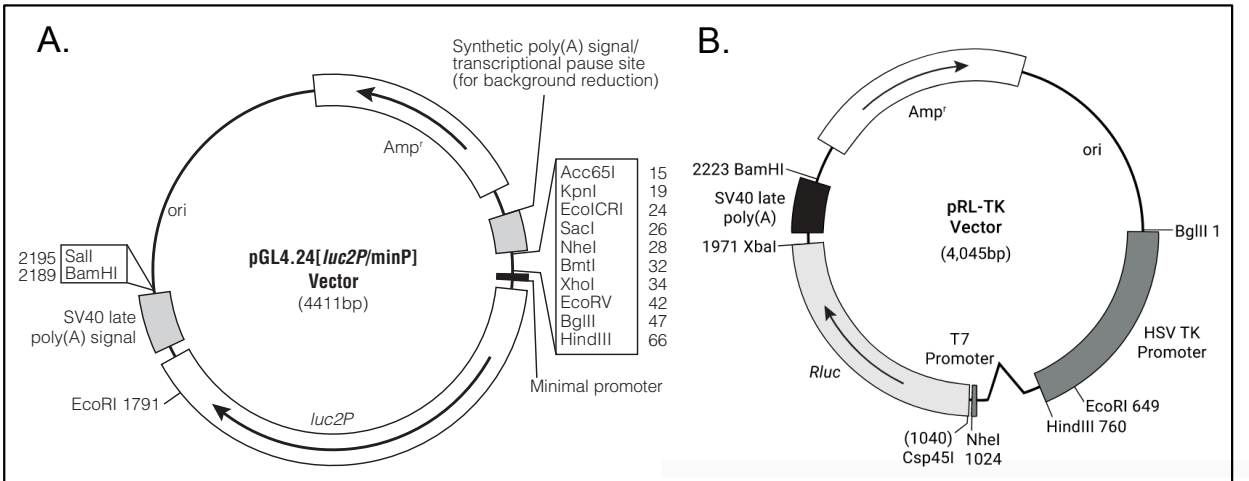

Figure 4.10 Maps of vectors used in functional studies of noncoding variants. A. Regulatory region subcloned into Promega pGL4.24 vector upstream of minimal promoter and luciferase gene. B. Control Renilla vector used in transfections for normalization of luciferase output. Promega Corporation (www.promega.com).

Dual Luciferase Reporter Assay for Regulatory Signal

To quantify the signaling potential of noncoding *AMH* and *AMHR2* variants, we employed a dual luciferase reporter assay. CHO-K1 cells were plated at 5,000 cells/well and transfected 24 hours later with a Firefly luciferase expressing pGL4.24 vector containing *AMH* or *AMHR2* reference or variant sequence regions as well as control *Renilla* luciferase reporter (pRL-TK, Promega Corporation, **Figure 4.10B**). Cells were incubated for 48 h. Firefly and *Renilla* luciferase readings were obtained using the Dual-Luciferase Reporter Assay System (Promega Corporation) according to manufacturer's instructions and luminescence was measured with the Synergy 2 plate reader (BioTek). Procedure for dual luciferase reporter assay testing regulatory variants is illustrated in **Figure 4.11**. Activity of reference and variant *AMH* and *AMHR2* were calculated with emissions of firefly luciferase divided by *Renilla* luminescence and normalized to empty vector control. Two-tailed t-test was used to determine degree of significance between variant and reference signal.

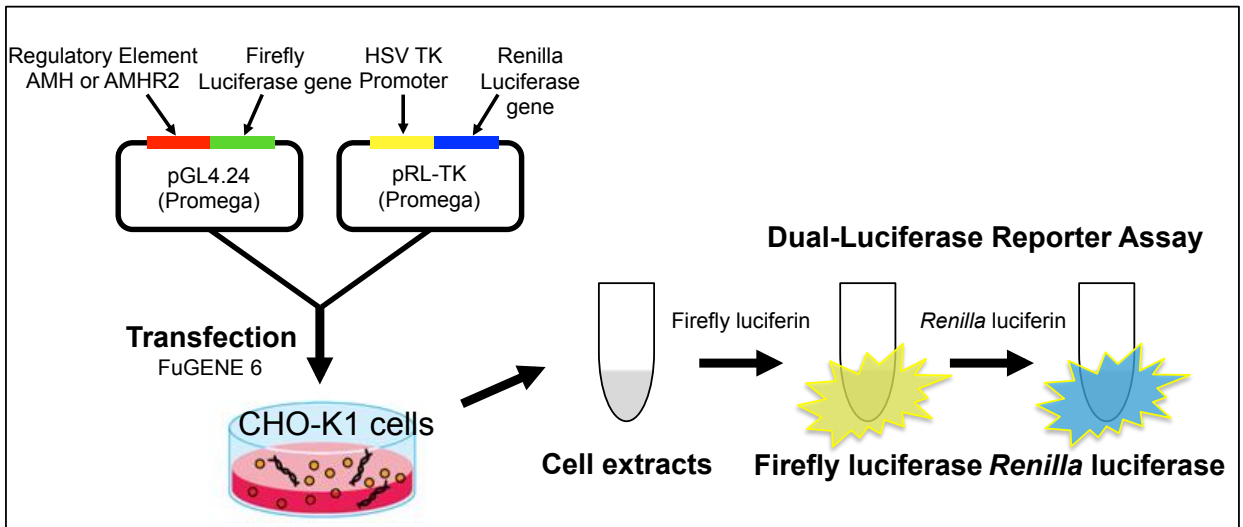

Figure 4.11 Method to test regulatory variants using a dual-luciferase reporter assay. (modified from http://photobiology.info/Ohmiya.html)

Dual Luciferase Reporter Assay for Potential *AMHR2* Splicing Variants

A modified *AMHR2* construct was created by Biomatik (Cambridge, ON, Canada) containing *AMHR2* cDNA sequence from start site to exon 7 and genomic sequence from exon 7 to the end of exon 11 (**Figure 4.12**). Q5 site-directed mutagenesis (as previously described) was conducted to achieve *AMHR2* intronic variants. Sanger sequencing confirmed each variant construct. To quantify the signaling potential of *AMHR2* intronic variants we performed a dual luciferase reporter assay where AMH binding to AMHR2 activates a firefly luciferase reporter (142, 265). COS7 cells were plated with 5,000 cells/well and transfected 24 h later with *AMHR2* variant or reference construct plus the *AMH* reference construct (265), bone morphogenetic protein (BMP)-responsive element (BRE) firefly luciferase reporter and control *Renilla* luciferase reporter (phRL-CMV) (142). Cells were incubated for 48 h. Firefly and *Renilla* luciferase readings were measured using the Dual-Luciferase Reporter Assay System (Promega Corporation, Milwaukee, WI) according to manufacturer's protocol and luminescence was measured using the Synergy 2

plate reader (BioTek, Winooski, VT). BRE induction of reference and variant *AMHR2* was calculated with emissions of firefly luciferase divided by *Renilla* luminescence and normalized to empty vector control. Two-tailed t-test was used to determine degree of significance between variant and reference activity. Similar to procedure previously summarized in **Figure 3.10**.

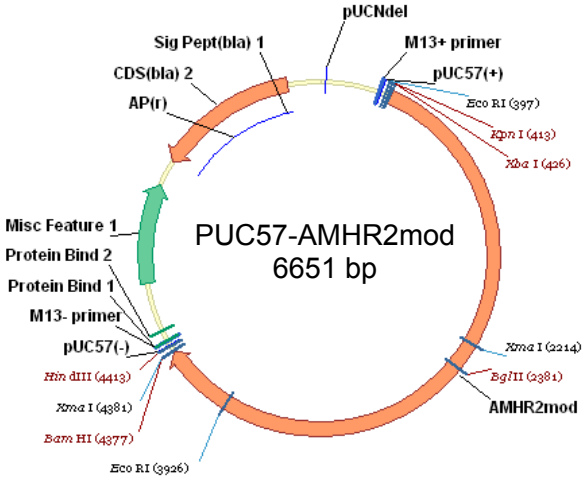

Figure 4.12 Plasmid map with modified *AMHR2* sequence. Image provided by Biomatik.

Evaluating AMHR2 Splicing Patterns

COS7 cell pellets were collected and RNA was isolated using the RNeasy Plus Mini kit (Qiagen). Resulting mRNA underwent DNase treatment to ensure minimal genomic DNA contamination. Reverse transcription was carried out using the High Capacity Reverse Transcription kit (Applied Biosystems) yielding final concentrations of 100 ng/µL. RT-PCR determined expression of *AMHR2* variant transcripts compared to reference. Applied Biosystem TaqMan primers measured *AMHR2* exon junctions 6/7 (Hs00179718_m1), 8/9 (Hs01086650_g1), 9/10 (Hs01086651_g1), and 10/11 (Hs01086644_m1), as well as housekeeping gene *GAPDH* (Hs02758991_g1). Complementary DNA samples were PCR-amplified targeting *AMHR2* exon regions 7 to 11 using forward (5'-CCCTGTGCCACTACTTGACC-3') and reverse (5'-GCTGAGGATTCCTGGAACAA-3')

primers. PCR samples were run on a 2% agarose gel to visualize changes in transcript size with 1 kb and 100 bp ladders (New England BioLabs Inc.).

4.7 CONCLUSIONS

Given that noncoding variants can affect regulatory elements and gene expression, we investigated noncoding variation in *AMH* and *AMHR2*. Our findings support the hypothesis that noncoding variation in members of the AMH pathway may have a functional impact on gene expression and signaling, similar to previously discussed coding variants. Specifically, we identified 3 PCOS-specific noncoding variants upstream of *AMH* that reduced signal in a dual luciferase reporter assay. Further, we evaluated 3 regions of *AMHR2*, which included an upstream region that contained acetylation and methylation marks, the proximal promoter region, and intron 1. Collectively, 7 of the 8 variants found in PCOS cases significantly decreased signal compared to reference. None of the variants identified in cases and controls showed a significant change in signal compared to reference (*AMH*: 0/1 and *AMHR2*: 0/2). Scores of deleteriousness, derived via CADD and FATHMM-MKL prediction tools, were advantageous in prioritization of variants/regions for functional studies; however, scores were not always consistent with outcome in *in vitro* assays.

Due to evidence of AMHR2 alternative splicing between exons 8 and 11, we also tested 12 variants in this region that were specific to PCOS subjects. Reference and variant *AMHR2* were examined for signaling impact, transcript expression and changes in transcript size. Nine of the 12 *AMHR2* variants were found to significantly reduce AMH signaling and 4 of these variants also resulted in altered splicing patterns. Our findings indicate that not only do noncoding variants impact regulatory elements and/or transcription factor binding motifs, but are

also capable of affecting canonical splicing patterns of *AMHR2*. Altered splicing of exons 9 and 10 impact the intracellular domain of the AMH receptor hindering type I receptor activation and downstream signaling. Defective AMHR2 protein is predicted to have similar effects on testosterone production as AMH variants, since AMH signaling is impaired. It is also possible that PCOS women with AMHR2 impairment have elevated AMH levels due to insufficient signaling ability through its receptor. These results indicate that rare variants causing *AMHR2* alternative splicing and subsequently decrease signaling capability contribute to PCOS.

Collectively, we found a total of 37 functional variants in/near *AMH* and *AMHR2* in 45 women affected with PCOS, equating to approximately 6.4% (45/700) of our PCOS cohort having pathogenic variants in two members of the AMH pathway (**Table 4.4**). We also tested for association between all functional *AMH*/*AMHR2* variants and PCOS using two independent control groups: the 165 reproductively normal control women sequenced in this study and population-based controls from the gnomAD Genome Aggregation Database (http://gnomad.broadinstitute.org/) (**Table 4.4**). Functional variants were significantly associated with PCOS in our cohort of 700 women with PCOS and 165 controls ($\chi = 22.046$; $p = 2.00 \times 10^{-5}$; OR = 12.7). Furthermore, evidence for association between functional *AMH*/*AMHR2* variants and PCOS was highly significant relative to a larger non-Finnish Europeans (gnomAD) population-based control cohort ($\chi = 71.5$; $p < 10^{-8}$; OR = 3.36). Notably, across our variant findings in *AMH* and *AMHR2*, variants found in controls often had higher MAF than variants identified in cases and are thus more likely to be polymorphisms with little if any impact on function as was observed in signaling assays. Our results support the hypothesis that rare genetic variation contributes to the missing heritability of PCOS and implicates the AMH pathway in its pathogenesis in a subgroup of affected women.

One pathway by which impaired AMH may contribute to PCOS phenotypes is through the loss of target gene *CYP17* inhibition, resulting in elevated levels of CYP17 and subsequent increased levels of testosterone. Interestingly, a recent study by de Medeiros *et al*. found increased levels of 17-hydroxypregnenolone (17-OHPE) in women with hyperandrogenemic PCOS compared to normoandrogenemic PCOS (266). 17-OHPE is the precursor to dehydroepiandrosterone (DHEA) directly regulated by CYP17 (**Figure 1.5**). Nevertheless, *CYP17* is not the sole target gene of AMH and, thus, other mechanisms must be considered for their role in PCOS. AMH regulation has also been demonstrated for several other genes (*CYP11A, CYP19A1, 3BHSD*) (267-271) with likely additional targets that remain yet undiscovered. Specifically, AMH has also been shown to inhibit *CYP11A* and *3BHSD*, however not to the same extent as *CYP17*. Nonetheless, we would predict a similar effect of impaired AMH on levels of *CYP11A* and *3BHSD* as with *CYP17*, resulting in elevated testosterone production. However, AMH has also been shown to inhibit *CYP19A1* expression, which encodes cytochrome P450 aromatase an enzyme responsible for the conversion of androgens to estrogens (106). Therefore, if AMH signaling were reduced in PCOS women we could also predict to see increased levels of *CYP19* expression. In circumstances of elevated aromatase levels, we would further expect women with PCOS to have higher estradiol levels given the availability of excess androgens for estrogen conversion. However, other factors may also act on *CYP19* expression that could substitute the inhibitory role of AMH. For example, researchers have found the promoter region of *CYP19* to be hypermethylated in women with PCOS compared to controls, thus causing reduced expression (272). Additionally, PPARγ has also been suggested to influence *CYP19* expression in granulosa cells treated with eicosapentaenoic

acid (273). While AMH has exhibited regulation of *CYP19*, there seem to be other complex mechanisms that also influence *CYP19* expression in various cell types (274-280).

AMH has also been shown to inhibit follicular transition from the primary to secondary stages (281), therefore suggesting another pathway in the development of PCOS. Specifically, decreased AMH signaling would result in an increased number of early stage follicles and PCOM, which are key characteristics of PCOS (282, 283). Our studies have provided evidence for one pathway by which compromised AMH could lead to PCOS via loss of *CYP17* inhibition; yet, questions still remain as to if and how other targets and pathways of AMH action contribute to PCOS pathogenesis.

Overall, this research has significantly contributed to the fields of PCOS and reproductive biology. Our findings were first to report pathogenic rare variants contributing to a common PCOS phenotype. Identifying these mutations in *AMH* and *AMHR2* has shed a new light into one of the pathways causing PCOS. For years, scientists and clinicians have followed the notion that elevated AMH levels in PCOS women meant greater hormone activity, which worsened the disease. However, our studies introduce a novel mechanism for the pathological underpinnings of PCOS in a subset of women: decreased AMH bioactivity. Furthermore, targeted resequencing of the genes encoding the insulin receptor and lamin a/c identified an extensive number of likely-to-be deleterious missense variants in PCOS subjects. The presence of *LMNA* and *INSR* variants in our PCOS cohort supports the hypothesis that genetic variants in genes associated with Mendelian forms of extreme insulin resistance also contribute to the etiology of common forms of insulin resistance. Our approach has provided the most comprehensive screen of genetic variation in these genes in women affected with PCOS and highlights important pathways in the pathogenesis of PCOS.

CHAPTER 5

FUTURE DIRECTIONS

5.1 OVERVIEW

Our results were the first to show rare variants associated with a common PCOS phenotype and illuminate a previously unrecognized pathway for PCOS: decreased AMH signaling. We have identified rare deleterious variants associated with PCOS in members of the AMH signaling cascade (*AMH* and *AMHR2*) as well as in additional genes that cause extreme phenotypes of PCOS (*INSR* and *LMNA*). We have also determined that PCOS-specific variants in *AMH* and *AMHR2* have damaging effects on signaling and downstream target gene expression of *CYP17 in vitro*. However, it remains unclear how these variants in *AMH* are disrupting the normal protein product, secretion and/or receptor binding processes. Given that our results have brought light to the importance of this pathway in PCOS, it is of interest to sequence other genes involved in this pathway. Additionally, functional investigation of *INSR* and *LMNA* variants would solidify the prediction that a subgroup of PCOS patients harbor mutations in genes that cause Mendelian disorders with PCOS symptoms.

Our cohort of PCOS cases was also of European ancestry and fulfilled the NIH criteria for PCOS of hyperandrogenism and chronic anovulation; ovarian morphology was not assessed (54, 179). Further studies are needed to assess the contribution of *AMH* mutations to the other Rotterdam PCOS phenotypes, hyperandrogenism and PCOM without anovulation and chronic anovulation and PCOM without hyperandrogenism (10) as well as to PCOS in other racial/ethnic groups.

5.2 IMPACT OF AMH VARIANTS ON PROTEIN FUNCTION AND PROCESSING

We have found 17 PCOS-specific *AMH* variants to reduce signaling capability in a cell line model (265) and also observed their loss of target gene *Cyp17* inhibition. However, we have yet

to determine how exactly these variants impact AMH protein activity. It, thus, remains unknown whether *AMH* variants affect protein synthesis, expression, processing, secretion and/or receptor binding ability. We would predict to see defects in various functions depending on the variant amino acid change and location within *AMH*. AMH protein levels can be assessed by ELISA and Western blot analysis using antibodies specific to the C-terminal mature domain as well as the N-terminal prodomain of AMH. Western blots testing cell lysates and media samples, can be used to determine changes in protein expression and/or secretion activity. Given that AMH requires proper processing in order to carry out functional signal, the Western blot approach can also be an informative tool to assess AMH cleavage into its prodomain and active mature domain of variant *AMH* compared to reference *AMH*. Completion of these experiments and evaluation of variants in certain locations within *AMH* would also offer insight into the specific domain characteristics of AMH itself.

5.3 MUTANT AMH ACTIVITY IN A MICROFLUIDIC SYSTEM THAT SUPPORTS FOLLICLE MATURATION

Now that our studies have shown PCOS-specific *AMH* variants to be pathogenic in an *in vitro* environment, it would be of interest to test their effects using a more applicable model system. *In vitro* models of ovarian follicle development have a bioengineered (hydrogel) microenvironment that have allowed the advancement and possibility to support follicle growth and maturation, hormone production, and oocyte maturation (284). A section of quarter mouse ovary and developing follicles are seen through microscope at day 6 of culturing in the microfluidic system (**Figure 5.1**). Utilizing a microenvironment suitable for follicle maturation would be particularly beneficial in further AMH studies, since this hormone has autocrine and

paracrine functions in follicular granulosa and theca cells of the ovary. The microfluidic platform enables a 28-day follicle cycle with a follicular phase, ovulation phase, and full luteal phase. This *in vitro* microfluidic system is able to recapitulate or "humanize" the 5-day ovarian cycle of the mouse to a 28-day cycle of the human by controlling gonadotropins, growth factors, and steroid hormone inputs (284). Therefore, this system can provide a controlled environment, where wild-type AMH and variant AMH can be tested for biological function in a high throughput manner. Downstream steroid enzymes can also be evaluated for changes in expression based on AMH treatment (285) (**Figure 5.2**).

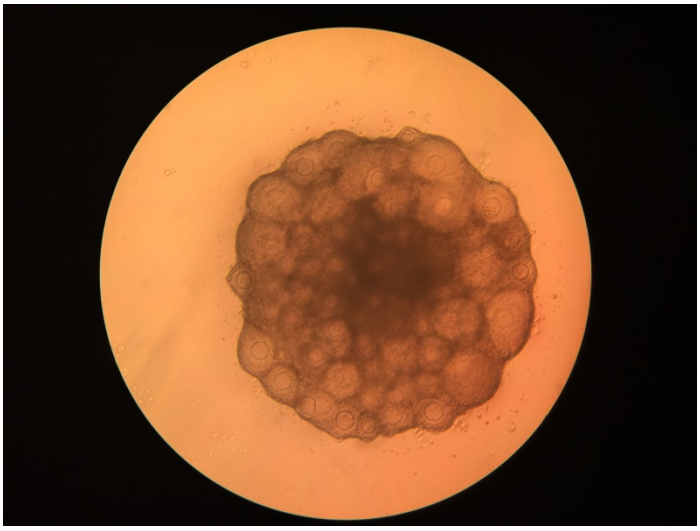

Figure 5.1 Follicular maturation in mouse ovary using the microfluidic system. Follicle at day 6 of culturing a quarter size ovary of mouse.

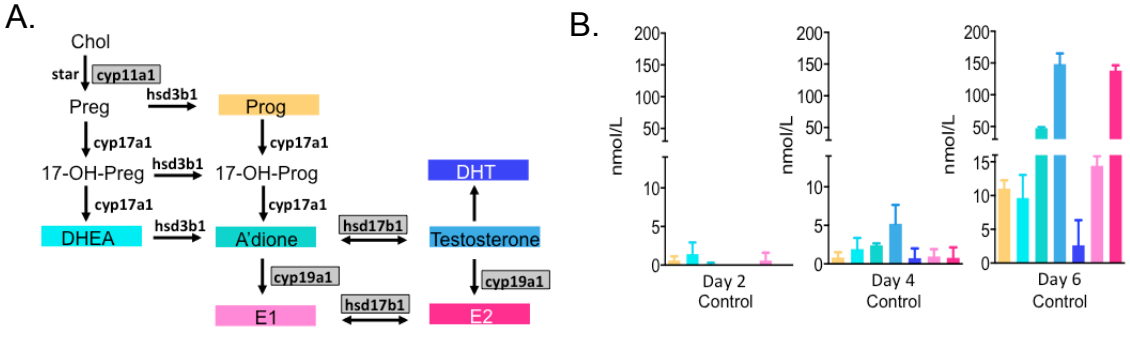

Figure 5.2 Steroid hormone production by cultured follicles. Hormones measured by liquid chromatography tandem mass spectrometry (LC-MS/MS), with 72-105 individual follicles at day 2, 4 and 6 of culture, and normalized to 100 follicles. Data are expressed as mean ± SD. A. Steroidogenic pathway and the murine steroidogenic enzymes involved in conversions; grey shaded boxes indicate significant upregulation of mRNA expression on day 6 of follicular development. B. Endogenous steroid production in the isolated follicle at day number indicated. Lebbe *et al*, *Endocrinology* 2017.

A number of approaches can be used to further understand the biological roles of AMH within the ovary using the microfluidic system. Ovarian murine sections can be treated with purified recombinant human AMH to determine the impact of excess AMH on peptide and steroid hormone production as well as follicular recruitment/growth/survival. Samples of media can be collected every 24 hours to evaluate estradiol, progesterone and testosterone levels. Histological staining can also be performed after the intended culturing period to determine follicle counts and health. Results from AMH treated ovarian sections can be compared to non-treated sections that only express murine endogenous AMH. Additionally, ovarian mouse sections cultured in the microfluidic system can also be treated with specific antibodies to inhibit endogenous mouse AMH activity. This treatment would mimic knockdown conditions of AMH signaling and exemplify the loss-of-function variants identified in our PCOS cohort. Finally, ovarian follicles in the microfluidic system can be treated with AMH variant proteins using conditions optimized by the bioactive AMH recombinant protein. Changes in follicular development and steroid production can then be assessed for each of the mutant AMH proteins. These studies would, furthermore, promote the use of the microfluidic platform for future studies of ovarian biology.

5.4 EXPANDED SEQUENCING SCREEN OF ADDITIONAL GENES ENCODING MEMBERS OF THE AMH SIGNALING PATHWAY

The pathogenic variants that we have identified in *AMH* and *AMHR2* highlight the importance of this pathway in PCOS etiology. Therefore, our findings suggest that mutations in other members of the AMH signaling pathway could also contribute to PCOS. Using next generation sequencing, a comprehensive catalog of rare coding and noncoding genetic variation can be

determined in additional genes that encode products involved in the AMH signaling cascade. Additional genes to perform sequencing on include those of which their products directly transduce the AMH signal (*ACVR1A, BMP15, BMPR1A, SMAD1, SMAD5, SMAD8*) (138), genes that regulate *AMH* expression (*SF1, GATA4, SMAD1*) (240, 286) and genes that are regulated by AMH (*CYP11A, CYP17, CYP19A1, 3BHSD*) (267-271). Therefore, it is likely that we have only discovered the tip of the iceberg, since *AMH* and *AMHR2* represent only two gene members of this pathway and an additional 23 known genes may harbor harmful variants leading to PCOS (**Figure 5.3**). A comprehensive study of genetic variation in other members of the AMH signaling cascade would determine the extent of AMH pathway impairment in PCOS etiology.

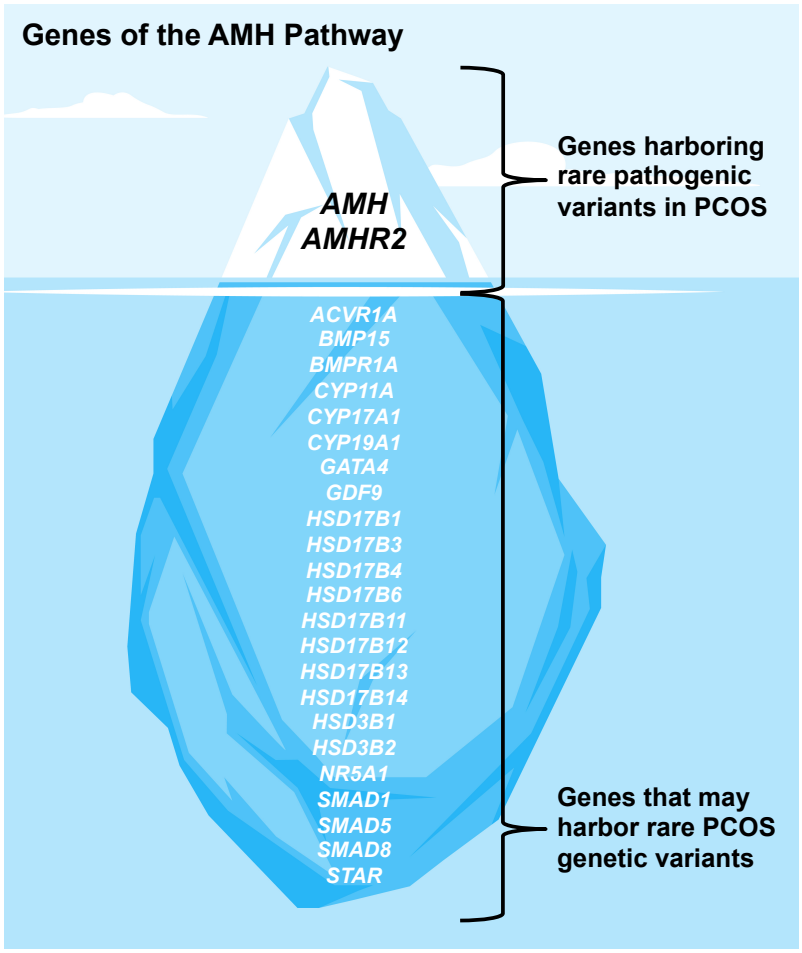

Figure 5.3 Identifying the tip of the iceberg: genes associated with the AMH pathway proposed for next generation sequencing in a PCOS case/control cohort. Iceberg image ID 49258005 © Oceloti, Dreamstime.com

5.5 FUNCTIONAL STUDIES OF LMNA AND INSR RARE VARIANTS

Given the complex, multifactorial nature of PCOS we would expect that other pathways also contribute to PCOS etiology. Rare, likely deleterious variants were identified in *LMNA* and *INSR* genes in women with PCOS. Studies showing the impact of these variants would verify their functional contribution to the PCOS phenotype and support the hypothesis that genes causing Mendelian disorders account for a subgroup of PCOS-affected women. As seen in our functional studies of *AMH* and *AMHR2*, not every nonsynonymous mutation has a functional impact on protein production and downstream signaling. Therefore, it is important to further investigate variant findings with functional tests. However, the *LMNA* and *INSR* genes are large and complex both producing multiple transcripts that ultimately lead to multiple protein products with various functions. It is, therefore, not surprising that different mutations can result in various phenotypes, ranging from mild to severe disorders (185, 186, 287, 288).

To determine the functional impact of *LMNA* variants, previous studies have used reference *LMNA* cDNA GFP-tagged constructs to generate mutant *LMNA* constructs (289). These constructs can be utilized in functional experiments using applicable *in vitro* models. For example, a recent study infected neonatal rat ventricular myocytes (NRVMs) to investigate the impact of *LMNA* mutations on cardiomyocytes and their role in the development of cardiomyopathies (289). Using GFP-tagged constructs, nuclear circularity, nuclear area and localization can be visualized and compared to wild-type LMNA using confocal immunofluorescence microscopy. Functional studies confirming abnormal protein action of *LMNA* variants found in our cohort would further provide strong evidence that *LMNA* mutations cause a PCOS phenotype in a subgroup of women.

To test deleterious *INSR* variants, cDNA constructs containing reference *INSR* sequence can undergo mutagenesis to achieve mutant *INSR*. Constructs can be transfected into cell line model systems for functional study. For instance, cells that have been transfected with reference and variant *INSR*, as well as stimulated with insulin, can be collected to assess differences in INSR protein expression and downstream protein expression of target genes. Using Western blot analysis, indicators of INSR-mediated signaling from the PI3K/Akt/mTOR and RAS pathways can be tested using specific antibodies. Targets for analysis could include Akt, P-Akt, Erk1/2 and P-Erk1/2, which are members of the insulin signaling pathway (176).

Performing functional analysis of variants would provide further insight into the processes involved in PCOS pathogenesis. While PCOS, generally speaking, is a common condition, it is possible that PCOS is a culmination of rare variation in multiple pathways causing similar, yet diverse, phenotypes. Thus, providing one possible explanation for the heterogeneous presentation of symptoms in PCOS women.

REFERENCES

1. Boyle J, Teede HJ. Polycystic ovary syndrome: an update. Australian family physician. 2012;41(10):752.
2. Diamanti-Kandarakis E, Dunaif A. Insulin resistance and the polycystic ovary syndrome revisited: an update on mechanisms and implications. Endocrine Reviews. 2012;33(6):981-1030. doi: 10.1210/er.2011-1034. PubMed PMID: 23065822.
3. Knochenhauer ES, Key TJ, Kahsar-Miller M, Waggoner W, Boots LR, Azziz R. Prevalence of the polycystic ovary syndrome in unselected black and white women of the southeastern United States: a prospective study. J Clin Endocrinol Metab. 1998;83(9):3078-82. Epub 1998/09/24. doi: 10.1210/jcem.83.9.5090. PubMed PMID: 9745406.
4. Diamanti-Kandarakis E, Kouli CR, Bergiele AT, Filandra FA, Tsianateli TC, Spina GG, Zapanti ED, Bartzis MI. A survey of the polycystic ovary syndrome in the Greek island of Lesbos: hormonal and metabolic profile. J Clin Endocrinol Metab. 1999;84(11):4006-11. Epub 1999/11/24. doi: 10.1210/jcem.84.11.6148. PubMed PMID: 10566641.
5. Azziz R, Woods KS, Reyna R, Key TJ, Knochenhauer ES, Yildiz BO. The prevalence and features of the polycystic ovary syndrome in an unselected population. J Clin Endocrinol Metab. 2004;89(6):2745-9. Epub 2004/06/08. doi: 10.1210/jc.2003-032046. PubMed PMID: 15181052.
6. Broekmans FJ, Knauff EA, Valkenburg O, Laven JS, Eijkemans MJ, Fauser BC. PCOS according to the Rotterdam consensus criteria: Change in prevalence among WHO-II anovulation and association with metabolic factors. BJOG. 2006;113(10):1210-7. Epub 2006/09/16. doi: 10.1111/j.1471-0528.2006.01008.x. PubMed PMID: 16972863.
7. March WA, Moore VM, Willson KJ, Phillips DI, Norman RJ, Davies MJ. The prevalence of polycystic ovary syndrome in a community sample assessed under contrasting diagnostic criteria. Hum Reprod. 2010;25(2):544-51. Epub 2009/11/17. doi: 10.1093/humrep/dep399. PubMed PMID: 19910321.
8. Mehrabian F, Khani B, Kelishadi R, Ghanbari E. The prevalence of polycystic ovary syndrome in Iranian women based on different diagnostic criteria. Endokrynol Pol. 2011;62(3):238-42. Epub 2011/07/01. PubMed PMID: 21717406.
9. Vink JM, Sadrzadeh S, Lambalk CB, Boomsma DI. Heritability of polycystic ovary syndrome in a Dutch twin-family study. Journal of Clinical Endocrinology & Metabolism. 2006;91(6):2100-4. doi: 10.1210/jc.2005-1494. PubMed PMID: 16219714.
10. Rotterdam EA-SPCWG. Revised 2003 consensus on diagnostic criteria and long-term health risks related to polycystic ovary syndrome. Fertility & Sterility. 2004;81(1):19-25. PubMed PMID: 14711538.
11. Sirmans SM, Pate KA. Epidemiology, diagnosis, and management of polycystic ovary syndrome. Clin Epidemiol. 2013;6:1-13. Epub 2014/01/01. doi: 10.2147/CLEP.S37559. PubMed PMID: 24379699; PubMed Central PMCID: PMC3872139.
12. Legro RS, Driscoll D, Strauss JF, 3rd, Fox J, Dunaif A. Evidence for a genetic basis for hyperandrogenemia in polycystic ovary syndrome. Proceedings of the National Academy of Sciences of the United States of America. 1998;95(25):14956-60. PubMed PMID: 9843997; PubMed Central PMCID: PMC24557.

13. Azziz R, Carmina E, Dewailly D, Diamanti-Kandarakis E, Escobar-Morreale HF, Futterweit W, Janssen OE, Legro RS, Norman RJ, Taylor AE, Witchel SF, Androgen Excess S. Positions statement: criteria for defining polycystic ovary syndrome as a predominantly hyperandrogenic syndrome: an Androgen Excess Society guideline. J Clin Endocrinol Metab. 2006;91(11):4237-45. Epub 2006/08/31. doi: 10.1210/jc.2006-0178. PubMed PMID: 16940456.
14. Sam S, Dunaif A. Polycystic ovary syndrome: syndrome XX? Trends Endocrinol Metab. 2003;14(8):365-70. Epub 2003/10/01. PubMed PMID: 14516934.
15. Jayasena CN, Franks S. The management of patients with polycystic ovary syndrome. Nat Rev Endocrinol. 2014;10(10):624-36. Epub 2014/07/16. doi: 10.1038/nrendo.2014.102. PubMed PMID: 25022814.
16. Ozcan Dag Z, Oguzturk O, Isik Y, Turkel Y, Bulcun E. Personality profile in patients with polycystic ovary syndrome. Gynecol Endocrinol. 2015:1-3. Epub 2015/04/18. doi: 10.3109/09513590.2015.1018162. PubMed PMID: 25884894.
17. Azziz R, Carmina E, Dewailly D, Diamanti-Kandarakis E, Escobar-Morreale HF, Futterweit W, Janssen OE, Legro RS, Norman RJ, Taylor AE, Witchel SF, Task Force on the Phenotype of the Polycystic Ovary Syndrome of The Androgen E, Society P. The Androgen Excess and PCOS Society criteria for the polycystic ovary syndrome: the complete task force report. Fertil Steril. 2009;91(2):456-88. Epub 2008/10/28. doi: 10.1016/j.fertnstert.2008.06.035. PubMed PMID: 18950759.
18. de-Medeiros SF, Yamamoto MMW, de-Medeiros MAS, Barbosa JS, Norman RJ. Should Subclinical Hypothyroidism Be an Exclusion Criterion for the Diagnosis of Polycystic Ovary Syndrome? J Reprod Infertil. 2017;18(2):242-50. Epub 2017/09/05. PubMed PMID: 28868249; PubMed Central PMCID: PMC5565908.
19. Stepto NK, Cassar S, Joham AE, Hutchison SK, Harrison CL, Goldstein RF, Teede HJ. Women with polycystic ovary syndrome have intrinsic insulin resistance on euglycaemic-hyperinsulaemic clamp. Hum Reprod. 2013;28(3):777-84. Epub 2013/01/15. doi: 10.1093/humrep/des463. PubMed PMID: 23315061.
20. Dunaif A, Segal KR, Futterweit W, Dobrjansky A. Profound peripheral insulin resistance, independent of obesity, in polycystic ovary syndrome. Diabetes. 1989;38(9):1165-74. Epub 1989/09/01. PubMed PMID: 2670645.
21. Ehrmann DA, Barnes RB, Rosenfield RL, Cavaghan MK, Imperial J. Prevalence of impaired glucose tolerance and diabetes in women with polycystic ovary syndrome. Diabetes Care. 1999;22(1):141-6. Epub 1999/05/20. PubMed PMID: 10333916.
22. Legro RS, Kunselman AR, Dodson WC, Dunaif A. Prevalence and predictors of risk for type 2 diabetes mellitus and impaired glucose tolerance in polycystic ovary syndrome: a prospective, controlled study in 254 affected women. J Clin Endocrinol Metab. 1999;84(1):165-9. Epub 1999/01/27. doi: 10.1210/jcem.84.1.5393. PubMed PMID: 9920077.
23. Moran LJ, Misso ML, Wild RA, Norman RJ. Impaired glucose tolerance, type 2 diabetes and metabolic syndrome in polycystic ovary syndrome: a systematic review and meta-analysis. Hum Reprod Update. 2010;16(4):347-63. Epub 2010/02/18. doi: 10.1093/humupd/dmq001. PubMed PMID: 20159883.
24. Mani H, Davies MJ, Bodicoat DH, Levy MJ, Gray LJ, Howlett TA, Khunti K. Clinical characteristics of polycystic ovary syndrome: investigating differences in white and South Asian women. Clin Endocrinol (Oxf). 2015. Epub 2015/04/01. doi: 10.1111/cen.12784. PubMed PMID: 25824095.

25. Sam S. Adiposity and metabolic dysfunction in polycystic ovary syndrome. Horm Mol Biol Clin Investig. 2015;21(2):107-16. Epub 2015/03/18. doi: 10.1515/hmbci-2015-0008. PubMed PMID: 25781555.
26. Lim SS, Davies MJ, Norman RJ, Moran LJ. Overweight, obesity and central obesity in women with polycystic ovary syndrome: a systematic review and meta-analysis. Hum Reprod Update. 2012;18(6):618-37. Epub 2012/07/07. doi: 10.1093/humupd/dms030. PubMed PMID: 22767467.
27. de Groot PC, Dekkers OM, Romijn JA, Dieben SW, Helmerhorst FM. PCOS, coronary heart disease, stroke and the influence of obesity: a systematic review and meta-analysis. Hum Reprod Update. 2011;17(4):495-500. Epub 2011/02/22. doi: 10.1093/humupd/dmr001. PubMed PMID: 21335359.
28. Mott MM, Kitos NR, Coviello AD. Practice Patterns in Screening for Metabolic Disease in Women with PCOS of Diverse Race-Ethnic Backgrounds. Endocr Pract. 2014;20(9):855-63. Epub 2014/03/20. doi: 10.4158/EP13414.OR. PubMed PMID: 24641921.
29. Barry JA, Azizia MM, Hardiman PJ. Risk of endometrial, ovarian and breast cancer in women with polycystic ovary syndrome: a systematic review and meta-analysis. Hum Reprod Update. 2014;20(5):748-58. Epub 2014/04/02. doi: 10.1093/humupd/dmu012. PubMed PMID: 24688118; PubMed Central PMCID: PMC4326303.
30. Gottschau M, Kjaer SK, Jensen A, Munk C, Mellemkjaer L. Risk of cancer among women with polycystic ovary syndrome: a Danish cohort study. Gynecol Oncol. 2015;136(1):99-103. Epub 2014/12/03. doi: 10.1016/j.ygyno.2014.11.012. PubMed PMID: 25451694.
31. Park JC, Lim SY, Jang TK, Bae JG, Kim JI, Rhee JH. Endometrial histology and predictable clinical factors for endometrial disease in women with polycystic ovary syndrome. Clin Exp Reprod Med. 2011;38(1):42-6. Epub 2012/03/03. doi: 10.5653/cerm.2011.38.1.42. PubMed PMID: 22384417; PubMed Central PMCID: PMC3283042.
32. Tantalaki E, Piperi C, Livadas S, Kollias A, Adamopoulos C, Koulouri A, Christakou C, Diamanti-Kandarakis E. Impact of dietary modification of advanced glycation end products (AGEs) on the hormonal and metabolic profile of women with polycystic ovary syndrome (PCOS). Hormones (Athens). 2014;13(1):65-73. Epub 2014/04/12. PubMed PMID: 24722128.
33. Spritzer PM, Motta AB, Sir-Petermann T, Diamanti-Kandarakis E. Novel strategies in the management of polycystic ovary syndrome. Minerva Endocrinol. 2015. Epub 2015/03/18. PubMed PMID: 25781065.
34. Naderpoor N, Shorakae S, Joham A, Boyle J, De Courten B, Teede HJ. Obesity and polycystic ovary syndrome. Minerva Endocrinol. 2015;40(1):37-51. Epub 2014/11/21. PubMed PMID: 25411807.
35. Rondanelli M, Perna S, Faliva M, Monteferrario F, Repaci E, Allieri F. Focus on metabolic and nutritional correlates of polycystic ovary syndrome and update on nutritional management of these critical phenomena. Arch Gynecol Obstet. 2014;290(6):1079-92. Epub 2014/09/10. doi: 10.1007/s00404-014-3433-z. PubMed PMID: 25200687.
36. Das M, Son WY, Buckett W, Tulandi T, Holzer H. In-vitro maturation versus IVF with GnRH antagonist for women with polycystic ovary syndrome: treatment outcome and rates of ovarian hyperstimulation syndrome. Reprod Biomed Online. 2014;29(5):545-51. Epub 2014/09/30. doi: 10.1016/j.rbmo.2014.07.019. PubMed PMID: 25262236.
37. Walls ML, Hunter T, Ryan JP, Keelan JA, Nathan E, Hart RJ. In vitro maturation as an alternative to standard in vitro fertilization for patients diagnosed with polycystic ovaries: a

comparative analysis of fresh, frozen and cumulative cycle outcomes. Hum Reprod. 2015;30(1):88-96. Epub 2014/10/31. doi: 10.1093/humrep/deu248. PubMed PMID: 25355587.
38. Wan HL, Hui PW, Li HW, Ng EH. Obstetric outcomes in women with polycystic ovary syndrome and isolated polycystic ovaries undergoing in vitro fertilization: a retrospective cohort analysis. J Matern Fetal Neonatal Med. 2015;28(4):475-8. Epub 2014/05/08. doi: 10.3109/14767058.2014.921673. PubMed PMID: 24803007.
39. Joham AE, Teede HJ, Ranasinha S, Zoungas S, Boyle J. Prevalence of infertility and use of fertility treatment in women with polycystic ovary syndrome: data from a large community-based cohort study. J Womens Health (Larchmt). 2015;24(4):299-307. Epub 2015/02/06. doi: 10.1089/jwh.2014.5000. PubMed PMID: 25654626.
40. Yildizhan R, Gokce AI, Yildizhan B, Cim N. Comparison of the effects of chlormadinone acetate versus drospirenone containing oral contraceptives on metabolic and hormonal parameters in women with PCOS for a period of two-year follow-up. Gynecol Endocrinol. 2015:1-5. Epub 2015/03/05. doi: 10.3109/09513590.2015.1006187. PubMed PMID: 25739031.
41. Rasmussen CB, Lindenberg S. The effect of liraglutide on weight loss in women with polycystic ovary syndrome: an observational study. Front Endocrinol (Lausanne). 2014;5:140. Epub 2014/09/16. doi: 10.3389/fendo.2014.00140. PubMed PMID: 25221543; PubMed Central PMCID: PMC4145240.
42. Dumitrescu R, Mehedintu C, Briceag I, Purcarea VL, Hudita D. Metformin-Clinical Pharmacology in PCOs. J Med Life. 2015;8(2):187-92. Epub 2015/04/14. PubMed PMID: 25866577; PubMed Central PMCID: PMC4392089.
43. Domecq JP, Prutsky G, Mullan RJ, Sundaresh V, Wang AT, Erwin PJ, Welt C, Ehrmann D, Montori VM, Murad MH. Adverse effects of the common treatments for polycystic ovary syndrome: a systematic review and meta-analysis. J Clin Endocrinol Metab. 2013;98(12):4646-54. Epub 2013/10/05. doi: 10.1210/jc.2013-2374. PubMed PMID: 24092830.
44. Chen ZJ, Zhao H, He L, Shi Y, Qin Y, Shi Y, Li Z, You L, Zhao J, Liu J, Liang X, Zhao X, Zhao J, Sun Y, Zhang B, Jiang H, Zhao D, Bian Y, Gao X, Geng L, Li Y, Zhu D, Sun X, Xu JE, Hao C, Ren CE, Zhang Y, Chen S, Zhang W, Yang A, Yan J, Li Y, Ma J, Zhao Y. Genome-wide association study identifies susceptibility loci for polycystic ovary syndrome on chromosome 2p16.3, 2p21 and 9q33.3. Nature Genetics. 2011;43(1):55-9. doi: 10.1038/ng.732. PubMed PMID: 21151128.
45. Shi Y, Zhao H, Shi Y, Cao Y, Yang D, Li Z, Zhang B, Liang X, Li T, Chen J, Shen J, Zhao J, You L, Gao X, Zhu D, Zhao X, Yan Y, Qin Y, Li W, Yan J, Wang Q, Zhao J, Geng L, Ma J, Zhao Y, He G, Zhang A, Zou S, Yang A, Liu J, Li W, Li B, Wan C, Qin Y, Shi J, Yang J, Jiang H, Xu JE, Qi X, Sun Y, Zhang Y, Hao C, Ju X, Zhao D, Ren CE, Li X, Zhang W, Zhang Y, Zhang J, Wu D, Zhang C, He L, Chen ZJ. Genome-wide association study identifies eight new risk loci for polycystic ovary syndrome. Nature Genetics. 2012;44(9):1020-5. doi: 10.1038/ng.2384. PubMed PMID: 22885925.
46. Biyasheva A, Legro RS, Dunaif A, Urbanek M. Evidence for association between polycystic ovary syndrome (PCOS) and TCF7L2 and glucose intolerance in women with PCOS and TCF7L2. J Clin Endocrinol Metab. 2009;94(7):2617-25. Epub 2009/04/09. doi: 10.1210/jc.2008-1664. PubMed PMID: 19351735; PubMed Central PMCID: PMC2708958.
47. Mutharasan P, Galdones E, Penalver Bernabe B, Garcia OA, Jafari N, Shea LD, Woodruff TK, Legro RS, Dunaif A, Urbanek M. Evidence for chromosome 2p16.3 polycystic

ovary syndrome susceptibility locus in affected women of European ancestry. J Clin Endocrinol Metab. 2013;98(1):E185-90. Epub 2012/11/03. doi: 10.1210/jc.2012-2471. PubMed PMID: 23118426; PubMed Central PMCID: PMC3537106.
48. Louwers YV, Stolk L, Uitterlinden AG, Laven JS. Cross-ethnic meta-analysis of genetic variants for polycystic ovary syndrome. J Clin Endocrinol Metab. 2013;98(12):E2006-12. Epub 2013/10/10. doi: 10.1210/jc.2013-2495. PubMed PMID: 24106282.
49. Goodarzi MO, Jones MR, Li X, Chua AK, Garcia OA, Chen YD, Krauss RM, Rotter JI, Ankener W, Legro RS, Azziz R, Strauss JF, 3rd, Dunaif A, Urbanek M. Replication of association of DENND1A and THADA variants with polycystic ovary syndrome in European cohorts. J Med Genet. 2012;49(2):90-5. Epub 2011/12/20. doi: 10.1136/jmedgenet-2011-100427. PubMed PMID: 22180642; PubMed Central PMCID: PMC3536488.
50. Li L, Gu ZP, Bo QM, Wang D, Yang XS, Cai GH. Association of CYP17A1 gene -34T/C polymorphism with polycystic ovary syndrome in Han Chinese population. Gynecol Endocrinol. 2015;31(1):40-3. Epub 2014/09/11. doi: 10.3109/09513590.2014.947948. PubMed PMID: 25208301.
51. McAllister JM, Legro RS, Modi BP, Strauss JF, 3rd. Functional genomics of PCOS: from GWAS to molecular mechanisms. Trends Endocrinol Metab. 2015;26(3):118-24. Epub 2015/01/21. doi: 10.1016/j.tem.2014.12.004. PubMed PMID: 25600292; PubMed Central PMCID: PMC4346470.
52. Barber TM, Franks S. Genetics of polycystic ovary syndrome. Front Horm Res. 2013;40:28-39. Epub 2013/09/05. doi: 10.1159/000341682. PubMed PMID: 24002403.
53. Zhao H, Lv Y, Li L, Chen ZJ. Genetic Studies on Polycystic Ovary Syndrome. Best Practice & Research in Clinical Obstetrics & Gynaecology. 2016. doi: 10.1016/j.bpobgyn.2016.04.002. PubMed PMID: 27264388.
54. Hayes MG, Urbanek M, Ehrmann DA, Armstrong LL, Lee JY, Sisk R, Karaderi T, Barber TM, McCarthy MI, Franks S, Lindgren CM, Welt CK, Diamanti-Kandarakis E, Panidis D, Goodarzi MO, Azziz R, Zhang Y, James RG, Olivier M, Kissebah AH, Reproductive Medicine N, Stener-Victorin E, Legro RS, Dunaif A. Genome-wide association of polycystic ovary syndrome implicates alterations in gonadotropin secretion in European ancestry populations. Nat Commun. 2015;6:7502. Epub 2015/08/19. doi: 10.1038/ncomms8502. PubMed PMID: 26284813; PubMed Central PMCID: PMC4557132.
55. Day FR, Hinds DA, Tung JY, Stolk L, Styrkarsdottir U, Saxena R, Bjonnes A, Broer L, Dunger DB, Halldorsson BV, Lawlor DA, Laval G, Mathieson I, McCardle WL, Louwers Y, Meun C, Ring S, Scott RA, Sulem P, Uitterlinden AG, Wareham NJ, Thorsteinsdottir U, Welt C, Stefansson K, Laven JS, Ong KK, Perry JR. Causal mechanisms and balancing selection inferred from genetic associations with polycystic ovary syndrome. Nat Commun. 2015;6:8464. Epub 2015/09/30. doi: 10.1038/ncomms9464. PubMed PMID: 26416764; PubMed Central PMCID: PMC4598835.
56. Manolio TA, Collins FS, Cox NJ, Goldstein DB, Hindorff LA, Hunter DJ, McCarthy MI, Ramos EM, Cardon LR, Chakravarti A, Cho JH, Guttmacher AE, Kong A, Kruglyak L, Mardis E, Rotimi CN, Slatkin M, Valle D, Whittemore AS, Boehnke M, Clark AG, Eichler EE, Gibson G, Haines JL, Mackay TF, McCarroll SA, Visscher PM. Finding the missing heritability of complex diseases. Nature. 2009;461(7265):747-53. doi: 10.1038/nature08494. PubMed PMID: 19812666; PubMed Central PMCID: PMC2831613.

57. Lee H, Oh JY, Sung YA, Chung H, Kim HL, Kim GS, Cho YS, Kim JT. Genome-wide association study identified new susceptibility loci for polycystic ovary syndrome. Human Reproduction. 2015;30(3):723-31. doi: 10.1093/humrep/deu352. PubMed PMID: 25574032.
58. Hirschhorn JN, Daly MJ. Genome-wide association studies for common diseases and complex traits. Nat Rev Genet. 2005;6(2):95-108. Epub 2005/02/18. doi: 10.1038/nrg1521. PubMed PMID: 15716906.
59. Iyengar SK, Elston RC. The genetic basis of complex traits: rare variants or "common gene, common disease"? Methods Mol Biol. 2007;376:71-84. Epub 2007/11/07. doi: 10.1007/978-1-59745-389-9_6. PubMed PMID: 17984539.
60. Schork NJ, Murray SS, Frazer KA, Topol EJ. Common vs. rare allele hypotheses for complex diseases. Curr Opin Genet Dev. 2009;19(3):212-9. Epub 2009/06/02. doi: 10.1016/j.gde.2009.04.010. PubMed PMID: 19481926; PubMed Central PMCID: PMC2914559.
61. Smith DJ, Lusis AJ. The allelic structure of common disease. Hum Mol Genet. 2002;11(20):2455-61. Epub 2002/09/28. PubMed PMID: 12351581.
62. Li B, Liu DJ, Leal SM. Identifying rare variants associated with complex traits via sequencing. Curr Protoc Hum Genet. 2013;Chapter 1:Unit 1 26. Epub 2013/07/16. doi: 10.1002/0471142905.hg0126s78. PubMed PMID: 23853079; PubMed Central PMCID: PMC3830981.
63. Florez JC, Sjogren M, Burtt N, Orho-Melander M, Schayer S, Sun M, Almgren P, Lindblad U, Tuomi T, Gaudet D, Hudson TJ, Daly MJ, Ardlie KG, Hirschhorn JN, Altshuler D, Groop L. Association testing in 9,000 people fails to confirm the association of the insulin receptor substrate-1 G972R polymorphism with type 2 diabetes. Diabetes. 2004;53(12):3313-8. PubMed PMID: 15561965.
64. Sanger F, Nicklen S, Coulson AR. DNA sequencing with chain-terminating inhibitors. Proc Natl Acad Sci U S A. 1977;74(12):5463-7. Epub 1977/12/01. PubMed PMID: 271968; PubMed Central PMCID: PMC431765.
65. Metzker ML. Sequencing technologies - the next generation. Nat Rev Genet. 2010;11(1):31-46. Epub 2009/12/10. doi: 10.1038/nrg2626. PubMed PMID: 19997069.
66. Shendure J, Ji H. Next-generation DNA sequencing. Nat Biotechnol. 2008;26(10):1135-45. Epub 2008/10/11. doi: 10.1038/nbt1486. PubMed PMID: 18846087.
67. Lazaridis KN, McAllister TM, Babovic-Vuksanovic D, Beck SA, Borad MJ, Bryce AH, Chanan-Khan AA, Ferber MJ, Fonseca R, Johnson KJ, Klee EW, Lindor NM, McCormick JB, McWilliams RR, Parker AS, Riegert-Johnson DL, Rohrer Vitek CR, Schahl KA, Schultz C, Stewart K, Then GC, Wieben ED, Farrugia G. Implementing individualized medicine into the medical practice. Am J Med Genet C Semin Med Genet. 2014;166C(1):15-23. Epub 2014/03/13. doi: 10.1002/ajmg.c.31387. PubMed PMID: 24616301.
68. Manolio TA, Chisholm RL, Ozenberger B, Roden DM, Williams MS, Wilson R, Bick D, Bottinger EP, Brilliant MH, Eng C, Frazer KA, Korf B, Ledbetter DH, Lupski JR, Marsh C, Mrazek D, Murray MF, O'Donnell PH, Rader DJ, Relling MV, Shuldiner AR, Valle D, Weinshilboum R, Green ED, Ginsburg GS. Implementing genomic medicine in the clinic: the future is here. Genet Med. 2013;15(4):258-67. Epub 2013/01/12. doi: 10.1038/gim.2012.157. PubMed PMID: 23306799; PubMed Central PMCID: PMC3835144.
69. Menezes MP, Waddell L, Lenk GM, Kaur S, MacArthur DG, Meisler MH, Clarke NF. Whole exome sequencing identifies three recessive FIG4 mutations in an apparently dominant pedigree with Charcot-Marie-Tooth disease. Neuromuscul Disord. 2014;24(8):666-70. Epub

2014/06/01. doi: 10.1016/j.nmd.2014.04.010. PubMed PMID: 24878229; PubMed Central PMCID: PMC4096049.
70. Worthey EA, Mayer AN, Syverson GD, Helbling D, Bonacci BB, Decker B, Serpe JM, Dasu T, Tschannen MR, Veith RL, Basehore MJ, Broeckel U, Tomita-Mitchell A, Arca MJ, Casper JT, Margolis DA, Bick DP, Hessner MJ, Routes JM, Verbsky JW, Jacob HJ, Dimmock DP. Making a definitive diagnosis: successful clinical application of whole exome sequencing in a child with intractable inflammatory bowel disease. Genet Med. 2011;13(3):255-62. Epub 2010/12/22. doi: 10.1097/GIM.0b013e3182088158. PubMed PMID: 21173700.
71. Ng SB, Buckingham KJ, Lee C, Bigham AW, Tabor HK, Dent KM, Huff CD, Shannon PT, Jabs EW, Nickerson DA, Shendure J, Bamshad MJ. Exome sequencing identifies the cause of a mendelian disorder. Nat Genet. 2010;42(1):30-5. Epub 2009/11/17. doi: 10.1038/ng.499. PubMed PMID: 19915526; PubMed Central PMCID: PMC2847889.
72. Tacik P, Guthrie KJ, Strongosky AJ, Broderick DF, Riegert-Johnson DL, Tang S, El-Khechen D, Parker AS, Ross OA, Wszolek ZK. Whole-exome sequencing as a diagnostic tool in a family with episodic ataxia type 1. Mayo Clin Proc. 2015;90(3):366-71. Epub 2015/02/11. doi: 10.1016/j.mayocp.2015.01.001. PubMed PMID: 25659636; PubMed Central PMCID: PMC4354704.
73. Eltzschig HK, Robson SC. NT5E mutations and arterial calcifications. N Engl J Med. 2011;364(16):1577-8; author reply 9-80. Epub 2011/04/22. doi: 10.1056/NEJMc1102515#SA1. PubMed PMID: 21506753.
74. Sallman Almen M, Rask-Andersen M, Jacobsson JA, Ameur A, Kalnina I, Moschonis G, Juhlin S, Bringeland N, Hedberg LA, Ignatovica V, Chrousos GP, Manios Y, Klovins J, Marcus C, Gyllensten U, Fredriksson R, Schioth HB. Determination of the obesity-associated gene variants within the entire FTO gene by ultra-deep targeted sequencing in obese and lean children. Int J Obes (Lond). 2013;37(3):424-31. Epub 2012/04/26. doi: 10.1038/ijo.2012.57. PubMed PMID: 22531089; PubMed Central PMCID: PMC3595467.
75. Bonnefond A, Clement N, Fawcett K, Yengo L, Vaillant E, Guillaume JL, Dechaume A, Payne F, Roussel R, Czernichow S, Hercberg S, Hadjadj S, Balkau B, Marre M, Lantieri O, Langenberg C, Bouatia-Naji N, Meta-Analysis of G, Insulin-Related Traits C, Charpentier G, Vaxillaire M, Rocheleau G, Wareham NJ, Sladek R, McCarthy MI, Dina C, Barroso I, Jockers R, Froguel P. Rare MTNR1B variants impairing melatonin receptor 1B function contribute to type 2 diabetes. Nat Genet. 2012;44(3):297-301. Epub 2012/01/31. doi: 10.1038/ng.1053. PubMed PMID: 22286214; PubMed Central PMCID: PMC3773908.
76. Rivas MA, Beaudoin M, Gardet A, Stevens C, Sharma Y, Zhang CK, Boucher G, Ripke S, Ellinghaus D, Burtt N, Fennell T, Kirby A, Latiano A, Goyette P, Green T, Halfvarson J, Haritunians T, Korn JM, Kuruvilla F, Lagace C, Neale B, Lo KS, Schumm P, Torkvist L, National Institute of D, Digestive Kidney Diseases Inflammatory Bowel Disease Genetics C, United Kingdom Inflammatory Bowel Disease Genetics C, International Inflammatory Bowel Disease Genetics C, Dubinsky MC, Brant SR, Silverberg MS, Duerr RH, Altshuler D, Gabriel S, Lettre G, Franke A, D'Amato M, McGovern DP, Cho JH, Rioux JD, Xavier RJ, Daly MJ. Deep resequencing of GWAS loci identifies independent rare variants associated with inflammatory bowel disease. Nat Genet. 2011;43(11):1066-73. Epub 2011/10/11. doi: 10.1038/ng.952. PubMed PMID: 21983784; PubMed Central PMCID: PMC3378381.
77. Han J, Ryu S, Moskowitz DM, Rothenberg D, Leahy DJ, Atzmon G, Barzilai N, Suh Y. Discovery of novel non-synonymous SNP variants in 988 candidate genes from 6 centenarians

by target capture and next-generation sequencing. Mech Ageing Dev. 2013;134(10):478-85. Epub 2013/02/05. doi: 10.1016/j.mad.2013.01.005. PubMed PMID: 23376243; PubMed Central PMCID: PMC3787996.
78. Rees MG, Raimondo A, Wang J, Ban MR, Davis MI, Barrett A, Ranft J, Jagdhuhn D, Waterstradt R, Baltrusch S, Simeonov A, Collins FS, Hegele RA, Gloyn AL. Inheritance of rare functional GCKR variants and their contribution to triglyceride levels in families. Human Molecular Genetics. 2014;23(20):5570-8. doi: 10.1093/hmg/ddu269. PubMed PMID: 24879641; PubMed Central PMCID: PMCPMC4168830.
79. Majithia AR, Flannick J, Shahinian P, Guo M, Bray MA, Fontanillas P, Gabriel SB, Go TDC, Project NJFAS, Consortium STD, Consortium TDG, Rosen ED, Altshuler D. Rare variants in PPARG with decreased activity in adipocyte differentiation are associated with increased risk of type 2 diabetes. Proceedings of the National Academy of Sciences of the United States of America. 2014;111(36):13127-32. doi: 10.1073/pnas.1410428111. PubMed PMID: 25157153; PubMed Central PMCID: PMCPMC4246964.
80. Pastor CL, Griffin-Korf ML, Aloi JA, Evans WS, Marshall JC. Polycystic ovary syndrome: evidence for reduced sensitivity of the gonadotropin-releasing hormone pulse generator to inhibition by estradiol and progesterone. J Clin Endocrinol Metab. 1998;83(2):582-90. Epub 1998/02/19. doi: 10.1210/jcem.83.2.4604. PubMed PMID: 9467578.
81. Diamanti-Kandarakis E. Polycystic ovarian syndrome: pathophysiology, molecular aspects and clinical implications. Expert Rev Mol Med. 2008;10:e3. Epub 2008/01/31. doi: 10.1017/S1462399408000598. PubMed PMID: 18230193.
82. Baculescu N. The role of androgen receptor activity mediated by the CAG repeat polymorphism in the pathogenesis of PCOS. J Med Life. 2013;6(1):18-25. Epub 2013/04/20. PubMed PMID: 23599814; PubMed Central PMCID: PMC3624640.
83. Chang RJ. The reproductive phenotype in polycystic ovary syndrome. Nat Clin Pract Endocrinol Metab. 2007;3(10):688-95. Epub 2007/09/26. doi: 10.1038/ncpendmet0637. PubMed PMID: 17893687.
84. Pellatt L, Hanna L, Brincat M, Galea R, Brain H, Whitehead S, Mason H. Granulosa cell production of anti-Mullerian hormone is increased in polycystic ovaries. J Clin Endocrinol Metab. 2007;92(1):240-5. Epub 2006/10/26. doi: 10.1210/jc.2006-1582. PubMed PMID: 17062765.
85. Dumont A, Robin G, Catteau-Jonard S, Dewailly D. Role of Anti-Mullerian Hormone in pathophysiology, diagnosis and treatment of Polycystic Ovary Syndrome: a review. Reproductive Biology & Endocrinology. 2015;13:137. doi: 10.1186/s12958-015-0134-9. PubMed PMID: 26691645; PubMed Central PMCID: PMCPMC4687350.
86. Rajpert-De Meyts E, Jorgensen N, Graem N, Muller J, Cate RL, Skakkebaek NE. Expression of anti-Mullerian hormone during normal and pathological gonadal development: association with differentiation of Sertoli and granulosa cells. J Clin Endocrinol Metab. 1999;84(10):3836-44. Epub 1999/10/16. doi: 10.1210/jcem.84.10.6047. PubMed PMID: 10523039.
87. Weenen C, Laven JS, Von Bergh AR, Cranfield M, Groome NP, Visser JA, Kramer P, Fauser BC, Themmen AP. Anti-Mullerian hormone expression pattern in the human ovary: potential implications for initial and cyclic follicle recruitment. Mol Hum Reprod. 2004;10(2):77-83. Epub 2004/01/27. PubMed PMID: 14742691.

88. Pellatt L, Rice S, Dilaver N, Heshri A, Galea R, Brincat M, Brown K, Simpson ER, Mason HD. Anti-Mullerian hormone reduces follicle sensitivity to follicle-stimulating hormone in human granulosa cells. Fertil Steril. 2011;96(5):1246-51 e1. Epub 2011/09/16. doi: 10.1016/j.fertnstert.2011.08.015. PubMed PMID: 21917251.
89. Carmina E. Reproductive System Outcome Among Patients with Polycystic Ovarian Syndrome. Endocrinol Metab Clin North Am. 2015;44(4):787-97. Epub 2015/11/17. doi: 10.1016/j.ecl.2015.07.006. PubMed PMID: 26568493.
90. Pigny P, Merlen E, Robert Y, Cortet-Rudelli C, Decanter C, Jonard S, Dewailly D. Elevated serum level of anti-mullerian hormone in patients with polycystic ovary syndrome: relationship to the ovarian follicle excess and to the follicular arrest. J Clin Endocrinol Metab. 2003;88(12):5957-62. Epub 2003/12/13. doi: 10.1210/jc.2003-030727. PubMed PMID: 14671196.
91. Dewailly D, Gronier H, Poncelet E, Robin G, Leroy M, Pigny P, Duhamel A, Catteau-Jonard S. Diagnosis of polycystic ovary syndrome (PCOS): revisiting the threshold values of follicle count on ultrasound and of the serum AMH level for the definition of polycystic ovaries. Hum Reprod. 2011;26(11):3123-9. Epub 2011/09/20. doi: 10.1093/humrep/der297. PubMed PMID: 21926054.
92. Eilertsen TB, Vanky E, Carlsen SM. Anti-Mullerian hormone in the diagnosis of polycystic ovary syndrome: can morphologic description be replaced? Hum Reprod. 2012;27(8):2494-502. Epub 2012/06/14. doi: 10.1093/humrep/des213. PubMed PMID: 22693172.
93. Piltonen T, Morin-Papunen L, Koivunen R, Perheentupa A, Ruokonen A, Tapanainen JS. Serum anti-Mullerian hormone levels remain high until late reproductive age and decrease during metformin therapy in women with polycystic ovary syndrome. Hum Reprod. 2005;20(7):1820-6. Epub 2005/04/02. doi: 10.1093/humrep/deh850. PubMed PMID: 15802325.
94. Iliodromiti S, Kelsey TW, Anderson RA, Nelson SM. Can anti-Mullerian hormone predict the diagnosis of polycystic ovary syndrome? A systematic review and meta-analysis of extracted data. J Clin Endocrinol Metab. 2013;98(8):3332-40. Epub 2013/06/19. doi: 10.1210/jc.2013-1393. PubMed PMID: 23775353.
95. Christiansen SC, Eilertsen TB, Vanky E, Carlsen SM. Does AMH Reflect Follicle Number Similarly in Women with and without PCOS? PLoS One. 2016;11(1):e0146739. Epub 2016/01/23. doi: 10.1371/journal.pone.0146739. PubMed PMID: 26799212; PubMed Central PMCID: PMC4723054.
96. Kucera R, Babuska V, Ulcova-Gallova Z, Kulda V, Topolcan O. Follicular fluid levels of anti-Mullerian hormone, insulin-like growth factor 1 and leptin in women with fertility disorders. Syst Biol Reprod Med. 2018:1-4. Epub 2018/03/30. doi: 10.1080/19396368.2018.1450906. PubMed PMID: 29595066.
97. Stracquadanio M, Ciotta L, Palumbo MA. Relationship between serum anti-Mullerian hormone and intrafollicular AMH levels in PCOS women. Gynecol Endocrinol. 2018;34(3):223-8. Epub 2017/09/26. doi: 10.1080/09513590.2017.1381838. PubMed PMID: 28944702.
98. Recabarren SE, Sir-Petermann T, Rios R, Maliqueo M, Echiburu B, Smith R, Rojas-Garcia P, Recabarren M, Rey RA. Pituitary and testicular function in sons of women with polycystic ovary syndrome from infancy to adulthood. Journal of Clinical Endocrinology & Metabolism. 2008;93(9):3318-24. doi: 10.1210/jc.2008-0255. PubMed PMID: 18544620.

99. Jamil AS, Alalaf SK, Al-Tawil NG, Al-Shawaf T. Comparison of clinical and hormonal characteristics among four phenotypes of polycystic ovary syndrome based on the Rotterdam criteria. Arch Gynecol Obstet. 2015. Epub 2015/09/27. doi: 10.1007/s00404-015-3889-5. PubMed PMID: 26408006.
100. Knight PG, Glister C. TGF-beta superfamily members and ovarian follicle development. Reproduction. 2006;132(2):191-206. Epub 2006/08/04. doi: 10.1530/rep.1.01074. PubMed PMID: 16885529.
101. Carlsson IB, Scott JE, Visser JA, Ritvos O, Themmen AP, Hovatta O. Anti-Mullerian hormone inhibits initiation of growth of human primordial ovarian follicles in vitro. Hum Reprod. 2006;21(9):2223-7. Epub 2006/05/25. doi: 10.1093/humrep/del165. PubMed PMID: 16720622.
102. Durlinger AL, Visser JA, Themmen AP. Regulation of ovarian function: the role of anti-Mullerian hormone. Reproduction. 2002;124(5):601-9. Epub 2002/11/06. PubMed PMID: 12416998.
103. Durlinger AL, Kramer P, Karels B, de Jong FH, Uilenbroek JT, Grootegoed JA, Themmen AP. Control of primordial follicle recruitment by anti-Mullerian hormone in the mouse ovary. Endocrinology. 1999;140(12):5789-96. Epub 1999/12/01. doi: 10.1210/endo.140.12.7204. PubMed PMID: 10579345.
104. Durlinger AL, Gruijters MJ, Kramer P, Karels B, Ingraham HA, Nachtigal MW, Uilenbroek JT, Grootegoed JA, Themmen AP. Anti-Mullerian hormone inhibits initiation of primordial follicle growth in the mouse ovary. Endocrinology. 2002;143(3):1076-84. Epub 2002/02/28. doi: 10.1210/endo.143.3.8691. PubMed PMID: 11861535.
105. Rouiller-Fabre V, Carmona S, Merhi RA, Cate R, Habert R, Vigier B. Effect of anti-Mullerian hormone on Sertoli and Leydig cell functions in fetal and immature rats. Endocrinology. 1998;139(3):1213-20. Epub 1998/03/10. doi: 10.1210/endo.139.3.5785. PubMed PMID: 9492056.
106. Chang HM, Klausen C, Leung PC. Antimullerian hormone inhibits follicle-stimulating hormone-induced adenylyl cyclase activation, aromatase expression, and estradiol production in human granulosa-lutein cells. Fertil Steril. 2013;100(2):585-92 e1. Epub 2013/05/15. doi: 10.1016/j.fertnstert.2013.04.019. PubMed PMID: 23663993.
107. Schmidt KL, Kryger-Baggesen N, Byskov AG, Andersen CY. Anti-Mullerian hormone initiates growth of human primordial follicles in vitro. Mol Cell Endocrinol. 2005;234(1-2):87-93. Epub 2005/04/20. doi: 10.1016/j.mce.2004.12.010. PubMed PMID: 15836957.
108. Campbell BK, Clinton M, Webb R. The role of anti-Mullerian hormone (AMH) during follicle development in a monovulatory species (sheep). Endocrinology. 2012;153(9):4533-43. doi: 10.1210/en.2012-1158. PubMed PMID: 22778215.
109. Teixeira J, Fynn-Thompson E, Payne AH, Donahoe PK. Mullerian-inhibiting substance regulates androgen synthesis at the transcriptional level. Endocrinology. 1999;140(10):4732-8. Epub 1999/09/28. doi: 10.1210/endo.140.10.7075. PubMed PMID: 10499532.
110. Trbovich AM, Sluss PM, Laurich VM, O'Neill FH, MacLaughlin DT, Donahoe PK, Teixeira J. Mullerian Inhibiting Substance lowers testosterone in luteinizing hormone-stimulated rodents. Proc Natl Acad Sci U S A. 2001;98(6):3393-7. Epub 2001/03/15. doi: 10.1073/pnas.051632298. PubMed PMID: 11248089; PubMed Central PMCID: PMC30664.

111. Teixeira J, Maheswaran S, Donahoe PK. Mullerian inhibiting substance: an instructive developmental hormone with diagnostic and possible therapeutic applications. Endocrine Reviews. 2001;22(5):657-74. doi: 10.1210/edrv.22.5.0445. PubMed PMID: 11588147.
112. Skaar KS, Nobrega RH, Magaraki A, Olsen LC, Schulz RW, Male R. Proteolytically activated, recombinant anti-mullerian hormone inhibits androgen secretion, proliferation, and differentiation of spermatogonia in adult zebrafish testis organ cultures. Endocrinology. 2011;152(9):3527-40. Epub 2011/07/14. doi: 10.1210/en.2010-1469. PubMed PMID: 21750047.
113. Kano M, Sosulski AE, Zhang L, Saatcioglu HD, Wang D, Nagykery N, Sabatini ME, Gao G, Donahoe PK, Pepin D. AMH/MIS as a contraceptive that protects the ovarian reserve during chemotherapy. Proceedings of the National Academy of Sciences of the United States of America. 2017;114(9):E1688-E97. doi: 10.1073/pnas.1620729114. PubMed PMID: 28137855.
114. Crisosto N, Sir-Petermann T, Greiner M, Maliqueo M, Moreno M, Aedo P, Lara HE. Testosterone-induced downregulation of anti-Mullerian hormone expression in granulosa cells from small bovine follicles. Endocrine. 2009;36(2):339-45. Epub 2009/08/29. doi: 10.1007/s12020-009-9227-6. PubMed PMID: 19714502.
115. Laird M, Thomson K, Fenwick M, Mora J, Franks S, Hardy K. Androgen Stimulates Growth of Mouse Preantral Follicles In Vitro: Interaction With Follicle-Stimulating Hormone and With Growth Factors of the TGFbeta Superfamily. Endocrinology. 2017;158(4):920-35. Epub 2017/03/23. doi: 10.1210/en.2016-1538. PubMed PMID: 28324051; PubMed Central PMCID: PMC5460807.
116. Hutson JM, Grover SR, O'Connell M, Pennell SD. Malformation syndromes associated with disorders of sex development. Nat Rev Endocrinol. 2014;10(8):476-87. Epub 2014/06/11. doi: 10.1038/nrendo.2014.83. PubMed PMID: 24913517.
117. Bedecarrats GY, O'Neill FH, Norwitz ER, Kaiser UB, Teixeira J. Regulation of gonadotropin gene expression by Mullerian inhibiting substance. Proc Natl Acad Sci U S A. 2003;100(16):9348-53. Epub 2003/07/25. doi: 10.1073/pnas.1633592100. PubMed PMID: 12878721; PubMed Central PMCID: PMC170921.
118. Josso N, Rey RA, Picard JY. Anti-mullerian hormone: a valuable addition to the toolbox of the pediatric endocrinologist. Int J Endocrinol. 2013;2013:674105. doi: 10.1155/2013/674105. PubMed PMID: 24382961; PubMed Central PMCID: PMCPMC3870610.
119. Josso N, Belville C, di Clemente N, Picard JY. AMH and AMH receptor defects in persistent Mullerian duct syndrome. Hum Reprod Update. 2005;11(4):351-6. Epub 2005/05/10. doi: 10.1093/humupd/dmi014. PubMed PMID: 15878900.
120. Picard JY, Cate RL, Racine C, Josso N. The Persistent Mullerian Duct Syndrome: An Update Based Upon a Personal Experience of 157 Cases. Sex Dev. 2017;11(3):109-25. Epub 2017/05/22. doi: 10.1159/000475516. PubMed PMID: 28528332.
121. Belville C, Josso N, Picard JY. Persistence of Mullerian derivatives in males. American Journal of Medical Genetics. 1999;89(4):218-23. PubMed PMID: 10727997.
122. Belville C, Van Vlijmen H, Ehrenfels C, Pepinsky B, Rezaie AR, Picard JY, Josso N, di Clemente N, Cate RL. Mutations of the anti-mullerian hormone gene in patients with persistent mullerian duct syndrome: biosynthesis, secretion, and processing of the abnormal proteins and analysis using a three-dimensional model. Mol Endocrinol. 2004;18(3):708-21. Epub 2003/12/16. doi: 10.1210/me.2003-0358. PubMed PMID: 14673134.

123. Mazen I, Abdel Hamid MS, El-Gammal M, Aref A, Amr K. AMH gene mutations in two Egyptian families with persistent mullerian duct syndrome. Sex Dev. 2011;5(6):277-80. Epub 2011/12/23. doi: 10.1159/000334854. PubMed PMID: 22188863.
124. Lee MM, Donahoe PK, Hasegawa T, Silverman B, Crist GB, Best S, Hasegawa Y, Noto RA, Schoenfeld D, MacLaughlin DT. Mullerian inhibiting substance in humans: normal levels from infancy to adulthood. J Clin Endocrinol Metab. 1996;81(2):571-6. Epub 1996/02/01. doi: 10.1210/jcem.81.2.8636269. PubMed PMID: 8636269.
125. Pankhurst MW, McLennan IS. Human blood contains both the uncleaved precursor of anti-Mullerian hormone and a complex of the NH2- and COOH-terminal peptides. American Journal of Physiology - Endocrinology & Metabolism. 2013;305(10):E1241-7. doi: 10.1152/ajpendo.00395.2013. PubMed PMID: 24045871.
126. Shi M, Zhu J, Wang R, Chen X, Mi L, Walz T, Springer TA. Latent TGF-beta structure and activation. Nature. 2011;474(7351):343-9. doi: 10.1038/nature10152. PubMed PMID: 21677751; PubMed Central PMCID: PMCPMC4717672.
127. Mi LZ, Brown CT, Gao Y, Tian Y, Le VQ, Walz T, Springer TA. Structure of bone morphogenetic protein 9 procomplex. Proceedings of the National Academy of Sciences of the United States of America. 2015;112(12):3710-5. doi: 10.1073/pnas.1501303112. PubMed PMID: 25751889; PubMed Central PMCID: PMCPMC4378411.
128. Wang X, Fischer G, Hyvonen M. Structure and activation of pro-activin A. Nature communications. 2016;7:12052. doi: 10.1038/ncomms12052. PubMed PMID: 27373274; PubMed Central PMCID: PMCPMC4932183.
129. Pepinsky RB, Sinclair LK, Chow EP, Mattaliano RJ, Manganaro TF, Donahoe PK, Cate RL. Proteolytic processing of mullerian inhibiting substance produces a transforming growth factor-beta-like fragment. J Biol Chem. 1988;263(35):18961-4. Epub 1988/12/15. PubMed PMID: 2974034.
130. Papakostas TD, Pieretti-Vanmarcke R, Nicolaou F, Thanos A, Trichonas G, Koufomichali X, Anago K, Donahoe PK, Teixeira J, MacLaughlin DT, Vavvas D. Development of an efficiently cleaved, bioactive, highly pure FLAG-tagged recombinant human Mullerian Inhibiting Substance. Protein Expr Purif. 2010;70(1):32-8. Epub 2009/09/17. doi: 10.1016/j.pep.2009.09.004. PubMed PMID: 19755162; PubMed Central PMCID: PMC3581853.
131. Salazar VS, Gamer LW, Rosen V. BMP signalling in skeletal development, disease and repair. Nat Rev Endocrinol. 2016;12(4):203-21. Epub 2016/02/20. doi: 10.1038/nrendo.2016.12. PubMed PMID: 26893264.
132. Catlin EA, Ezzell RM, Donahoe PK, Manganaro TF, Ebb RG, MacLaughlin DT. Mullerian inhibiting substance binding and uptake. Developmental Dynamics. 1992;193(4):295-9. doi: 10.1002/aja.1001930402. PubMed PMID: 1511169.
133. Wang T, Li BY, Danielson PD, Shah PC, Rockwell S, Lechleider RJ, Martin J, Manganaro T, Donahoe PK. The immunophilin FKBP12 functions as a common inhibitor of the TGF beta family type I receptors. Cell. 1996;86(3):435-44. PubMed PMID: 8756725.
134. Gordon KJ, Blobe GC. Role of transforming growth factor-beta superfamily signaling pathways in human disease. Biochim Biophys Acta. 2008;1782(4):197-228. Epub 2008/03/04. doi: 10.1016/j.bbadis.2008.01.006. PubMed PMID: 18313409.
135. Raja-Khan N, Urbanek M, Rodgers RJ, Legro RS. The role of TGF-beta in polycystic ovary syndrome. Reprod Sci. 2014;21(1):20-31. Epub 2013/04/16. doi: 10.1177/1933719113485294. PubMed PMID: 23585338.

136. Innis CA, Shi J, Blundell TL. Evolutionary trace analysis of TGF-beta and related growth factors: implications for site-directed mutagenesis. Protein Eng. 2000;13(12):839-47. PubMed PMID: 11239083.
137. di Clemente N, Wilson C, Faure E, Boussin L, Carmillo P, Tizard R, Picard JY, Vigier B, Josso N, Cate R. Cloning, expression, and alternative splicing of the receptor for anti-Mullerian hormone. Molecular Endocrinology. 1994;8(8):1006-20. doi: 10.1210/mend.8.8.7997230. PubMed PMID: 7997230.
138. Kristensen SG, Andersen K, Clement CA, Franks S, Hardy K, Andersen CY. Expression of TGF-beta superfamily growth factors, their receptors, the associated SMADs and antagonists in five isolated size-matched populations of pre-antral follicles from normal human ovaries. Mol Hum Reprod. 2014;20(4):293-308. Epub 2013/11/26. doi: 10.1093/molehr/gat089. PubMed PMID: 24270394.
139. Baarends WM, van Helmond MJ, Post M, van der Schoot PJ, Hoogerbrugge JW, de Winter JP, Uilenbroek JT, Karels B, Wilming LG, Meijers JH, et al. A novel member of the transmembrane serine/threonine kinase receptor family is specifically expressed in the gonads and in mesenchymal cells adjacent to the mullerian duct. Development. 1994;120(1):189-97. PubMed PMID: 8119126.
140. Clarke TR, Hoshiya Y, Yi SE, Liu X, Lyons KM, Donahoe PK. Mullerian inhibiting substance signaling uses a bone morphogenetic protein (BMP)-like pathway mediated by ALK2 and induces SMAD6 expression. Molecular Endocrinology. 2001;15(6):946-59. doi: 10.1210/mend.15.6.0664. PubMed PMID: 11376113.
141. Jamin SP, Arango NA, Mishina Y, Hanks MC, Behringer RR. Requirement of Bmpr1a for Mullerian duct regression during male sexual development. Nature Genetics. 2002;32(3):408-10. doi: 10.1038/ng1003. PubMed PMID: 12368913.
142. Renlund N, Pieretti-Vanmarcke R, O'Neill FH, Zhang L, Donahoe PK, Teixeira J. c-Jun N-terminal kinase inhibitor II (SP600125) activates Mullerian inhibiting substance type II receptor-mediated signal transduction. Endocrinology. 2008;149(1):108-15. doi: 10.1210/en.2007-0529. PubMed PMID: 17947357; PubMed Central PMCID: PMC2194615.
143. Massague J, Wotton D. Transcriptional control by the TGF-beta/Smad signaling system. EMBO J. 2000;19(8):1745-54. Epub 2000/04/25. doi: 10.1093/emboj/19.8.1745. PubMed PMID: 10775259; PubMed Central PMCID: PMC302010.
144. Rocha A, Zanuy S, Gomez A. Conserved Anti-Mullerian Hormone: Anti-Mullerian Hormone Type-2 Receptor Specific Interaction and Intracellular Signaling in Teleosts. Biol Reprod. 2016;94(6):141. Epub 2016/05/27. doi: 10.1095/biolreprod.115.137547. PubMed PMID: 27226310.
145. Zheng MX, Li Y, Hu R, Wang FM, Zhang XM, Guan B. Anti-Mullerian hormone gene polymorphism is associated with androgen levels in Chinese polycystic ovary syndrome patients with insulin resistance. J Assist Reprod Genet. 2016;33(2):199-205. Epub 2016/01/07. doi: 10.1007/s10815-015-0641-9. PubMed PMID: 26732661; PubMed Central PMCID: PMC4759001.
146. Yalamanchi SK, Sam S, Cardenas MO, Holaday LW, Urbanek M, Dunaif A. Association of fibrillin-3 and transcription factor-7-like 2 gene variants with metabolic phenotypes in PCOS. Obesity (Silver Spring). 2012;20(6):1273-8. Epub 2012/02/04. doi: 10.1038/oby.2011.400. PubMed PMID: 22301903; PubMed Central PMCID: PMC3346885.

147. Dunaif A. Perspectives in Polycystic Ovary Syndrome: From Hair to Eternity. J Clin Endocrinol Metab. 2016;101(3):759-68. Epub 2016/02/26. doi: 10.1210/jc.2015-3780. PubMed PMID: 26908109; PubMed Central PMCID: PMC4803161.
148. Kevenaar ME, Laven JS, Fong SL, Uitterlinden AG, de Jong FH, Themmen AP, Visser JA. A functional anti-mullerian hormone gene polymorphism is associated with follicle number and androgen levels in polycystic ovary syndrome patients. Journal of Clinical Endocrinology & Metabolism. 2008;93(4):1310-6. doi: 10.1210/jc.2007-2205. PubMed PMID: 18230658.
149. Kevenaar ME, Themmen AP, van Kerkwijk AJ, Valkenburg O, Uitterlinden AG, de Jong FH, Laven JS, Visser JA. Variants in the ACVR1 gene are associated with AMH levels in women with polycystic ovary syndrome. Human Reproduction. 2009;24(1):241-9. doi: 10.1093/humrep/den353. PubMed PMID: 18854405.
150. Georgopoulos NA, Karagiannidou E, Koika V, Roupas ND, Armeni A, Marioli D, Papadakis E, Welt CK, Panidis D. Increased frequency of the anti-mullerian-inhibiting hormone receptor 2 (AMHR2) 482 A>G polymorphism in women with polycystic ovary syndrome: relationship to luteinizing hormone levels. Journal of Clinical Endocrinology & Metabolism. 2013;98(11):E1866-70. doi: 10.1210/jc.2013-2458. PubMed PMID: 23969185.
151. Kaur R, Kaur T, Kaur A. Genetic association study from North India to analyze association of CYP19A1 and CYP17A1 with polycystic ovary syndrome. J Assist Reprod Genet. 2018. Epub 2018/03/23. doi: 10.1007/s10815-018-1162-0. PubMed PMID: 29564739.
152. Urbanek M, Legro RS, Driscoll DA, Azziz R, Ehrmann DA, Norman RJ, Strauss JF, 3rd, Spielman RS, Dunaif A. Thirty-seven candidate genes for polycystic ovary syndrome: strongest evidence for linkage is with follistatin. Proc Natl Acad Sci U S A. 1999;96(15):8573-8. Epub 1999/07/21. PubMed PMID: 10411917; PubMed Central PMCID: PMC17558.
153. Urbanek M. The genetics of the polycystic ovary syndrome. Nat Clin Pract Endocrinol Metab. 2007;3(2):103-11. Epub 2007/01/24. doi: 10.1038/ncpendmet0400. PubMed PMID: 17237837.
154. Franks S, Stark J, Hardy K. Follicle dynamics and anovulation in polycystic ovary syndrome. Hum Reprod Update. 2008;14(4):367-78. Epub 2008/05/24. doi: 10.1093/humupd/dmn015. PubMed PMID: 18499708.
155. McAllister JM, Modi B, Miller BA, Biegler J, Bruggeman R, Legro RS, Strauss JF, 3rd. Overexpression of a DENND1A isoform produces a polycystic ovary syndrome theca phenotype. Proc Natl Acad Sci U S A. 2014;111(15):E1519-27. Epub 2014/04/08. doi: 10.1073/pnas.1400574111. PubMed PMID: 24706793; PubMed Central PMCID: PMC3992676.
156. Zeggini E, Scott LJ, Saxena R, Voight BF, Marchini JL, Hu T, de Bakker PI, Abecasis GR, Almgren P, Andersen G, Ardlie K, Bostrom KB, Bergman RN, Bonnycastle LL, Borch-Johnsen K, Burtt NP, Chen H, Chines PS, Daly MJ, Deodhar P, Ding CJ, Doney AS, Duren WL, Elliott KS, Erdos MR, Frayling TM, Freathy RM, Gianniny L, Grallert H, Grarup N, Groves CJ, Guiducci C, Hansen T, Herder C, Hitman GA, Hughes TE, Isomaa B, Jackson AU, Jorgensen T, Kong A, Kubalanza K, Kuruvilla FG, Kuusisto J, Langenberg C, Lango H, Lauritzen T, Li Y, Lindgren CM, Lyssenko V, Marvelle AF, Meisinger C, Midthjell K, Mohlke KL, Morken MA, Morris AD, Narisu N, Nilsson P, Owen KR, Palmer CN, Payne F, Perry JR, Pettersen E, Platou C, Prokopenko I, Qi L, Qin L, Rayner NW, Rees M, Roix JJ, Sandbaek A, Shields B, Sjogren M, Steinthorsdottir V, Stringham HM, Swift AJ, Thorleifsson G, Thorsteinsdottir U, Timpson NJ, Tuomi T, Tuomilehto J, Walker M, Watanabe RM, Weedon MN, Willer CJ, Wellcome Trust Case Control C, Illig T, Hveem K, Hu FB, Laakso M, Stefansson K, Pedersen O, Wareham NJ,

Barroso I, Hattersley AT, Collins FS, Groop L, McCarthy MI, Boehnke M, Altshuler D. Meta-analysis of genome-wide association data and large-scale replication identifies additional susceptibility loci for type 2 diabetes. Nat Genet. 2008;40(5):638-45. Epub 2008/04/01. doi: 10.1038/ng.120. PubMed PMID: 18372903; PubMed Central PMCID: PMC2672416.
157. Semple RK, Savage DB, Cochran EK, Gorden P, O'Rahilly S. Genetic syndromes of severe insulin resistance. Endocrine Reviews. 2011;32(4):498-514. doi: 10.1210/er.2010-0020. PubMed PMID: 21536711.
158. Garg A, Misra A. Lipodystrophies: rare disorders causing metabolic syndrome. Endocrinol Metab Clin North Am. 2004;33(2):305-31. Epub 2004/05/26. doi: 10.1016/j.ecl.2004.03.003. PubMed PMID: 15158521.
159. Hegele RA, Joy TR, Al-Attar SA, Rutt BK. Thematic review series: Adipocyte Biology. Lipodystrophies: windows on adipose biology and metabolism. J Lipid Res. 2007;48(7):1433-44. Epub 2007/03/22. doi: 10.1194/jlr.R700004-JLR200. PubMed PMID: 17374881.
160. Capeau J, Magre J, Caron-Debarle M, Lagathu C, Antoine B, Bereziat V, Lascols O, Bastard JP, Vigouroux C. Human lipodystrophies: genetic and acquired diseases of adipose tissue. Endocr Dev. 2010;19:1-20. Epub 2010/06/17. doi: 10.1159/000316893. PubMed PMID: 20551664; PubMed Central PMCID: PMC3892722.
161. Wojtanik KM, Edgemon K, Viswanadha S, Lindsey B, Haluzik M, Chen W, Poy G, Reitman M, Londos C. The role of LMNA in adipose: a novel mouse model of lipodystrophy based on the Dunnigan-type familial partial lipodystrophy mutation. J Lipid Res. 2009;50(6):1068-79. Epub 2009/02/10. doi: 10.1194/jlr.M800491-JLR200. PubMed PMID: 19201734; PubMed Central PMCID: PMC2681389.
162. Hutchison CJ, Worman HJ. A-type lamins: guardians of the soma? Nat Cell Biol. 2004;6(11):1062-7. Epub 2004/11/02. doi: 10.1038/ncb1104-1062. PubMed PMID: 15517000.
163. Goldman RD, Goldman AE, Shumaker DK. Nuclear lamins: building blocks of nuclear structure and function. Novartis Found Symp. 2005;264:3-16; discussion -21, 227-30. Epub 2005/03/19. PubMed PMID: 15773744.
164. Capanni C, Mattioli E, Columbaro M, Lucarelli E, Parnaik VK, Novelli G, Wehnert M, Cenni V, Maraldi NM, Squarzoni S, Lattanzi G. Altered pre-lamin A processing is a common mechanism leading to lipodystrophy. Hum Mol Genet. 2005;14(11):1489-502. Epub 2005/04/22. doi: 10.1093/hmg/ddi158. PubMed PMID: 15843404.
165. Lloyd DJ, Trembath RC, Shackleton S. A novel interaction between lamin A and SREBP1: implications for partial lipodystrophy and other laminopathies. Hum Mol Genet. 2002;11(7):769-77. Epub 2002/04/04. PubMed PMID: 11929849.
166. Hosoe J, Kadowaki H, Miya F, Aizu K, Kawamura T, Miyata I, Satomura K, Ito T, Hara K, Tanaka M, Ishiura H, Tsuji S, Suzuki K, Takakura M, Boroevich KA, Tsunoda T, Yamauchi T, Shojima N, Kadowaki T. Structural Basis and Genotype-Phenotype Correlations of INSR Mutations Causing Severe Insulin Resistance. Diabetes. 2017;66(10):2713-23. Epub 2017/08/03. doi: 10.2337/db17-0301. PubMed PMID: 28765322.
167. Huang Z, Liu J, Ng K, Wan X, Xu L, He X, Liao Z, Li Y. Glimepiride treatment in a patient with type A insulin resistance syndrome due to a novel heterozygous missense mutation in the insulin receptor gene. J Diabetes Investig. 2018. Epub 2018/02/23. doi: 10.1111/jdi.12824. PubMed PMID: 29469970.
168. Qin L, Li X, Hou Q, Wang H, Lou G, Li T, Wang L, Liu H, Li X, Liao S. Novel heterozygous mutations of the INSR gene in a familial case of Donohue syndrome. Clin Chim

Acta. 2017;473:26-31. Epub 2017/08/15. doi: 10.1016/j.cca.2017.08.007. PubMed PMID: 28803747.
169. Chen X, Wang H, Wu B, Dong X, Liu B, Chen H, Lu Y, Zhou W, Yang L. One novel 2.43Kb deletion and one single nucleotide mutation of the INSR gene in a Chinese neonate with Rabson-Mendenhall syndrome. J Clin Res Pediatr Endocrinol. 2017. Epub 2017/10/31. doi: 10.4274/jcrpe.5080. PubMed PMID: 29082893.
170. Sinnarajah K, Dayasiri MB, Dissanayake ND, Kudagammana ST, Jayaweera AH. Rabson Mendenhall Syndrome caused by a novel missense mutation. Int J Pediatr Endocrinol. 2016;2016:21. Epub 2016/11/29. doi: 10.1186/s13633-016-0039-1. PubMed PMID: 27891155; PubMed Central PMCID: PMC5114824.
171. Moller DE, Flier JS. Detection of an alteration in the insulin-receptor gene in a patient with insulin resistance, acanthosis nigricans, and the polycystic ovary syndrome (type A insulin resistance). N Engl J Med. 1988;319(23):1526-9. Epub 1988/12/08. doi: 10.1056/NEJM198812083192306. PubMed PMID: 2460770.
172. Moller DE, Yokota A, White MF, Pazianos AG, Flier JS. A naturally occurring mutation of insulin receptor alanine 1134 impairs tyrosine kinase function and is associated with dominantly inherited insulin resistance. J Biol Chem. 1990;265(25):14979-85. Epub 1990/09/05. PubMed PMID: 2168397.
173. Taylor SI, Kadowaki T, Kadowaki H, Accili D, Cama A, McKeon C. Mutations in insulin-receptor gene in insulin-resistant patients. Diabetes Care. 1990;13(3):257-79. Epub 1990/03/01. PubMed PMID: 1968373.
174. Hojlund K. Metabolism and insulin signaling in common metabolic disorders and inherited insulin resistance. Dan Med J. 2014;61(7):B4890. Epub 2014/08/16. PubMed PMID: 25123125.
175. Hubbard SR. The insulin receptor: both a prototypical and atypical receptor tyrosine kinase. Cold Spring Harb Perspect Biol. 2013;5(3):a008946. Epub 2013/03/05. doi: 10.1101/cshperspect.a008946. PubMed PMID: 23457259; PubMed Central PMCID: PMC3578362.
176. Kim B, Feldman EL. Insulin resistance in the nervous system. Trends Endocrinol Metab. 2012;23(3):133-41. Epub 2012/01/17. doi: 10.1016/j.tem.2011.12.004. PubMed PMID: 22245457; PubMed Central PMCID: PMC3392648.
177. Chen ZJ, Shi YH, Zhao YR, Li Y, Tang R, Zhao LX, Chang ZH. [Correlation between single nucleotide polymorphism of insulin receptor gene with polycystic ovary syndrome]. Zhonghua Fu Chan Ke Za Zhi. 2004;39(9):582-5. Epub 2004/10/23. PubMed PMID: 15498182.
178. Siegel S, Futterweit W, Davies TF, Concepcion ES, Greenberg DA, Villanueva R, Tomer Y. A C/T single nucleotide polymorphism at the tyrosine kinase domain of the insulin receptor gene is associated with polycystic ovary syndrome. Fertil Steril. 2002;78(6):1240-3. Epub 2002/12/13. PubMed PMID: 12477518.
179. Legro RS, Spielman R, Urbanek M, Driscoll D, Strauss JF, 3rd, Dunaif A. Phenotype and genotype in polycystic ovary syndrome. Recent Progress in Hormone Research. 1998;53:217-56. PubMed PMID: 9769710.
180. Kircher M, Witten DM, Jain P, O'Roak BJ, Cooper GM, Shendure J. A general framework for estimating the relative pathogenicity of human genetic variants. Nat Genet. 2014;46(3):310-5. Epub 2014/02/04. doi: 10.1038/ng.2892. PubMed PMID: 24487276; PubMed Central PMCID: PMC3992975.

181. Adzhubei IA, Schmidt S, Peshkin L, Ramensky VE, Gerasimova A, Bork P, Kondrashov AS, Sunyaev SR. A method and server for predicting damaging missense mutations. Nat Methods. 2010;7(4):248-9. Epub 2010/04/01. doi: 10.1038/nmeth0410-248. PubMed PMID: 20354512; PubMed Central PMCID: PMC2855889.
182. Ng PC, Henikoff S. SIFT: Predicting amino acid changes that affect protein function. Nucleic Acids Research. 2003;31(13):3812-4. PubMed PMID: 12824425; PubMed Central PMCID: PMCPMC168916.
183. Davydov EV, Goode DL, Sirota M, Cooper GM, Sidow A, Batzoglou S. Identifying a high fraction of the human genome to be under selective constraint using GERP++. PLoS Computational Biology. 2010;6(12):e1001025. doi: 10.1371/journal.pcbi.1001025. PubMed PMID: 21152010; PubMed Central PMCID: PMCPMC2996323.
184. Shihab HA, Rogers MF, Gough J, Mort M, Cooper DN, Day IN, Gaunt TR, Campbell C. An integrative approach to predicting the functional effects of non-coding and coding sequence variation. Bioinformatics. 2015;31(10):1536-43. Epub 2015/01/15. doi: 10.1093/bioinformatics/btv009. PubMed PMID: 25583119; PubMed Central PMCID: PMC4426838.
185. Yang L, Munck M, Swaminathan K, Kapinos LE, Noegel AA, Neumann S. Mutations in LMNA modulate the lamin A--Nesprin-2 interaction and cause LINC complex alterations. PLoS One. 2013;8(8):e71850. Epub 2013/08/27. doi: 10.1371/journal.pone.0071850. PubMed PMID: 23977161; PubMed Central PMCID: PMC3748058.
186. Vigouroux C, Guenantin AC, Vatier C, Capel E, Dour CL, Afonso P, Bidault G, Bereziat V, Lascols O, Capeau J, Briand N, Jeru I. Lipodystrophic syndromes due to LMNA mutations: recent developments on biomolecular aspects, pathophysiological hypotheses and therapeutic perspectives. Nucleus. 2018:1-32. Epub 2018/03/27. doi: 10.1080/19491034.2018.1456217. PubMed PMID: 29578370.
187. Bonne G, Quijano-Roy S. Emery-Dreifuss muscular dystrophy, laminopathies, and other nuclear envelopathies. Handb Clin Neurol. 2013;113:1367-76. Epub 2013/04/30. doi: 10.1016/B978-0-444-59565-2.00007-1. PubMed PMID: 23622360.
188. Bonne G, Di Barletta MR, Varnous S, Becane HM, Hammouda EH, Merlini L, Muntoni F, Greenberg CR, Gary F, Urtizberea JA, Duboc D, Fardeau M, Toniolo D, Schwartz K. Mutations in the gene encoding lamin A/C cause autosomal dominant Emery-Dreifuss muscular dystrophy. Nat Genet. 1999;21(3):285-8. Epub 1999/03/18. doi: 10.1038/6799. PubMed PMID: 10080180.
189. Agarwal AK, Arioglu E, De Almeida S, Akkoc N, Taylor SI, Bowcock AM, Barnes RI, Garg A. AGPAT2 is mutated in congenital generalized lipodystrophy linked to chromosome 9q34. Nat Genet. 2002;31(1):21-3. Epub 2002/04/23. doi: 10.1038/ng880. PubMed PMID: 11967537.
190. Tobita T, Nomura S, Fujita T, Morita H, Asano Y, Onoue K, Ito M, Imai Y, Suzuki A, Ko T, Satoh M, Fujita K, Naito AT, Furutani Y, Toko H, Harada M, Amiya E, Hatano M, Takimoto E, Shiga T, Nakanishi T, Sakata Y, Ono M, Saito Y, Takashima S, Hagiwara N, Aburatani H, Komuro I. Genetic basis of cardiomyopathy and the genotypes involved in prognosis and left ventricular reverse remodeling. Sci Rep. 2018;8(1):1998. Epub 2018/02/02. doi: 10.1038/s41598-018-20114-9. PubMed PMID: 29386531; PubMed Central PMCID: PMC5792481.

191. Tazir M, Bellatache M, Nouioua S, Vallat JM. Autosomal recessive Charcot-Marie-Tooth disease: from genes to phenotypes. J Peripher Nerv Syst. 2013;18(2):113-29. Epub 2013/06/21. doi: 10.1111/jns5.12026. PubMed PMID: 23781959.
192. Hussain I, Patni N, Ueda M, Sorkina E, Valerio CM, Cochran E, Brown RJ, Peeden J, Tikhonovich Y, Tiulpakov A, Stender SRS, Klouda E, Tayeh MK, Innis JW, Meyer A, Lal P, Godoy-Matos AF, Teles MG, Adams-Huet B, Rader DJ, Hegele RA, Oral EA, Garg A. A Novel Generalized Lipodystrophy-Associated Progeroid Syndrome Due to Recurrent Heterozygous LMNA p.T10I Mutation. J Clin Endocrinol Metab. 2018;103(3):1005-14. Epub 2017/12/22. doi: 10.1210/jc.2017-02078. PubMed PMID: 29267953.
193. Villa F, Maciag A, Spinelli CC, Ferrario A, Carrizzo A, Parisi A, Torella A, Montenero C, Condorelli G, Vecchione C, Nigro V, Montenero AS, Puca AA. A G613A missense in the Hutchinson's progeria lamin A/C gene causes a lone, autosomal dominant atrioventricular block. Immun Ageing. 2014;11(1):19. Epub 2014/12/04. doi: 10.1186/s12979-014-0019-3. PubMed PMID: 25469153; PubMed Central PMCID: PMC4251685.
194. Torchen LC, Kumar A, Kalra B, Savjani G, Sisk R, Legro RS, Dunaif A. Increased antimullerian hormone levels and other reproductive endocrine changes in adult male relatives of women with polycystic ovary syndrome. Fertility & Sterility. 2016;106(1):50-5. doi: 10.1016/j.fertnstert.2016.03.029. PubMed PMID: 27042970; PubMed Central PMCID: PMCPMC4930891.
195. Zawadzki J, Dunaif A, editors. Diagnostic criteria for polycystic ovary syndrome; towards a rational apporach.: Blackwell Scientific; 1991.
196. Sam S, Legro RS, Bentley-Lewis R, Dunaif A. Dyslipidemia and metabolic syndrome in the sisters of women with polycystic ovary syndrome. Journal of Clinical Endocrinology & Metabolism. 2005;90(8):4797-802. doi: 10.1210/jc.2004-2217. PubMed PMID: 15899949; PubMed Central PMCID: PMC4428585.
197. Carnevali P, Baccash J, Halpern AL, Nazarenko I, Nilsen GB, Pant KP, Ebert JC, Brownley A, Morenzoni M, Karpinchyk V, Martin B, Ballinger DG, Drmanac R. Computational techniques for human genome resequencing using mated gapped reads. J Comput Biol. 2012;19(3):279-92. doi: 10.1089/cmb.2011.0201. PubMed PMID: 22175250.
198. Wang K, Li M, Hakonarson H. ANNOVAR: functional annotation of genetic variants from high-throughput sequencing data. Nucleic Acids Research. 2010;38(16):e164. doi: 10.1093/nar/gkq603. PubMed PMID: 20601685; PubMed Central PMCID: PMCPMC2938201.
199. Wilson CA, di Clemente N, Ehrenfels C, Pepinsky RB, Josso N, Vigier B, Cate RL. Mullerian inhibiting substance requires its N-terminal domain for maintenance of biological activity, a novel finding within the transforming growth factor-beta superfamily. Molecular Endocrinology. 1993;7(2):247-57. doi: 10.1210/mend.7.2.8469238. PubMed PMID: 8469238.
200. di Clemente N, Jamin SP, Lugovskoy A, Carmillo P, Ehrenfels C, Picard JY, Whitty A, Josso N, Pepinsky RB, Cate RL. Processing of anti-mullerian hormone regulates receptor activation by a mechanism distinct from TGF-beta. Mol Endocrinol. 2010;24(11):2193-206. Epub 2010/09/24. doi: 10.1210/me.2010-0273. PubMed PMID: 20861221.
201. Imbeaud S, Carre-Eusebe D, Rey R, Belville C, Josso N, Picard JY. Molecular genetics of the persistent mullerian duct syndrome: a study of 19 families. Hum Mol Genet. 1994;3(1):125-31. Epub 1994/01/01. PubMed PMID: 8162013.

202. Mazen I, El-Gammal M, McElreavey K, Elaidy A, Abdel-Hamid MS. Novel AMH and AMHR2 Mutations in Two Egyptian Families with Persistent Mullerian Duct Syndrome. Sex Dev. 2017;11(1):29-33. Epub 2017/02/01. doi: 10.1159/000455019. PubMed PMID: 28142151.
203. van der Zwan YG, Bruggenwirth HT, Drop SL, Wolffenbuttel KP, Madern GC, Looijenga LH, Visser JA. A novel AMH missense mutation in a patient with persistent Mullerian duct syndrome. Sex Dev. 2012;6(6):279-83. Epub 2012/07/17. doi: 10.1159/000339704. PubMed PMID: 22797409.
204. Zeller J, Imbeaud S, Rey R, Adamsbaum C, Fourmaintraux A, Donnet J, van Kote G, Josso N, Chaussain JL. [Persistent mullerian duct syndrome (males with uterus): a pediatric problem]. Arch Pediatr. 1994;1(11):991-7. Epub 1994/11/01. PubMed PMID: 7834048.
205. Nishi MY, Domenice S, Maciel-Guerra AT, Zaba Neto A, Silva MA, Costa EM, Guerra-Junior G, Mendonca BB. Analysis of anti-Mullerian hormone (AMH) and its receptor (AMHR2) genes in patients with persistent Mullerian duct syndrome. Arq Bras Endocrinol Metabol. 2012;56(8):473-8. Epub 2013/01/09. PubMed PMID: 23295284.
206. Loeff DS, Imbeaud S, Reyes HM, Meller JL, Rosenthal IM. Surgical and genetic aspects of persistent mullerian duct syndrome. J Pediatr Surg. 1994;29(1):61-5. Epub 1994/01/01. PubMed PMID: 7907140.
207. Gricourt S, Treton D, Renard-Pennat R, Samuel Lajeunesse J, Bitker MO, Bichet JC, Picard JY, Touraine P. Novel anti-mullerian hormone mutation revealed by haematospermia in a 60-year-old patient. Clin Endocrinol (Oxf). 2011;74(3):404-5. Epub 2010/11/09. doi: 10.1111/j.1365-2265.2010.03903.x. PubMed PMID: 21054481.
208. Carre-Eusebe D, Imbeaud S, Harbison M, New MI, Josso N, Picard JY. Variants of the anti-Mullerian hormone gene in a compound heterozygote with the persistent Mullerian duct syndrome and his family. Hum Genet. 1992;90(4):389-94. Epub 1992/12/01. PubMed PMID: 1483695.
209. Knebelmann B, Boussin L, Guerrier D, Legeai L, Kahn A, Josso N, Picard JY. Anti-Mullerian hormone Bruxelles: a nonsense mutation associated with the persistent Mullerian duct syndrome. Proc Natl Acad Sci U S A. 1991;88(9):3767-71. Epub 1991/05/01. PubMed PMID: 2023927; PubMed Central PMCID: PMC51534.
210. Lang-Muritano M, Biason-Lauber A, Gitzelmann C, Belville C, Picard Y, Schoenle EJ. A novel mutation in the anti-mullerian hormone gene as cause of persistent mullerian duct syndrome. Eur J Pediatr. 2001;160(11):652-4. Epub 2002/01/05. PubMed PMID: 11760020.
211. Morikawa S, Moriya K, Ishizu K, Tajima T. Two heterozygous mutations of the AMH gene in a Japanese patient with persistent Mullerian duct syndrome. J Pediatr Endocrinol Metab. 2014;27(11-12):1223-6. Epub 2014/07/16. doi: 10.1515/jpem-2014-0111. PubMed PMID: 25026127.
212. Altincik A, Karaca F, Onay H. Persistent Mullerian duct syndrome: A novel mutation in the Alphanti-Mullerian Etaormone gene. Hormones (Athens). 2017;16(2):205-8. Epub 2017/07/26. doi: 10.14310/horm.2002.1735. PubMed PMID: 28742509.
213. Nalbantoglu O, Demir K, Korkmaz HA, Buyukinan M, Yildiz M, Tunc S, Ozkan B. A novel mutation of AMH in three siblings with persistent Mullerian duct syndrome. J Pediatr Endocrinol Metab. 2015;28(11-12):1379-82. Epub 2015/07/17. doi: 10.1515/jpem-2014-0501. PubMed PMID: 26181047.
214. Guerrier D, Tran D, Vanderwinden JM, Hideux S, Van Outryve L, Legeai L, Bouchard M, Van Vliet G, De Laet MH, Picard JY, et al. The persistent Mullerian duct syndrome: a

molecular approach. J Clin Endocrinol Metab. 1989;68(1):46-52. Epub 1989/01/01. doi: 10.1210/jcem-68-1-46. PubMed PMID: 2562843.
215. Messika-Zeitoun L, Gouedard L, Belville C, Dutertre M, Lins L, Imbeaud S, Hughes IA, Picard JY, Josso N, di Clemente N. Autosomal recessive segregation of a truncating mutation of anti-Mullerian type II receptor in a family affected by the persistent Mullerian duct syndrome contrasts with its dominant negative activity in vitro. J Clin Endocrinol Metab. 2001;86(9):4390-7. Epub 2001/09/11. doi: 10.1210/jcem.86.9.7839. PubMed PMID: 11549681.
216. Hoshiya M, Christian BP, Cromie WJ, Kim H, Zhan Y, MacLaughlin DT, Donahoe PK. Persistent Mullerian duct syndrome caused by both a 27-bp deletion and a novel splice mutation in the MIS type II receptor gene. Birth Defects Res A Clin Mol Teratol. 2003;67(10):868-74. Epub 2004/01/28. doi: 10.1002/bdra.10091. PubMed PMID: 14745940.
217. Abduljabbar M, Taheini K, Picard JY, Cate RL, Josso N. Mutations of the AMH type II receptor in two extended families with persistent Mullerian duct syndrome: lack of phenotype/genotype correlation. Horm Res Paediatr. 2012;77(5):291-7. Epub 2012/05/16. doi: 10.1159/000338343. PubMed PMID: 22584735.
218. Imbeaud S, Rey R, Berta P, Chaussain JL, Wit JM, Lustig RH, De Vroede MA, Picard JY, Josso N. Testicular degeneration in three patients with the persistent mullerian duct syndrome. Eur J Pediatr. 1995;154(3):187-90. Epub 1995/03/01. PubMed PMID: 7758514.
219. Elias-Assad G, Elias M, Kanety H, Pressman A, Tenenbaum-Rakover Y. Persistent Mullerian Duct Syndrome Caused by a Novel Mutation of an Anti-MuIlerian Hormone Receptor Gene: Case Presentation and Literature Review. Pediatr Endocrinol Rev. 2016;13(4):731-40. Epub 2016/07/29. PubMed PMID: 27464416.
220. Imbeaud S, Belville C, Messika-Zeitoun L, Rey R, di Clemente N, Josso N, Picard JY. A 27 base-pair deletion of the anti-mullerian type II receptor gene is the most common cause of the persistent mullerian duct syndrome. Hum Mol Genet. 1996;5(9):1269-77. Epub 1996/09/01. PubMed PMID: 8872466.
221. Cakir AD, Turan H, Onay H, Emir H, Emre S, Comunoglu N, Ercan O, Evliyaoglu O. A Novel Mutation of AMHR2 In Two Siblings with Persistent Mullerian Duct Syndrome. Sex Dev. 2017;11(5-6):289-92. Epub 2018/01/15. doi: 10.1159/000485882. PubMed PMID: 29332065.
222. Ren X, Wu D, Gong C. Persistent Mullerian duct syndrome: A case report and review. Exp Ther Med. 2017;14(6):5779-84. Epub 2017/12/30. doi: 10.3892/etm.2017.5281. PubMed PMID: 29285121; PubMed Central PMCID: PMC5740701.
223. Avolio L, Belville C, Bragheri R. Persistent mullerian duct syndrome with crossed testicular ectopia. Urology. 2003;62(2):350. Epub 2003/08/02. PubMed PMID: 12893352.
224. Rosal-Goncalves M, Almeida C, Barber J, Kay T, Limbert C, Lopes L, Fonseca G. Mutation of the MIF type II receptor in two brothers. J Pediatr Endocrinol Metab. 2010;23(3):315-7. Epub 2010/05/20. PubMed PMID: 20480734.
225. Korkmaz O, Ozen S, Ozcan N, Bayindir P, Sen S, Onay H, Goksen D, Avanoglu A, Ozkinay F, Darcan S. Persistent Mullerian Duct Syndrome with Transverse Testicular Ectopia: A Novel Anti-Mullerian Hormone Receptor Mutation. J Clin Res Pediatr Endocrinol. 2017;9(2):179-81. Epub 2017/01/18. doi: 10.4274/jcrpe.4058. PubMed PMID: 28094762; PubMed Central PMCID: PMC5463293.
226. Wongprasert H, Somanunt S, De Filippo R, Picard JY, Pitukcheewanont P. A novel mutation of anti-Mullerian hormone gene in Persistent Mullerian Duct Syndrome presented with

bilateral cryptorchidism: a case report. J Pediatr Urol. 2013;9(4):e147-9. Epub 2013/04/25. doi: 10.1016/j.jpurol.2013.03.004. PubMed PMID: 23611722.
227. Al-Faris A, Jabari M, Al-Sayed M, Al-Shehri H. Bilateral Cryptorchidism, a rare presentation for persistent Mullerian duct syndrome. Electron Physician. 2016;8(12):3395-7. Epub 2017/02/07. doi: 10.19082/3395. PubMed PMID: 28163853; PubMed Central PMCID: PMC5279971.
228. Menabo S, Balsamo A, Nicoletti A, Gennari M, Pirazzoli P, Cicognani A, Baldazzi L. Three novel AMH gene mutations in a patient with persistent mullerian duct syndrome and normal AMH serum dosage. Horm Res. 2008;70(2):124-8. Epub 2008/06/13. doi: 10.1159/000137664. PubMed PMID: 18547961.
229. Oros-Millan ME, Munoz-Calvo MT, Nishi MY, Bilharinho Mendonca B, Argente J. [Persistent Mullerian duct syndrome due to a mutation in the anti-Mullerian hormone receptor gene (AMHR2)]. An Pediatr (Barc). 2017;86(2):94-5. Epub 2016/07/28. doi: 10.1016/j.anpedi.2016.06.011. PubMed PMID: 27461869.
230. Chan AO, But WM, Lee CY, Lam YY, Ng KL, Loung PY, Lam A, Cheng CW, Shek CC, Wong WS, Wong KF, Wong MY, Tse WY. Aetiological bases of 46,XY disorders of sex development in the Hong Kong Chinese population. Hong Kong Med J. 2015;21(6):499-510. Epub 2015/10/24. doi: 10.12809/hkmj144402. PubMed PMID: 26492835.
231. Trbovich AM, Martinelle N, O'Neill FH, Pearson EJ, Donahoe PK, Sluss PM, Teixeira J. Steroidogenic activities in MA-10 Leydig cells are differentially altered by cAMP and Mullerian inhibiting substance. J Steroid Biochem Mol Biol. 2004;92(3):199-208. Epub 2004/11/24. doi: 10.1016/j.jsbmb.2004.07.002. PubMed PMID: 15555913.
232. Nelson VL, Legro RS, Strauss JF, 3rd, McAllister JM. Augmented androgen production is a stable steroidogenic phenotype of propagated theca cells from polycystic ovaries. Mol Endocrinol. 1999;13(6):946-57. Epub 1999/06/24. doi: 10.1210/mend.13.6.0311. PubMed PMID: 10379893.
233. Salhi I, Cambon-Roques S, Lamarre I, Laune D, Molina F, Pugniere M, Pourquier D, Gutowski M, Picard JY, Xavier F, Pelegrin A, Navarro-Teulon I. The anti-Mullerian hormone type II receptor: insights into the binding domains recognized by a monoclonal antibody and the natural ligand. Biochem J. 2004;379(Pt 3):785-93. Epub 2004/01/31. doi: 10.1042/BJ20031961. PubMed PMID: 14750901; PubMed Central PMCID: PMC1224123.
234. Morgenthaler S, Thilly WG. A strategy to discover genes that carry multi-allelic or mono-allelic risk for common diseases: a cohort allelic sums test (CAST). Mutation Research. 2007;615(1-2):28-56. doi: 10.1016/j.mrfmmm.2006.09.003. PubMed PMID: 17101154.
235. Morikawa N, Clarke TR, Novina CD, Watanabe K, Haqq C, Weiss M, Roy AL, Donahoe PK. Human Mullerian-inhibiting substance promoter contains a functional TFII-I-binding initiator. Biol Reprod. 2000;63(4):1075-83. Epub 2000/09/20. PubMed PMID: 10993829.
236. Rey R, Lukas-Croisier C, Lasala C, Bedecarras P. AMH/MIS: what we know already about the gene, the protein and its regulation. Mol Cell Endocrinol. 2003;211(1-2):21-31. Epub 2003/12/06. PubMed PMID: 14656472.
237. Ito M, Yu R, Jameson JL. DAX-1 inhibits SF-1-mediated transactivation via a carboxy-terminal domain that is deleted in adrenal hypoplasia congenita. Mol Cell Biol. 1997;17(3):1476-83. Epub 1997/03/01. PubMed PMID: 9032275; PubMed Central PMCID: PMC231873.

238. Nachtigal MW, Hirokawa Y, Enyeart-VanHouten DL, Flanagan JN, Hammer GD, Ingraham HA. Wilms' tumor 1 and Dax-1 modulate the orphan nuclear receptor SF-1 in sex-specific gene expression. Cell. 1998;93(3):445-54. Epub 1998/05/20. PubMed PMID: 9590178.
239. Schepers G, Wilson M, Wilhelm D, Koopman P. SOX8 is expressed during testis differentiation in mice and synergizes with SF1 to activate the Amh promoter in vitro. J Biol Chem. 2003;278(30):28101-8. Epub 2003/05/07. doi: 10.1074/jbc.M304067200. PubMed PMID: 12732652.
240. Tremblay JJ, Viger RS. Transcription factor GATA-4 enhances Mullerian inhibiting substance gene transcription through a direct interaction with the nuclear receptor SF-1. Mol Endocrinol. 1999;13(8):1388-401. Epub 1999/08/14. doi: 10.1210/mend.13.8.0330. PubMed PMID: 10446911.
241. De Santa Barbara P, Bonneaud N, Boizet B, Desclozeaux M, Moniot B, Sudbeck P, Scherer G, Poulat F, Berta P. Direct interaction of SRY-related protein SOX9 and steroidogenic factor 1 regulates transcription of the human anti-Mullerian hormone gene. Mol Cell Biol. 1998;18(11):6653-65. Epub 1998/10/17. PubMed PMID: 9774680; PubMed Central PMCID: PMC109250.
242. Hong CY, Park JH, Seo KH, Kim JM, Im SY, Lee JW, Choi HS, Lee K. Expression of MIS in the testis is downregulated by tumor necrosis factor alpha through the negative regulation of SF-1 transactivation by NF-kappa B. Mol Cell Biol. 2003;23(17):6000-12. Epub 2003/08/15. PubMed PMID: 12917325; PubMed Central PMCID: PMC180915.
243. Jin H, Won M, Park SE, Lee S, Park M, Bae J. FOXL2 Is an Essential Activator of SF-1-Induced Transcriptional Regulation of Anti-Mullerian Hormone in Human Granulosa Cells. PLoS One. 2016;11(7):e0159112. Epub 2016/07/16. doi: 10.1371/journal.pone.0159112. PubMed PMID: 27414805; PubMed Central PMCID: PMC4944948.
244. Consortium EP. An integrated encyclopedia of DNA elements in the human genome. Nature. 2012;489(7414):57-74. doi: 10.1038/nature11247. PubMed PMID: 22955616; PubMed Central PMCID: PMCPMC3439153.
245. Kheradpour P, Kellis M. Systematic discovery and characterization of regulatory motifs in ENCODE TF binding experiments. Nucleic Acids Res. 2014;42(5):2976-87. doi: 10.1093/nar/gkt1249. PubMed PMID: 24335146; PubMed Central PMCID: PMCPMC3950668.
246. Kerr ID, Cox HC, Moyes K, Evans B, Burdett BC, van Kan A, McElroy H, Vail PJ, Brown KL, Sumampong DB, Monteferrante NJ, Hardman KL, Theisen A, Mundt E, Wenstrup RJ, Eggington JM. Assessment of in silico protein sequence analysis in the clinical classification of variants in cancer risk genes. J Community Genet. 2017;8(2):87-95. Epub 2017/01/05. doi: 10.1007/s12687-016-0289-x. PubMed PMID: 28050887; PubMed Central PMCID: PMC5386911.
247. Walters-Sen LC, Hashimoto S, Thrush DL, Reshmi S, Gastier-Foster JM, Astbury C, Pyatt RE. Variability in pathogenicity prediction programs: impact on clinical diagnostics. Mol Genet Genomic Med. 2015;3(2):99-110. Epub 2015/03/25. doi: 10.1002/mgg3.116. PubMed PMID: 25802880; PubMed Central PMCID: PMC4367082.
248. Gong L, Xia Y, Qian Z, Shi J, Luo J, Song G, Xu J, Ye Z. Overexpression of MYC binding protein promotes invasion and migration in gastric cancer. Oncol Lett. 2018;15(4):5243-9. Epub 2018/03/20. doi: 10.3892/ol.2018.7944. PubMed PMID: 29552163; PubMed Central PMCID: PMC5840499.

249. Mai S, Mushinski JF. c-Myc-induced genomic instability. J Environ Pathol Toxicol Oncol. 2003;22(3):179-99. Epub 2003/10/08. PubMed PMID: 14529093.
250. Briggs MR, Kadonaga JT, Bell SP, Tjian R. Purification and biochemical characterization of the promoter-specific transcription factor, Sp1. Science. 1986;234(4772):47-52. Epub 1986/10/03. PubMed PMID: 3529394.
251. O'Connor L, Gilmour J, Bonifer C. The Role of the Ubiquitously Expressed Transcription Factor Sp1 in Tissue-specific Transcriptional Regulation and in Disease. Yale J Biol Med. 2016;89(4):513-25. Epub 2016/12/27. PubMed PMID: 28018142; PubMed Central PMCID: PMC5168829.
252. Teixeira J, Kehas DJ, Antun R, Donahoe PK. Transcriptional regulation of the rat Mullerian inhibiting substance type II receptor in rodent Leydig cells. Proc Natl Acad Sci U S A. 1999;96(24):13831-8. Epub 1999/11/26. PubMed PMID: 10570158; PubMed Central PMCID: PMC24150.
253. Klattig J, Sierig R, Kruspe D, Besenbeck B, Englert C. Wilms' tumor protein Wt1 is an activator of the anti-Mullerian hormone receptor gene Amhr2. Mol Cell Biol. 2007;27(12):4355-64. Epub 2007/04/11. doi: 10.1128/MCB.01780-06. PubMed PMID: 17420277; PubMed Central PMCID: PMC1900060.
254. Li R, Cauchy P, Ramamoorthy S, Boller S, Chavez L, Grosschedl R. Dynamic EBF1 occupancy directs sequential epigenetic and transcriptional events in B-cell programming. Genes Dev. 2018;32(2):96-111. Epub 2018/02/15. doi: 10.1101/gad.309583.117. PubMed PMID: 29440261; PubMed Central PMCID: PMC5830932.
255. Morra F, Luise C, Visconti R, Staibano S, Merolla F, Ilardi G, Guggino G, Paladino S, Sarnataro D, Franco R, Monaco R, Zitomarino F, Pacelli R, Monaco G, Rocco G, Cerrato A, Linardopoulos S, Muller MT, Celetti A. New therapeutic perspectives in CCDC6 deficient lung cancer cells. Int J Cancer. 2015;136(9):2146-57. Epub 2014/10/11. doi: 10.1002/ijc.29263. PubMed PMID: 25302833.
256. Andris F, Denanglaire S, Anciaux M, Hercor M, Hussein H, Leo O. The Transcription Factor c-Maf Promotes the Differentiation of Follicular Helper T Cells. Front Immunol. 2017;8:480. Epub 2017/05/13. doi: 10.3389/fimmu.2017.00480. PubMed PMID: 28496444; PubMed Central PMCID: PMC5406410.
257. DeFalco T, Takahashi S, Capel B. Two distinct origins for Leydig cell progenitors in the fetal testis. Dev Biol. 2011;352(1):14-26. Epub 2011/01/25. doi: 10.1016/j.ydbio.2011.01.011. PubMed PMID: 21255566; PubMed Central PMCID: PMC3055913.
258. Imhoff FM, Yang D, Mathew SF, Clarkson AN, Kawagishi Y, Tate WP, Koishi K, McLennan IS. The type 2 anti-Mullerian hormone receptor has splice variants that are dominant-negative inhibitors. FEBS Lett. 2013;587(12):1749-53. Epub 2013/04/30. doi: 10.1016/j.febslet.2013.04.014. PubMed PMID: 23624077.
259. Chan HP, Zhang NR, Chen LH. Importance sampling of word patterns in DNA and protein sequences. J Comput Biol. 2010;17(12):1697-709. doi: 10.1089/cmb.2008.0233. PubMed PMID: 21128856; PubMed Central PMCID: PMCPMC3787731.
260. Macintyre G, Bailey J, Haviv I, Kowalczyk A. is-rSNP: a novel technique for in silico regulatory SNP detection. Bioinformatics. 2010;26(18):i524-30. doi: 10.1093/bioinformatics/btq378. PubMed PMID: 20823317; PubMed Central PMCID: PMCPMC2935445.

261. Zuo C, Shin S, Keles S. atSNP: transcription factor binding affinity testing for regulatory SNP detection. Bioinformatics. 2015;31(20):3353-5. Epub 2015/06/21. doi: 10.1093/bioinformatics/btv328. PubMed PMID: 26092860; PubMed Central PMCID: PMC4643619.
262. Benjamini Y, Hochberg Y. Controlling the False Discovery Rate - a Practical and Powerful Approach to Multiple Testing. Journal of the Royal Statistical Society Series B-Methodological. 1995;57(1):289-300. PubMed PMID: WOS:A1995QE45300017.
263. Ye S. Computational approaches for motif-finding in DNA sequences [Doctoral dissertation]: University of South Dakota; 2008.
264. Consortium GT. The Genotype-Tissue Expression (GTEx) project. Nat Genet. 2013;45(6):580-5. doi: 10.1038/ng.2653. PubMed PMID: 23715323; PubMed Central PMCID: PMCPMC4010069.
265. Gorsic LK, Kosova G, Werstein B, Sisk R, Legro RS, Hayes MG, Teixeira JM, Dunaif A, Urbanek M. Pathogenic Anti-Mullerian Hormone Variants in Polycystic Ovary Syndrome. J Clin Endocrinol Metab. 2017;102(8):2862-72. Epub 2017/05/16. doi: 10.1210/jc.2017-00612. PubMed PMID: 28505284; PubMed Central PMCID: PMC5546867.
266. de Medeiros SF, Ormond CM, de Medeiros MAS, de Souza Santos N, Banhara CR, Yamamoto MMW. Metabolic and endocrine connections of 17-hydroxypregnenolone in polycystic ovary syndrome women. Endocr Connect. 2017;6(7):479-88. Epub 2017/08/09. doi: 10.1530/EC-17-0151. PubMed PMID: 28784626; PubMed Central PMCID: PMC5592777.
267. Belville C, Jamin SP, Picard JY, Josso N, di Clemente N. Role of type I receptors for anti-Mullerian hormone in the SMAT-1 Sertoli cell line. Oncogene. 2005;24(31):4984-92. Epub 2005/05/18. doi: 10.1038/sj.onc.1208686. PubMed PMID: 15897891.
268. Racine C, Rey R, Forest MG, Louis F, Ferre A, Huhtaniemi I, Josso N, di Clemente N. Receptors for anti-mullerian hormone on Leydig cells are responsible for its effects on steroidogenesis and cell differentiation. Proc Natl Acad Sci U S A. 1998;95(2):594-9. Epub 1998/01/22. PubMed PMID: 9435237; PubMed Central PMCID: PMC18465.
269. Fynn-Thompson E, Cheng H, Teixeira J. Inhibition of steroidogenesis in Leydig cells by Mullerian-inhibiting substance. Mol Cell Endocrinol. 2003;211(1-2):99-104. Epub 2003/12/06. PubMed PMID: 14656482.
270. Grossman MP, Nakajima ST, Fallat ME, Siow Y. Mullerian-inhibiting substance inhibits cytochrome P450 aromatase activity in human granulosa lutein cell culture. Fertil Steril. 2008;89(5 Suppl):1364-70. Epub 2007/05/23. doi: 10.1016/j.fertnstert.2007.03.066. PubMed PMID: 17517397.
271. Sedes L, Leclerc A, Moindjie H, Cate RL, Picard JY, di Clemente N, Jamin SP. Anti-Mullerian hormone recruits BMPR-IA in immature granulosa cells. PLoS One. 2013;8(11):e81551. Epub 2013/12/07. doi: 10.1371/journal.pone.0081551. PubMed PMID: 24312319; PubMed Central PMCID: PMC3842941.
272. Yu YY, Sun CX, Liu YK, Li Y, Wang L, Zhang W. Promoter methylation of CYP19A1 gene in Chinese polycystic ovary syndrome patients. Gynecol Obstet Invest. 2013;76(4):209-13. Epub 2013/10/26. doi: 10.1159/000355314. PubMed PMID: 24157654.
273. Zaree M, Shahnazi V, Fayezi S, Darabi M, Mehrzad-Sadaghiani M, Darabi M, Khani S, Nouri M. Expression Levels of PPARgamma and CYP-19 in Polycystic Ovarian Syndrome Primary Granulosa Cells: Influence of omega-3 Fatty Acid. Int J Fertil Steril. 2015;9(2):197-204. Epub 2015/08/08. PubMed PMID: 26246878; PubMed Central PMCID: PMC4518488.

274. Golovine K, Schwerin M, Vanselow J. Three different promoters control expression of the aromatase cytochrome p450 gene (cyp19) in mouse gonads and brain. Biol Reprod. 2003;68(3):978-84. Epub 2003/02/27. PubMed PMID: 12604651.
275. Zhao Y, Agarwal VR, Mendelson CR, Simpson ER. Transcriptional regulation of CYP19 gene (aromatase) expression in adipose stromal cells in primary culture. J Steroid Biochem Mol Biol. 1997;61(3-6):203-10. Epub 1997/04/01. PubMed PMID: 9365191.
276. Prosperi JR, Robertson FM. Cyclooxygenase-2 directly regulates gene expression of P450 Cyp19 aromatase promoter regions pII, pI.3 and pI.7 and estradiol production in human breast tumor cells. Prostaglandins Other Lipid Mediat. 2006;81(1-2):55-70. Epub 2006/09/26. doi: 10.1016/j.prostaglandins.2006.07.003. PubMed PMID: 16997132.
277. Subbaramaiah K, Hudis C, Chang SH, Hla T, Dannenberg AJ. EP2 and EP4 receptors regulate aromatase expression in human adipocytes and breast cancer cells. Evidence of a BRCA1 and p300 exchange. J Biol Chem. 2008;283(6):3433-44. Epub 2007/12/18. doi: 10.1074/jbc.M705409200. PubMed PMID: 18083712.
278. Stocco C, Kwintkiewicz J, Cai Z. Identification of regulatory elements in the Cyp19 proximal promoter in rat luteal cells. J Mol Endocrinol. 2007;39(4):211-21. Epub 2007/10/03. doi: 10.1677/JME-07-0026. PubMed PMID: 17909262.
279. Parakh TN, Hernandez JA, Grammer JC, Weck J, Hunzicker-Dunn M, Zeleznik AJ, Nilson JH. Follicle-stimulating hormone/cAMP regulation of aromatase gene expression requires beta-catenin. Proc Natl Acad Sci U S A. 2006;103(33):12435-40. Epub 2006/08/10. doi: 10.1073/pnas.0603006103. PubMed PMID: 16895991; PubMed Central PMCID: PMC1533882.
280. Wang ZJ, Jeffs B, Ito M, Achermann JC, Yu RN, Hales DB, Jameson JL. Aromatase (Cyp19) expression is up-regulated by targeted disruption of Dax1. Proc Natl Acad Sci U S A. 2001;98(14):7988-93. Epub 2001/06/28. doi: 10.1073/pnas.141543298. PubMed PMID: 11427738; PubMed Central PMCID: PMC35455.
281. Park JH, Maclaughlin DT, Teixeira JM. The rate of in vitro maturation of primary follicles from adult mice and the quality of oocytes is improved in the absence of anti-mullerian hormone. Reprod Sci. 2011;18(4):334-41. Epub 2010/11/26. doi: 10.1177/1933719110388294. PubMed PMID: 21098214.
282. Webber LJ, Stubbs S, Stark J, Trew GH, Margara R, Hardy K, Franks S. Formation and early development of follicles in the polycystic ovary. Lancet. 2003;362(9389):1017-21. Epub 2003/10/03. PubMed PMID: 14522531.
283. Maciel GA, Baracat EC, Benda JA, Markham SM, Hensinger K, Chang RJ, Erickson GF. Stockpiling of transitional and classic primary follicles in ovaries of women with polycystic ovary syndrome. J Clin Endocrinol Metab. 2004;89(11):5321-7. Epub 2004/11/09. doi: 10.1210/jc.2004-0643. PubMed PMID: 15531477.
284. Xiao S, Coppeta JR, Rogers HB, Isenberg BC, Zhu J, Olalekan SA, McKinnon KE, Dokic D, Rashedi AS, Haisenleder DJ, Malpani SS, Arnold-Murray CA, Chen K, Jiang M, Bai L, Nguyen CT, Zhang J, Laronda MM, Hope TJ, Maniar KP, Pavone ME, Avram MJ, Sefton EC, Getsios S, Burdette JE, Kim JJ, Borenstein JT, Woodruff TK. A microfluidic culture model of the human reproductive tract and 28-day menstrual cycle. Nat Commun. 2017;8:14584. Epub 2017/03/30. doi: 10.1038/ncomms14584. PubMed PMID: 28350383; PubMed Central PMCID: PMC5379057.
285. Lebbe M, Taylor AE, Visser JA, Kirkman-Brown JC, Woodruff TK, Arlt W. The Steroid Metabolome in the Isolated Ovarian Follicle and Its Response to Androgen Exposure and

Antagonism. Endocrinology. 2017;158(5):1474-85. Epub 2017/03/23. doi: 10.1210/en.2016-1851. PubMed PMID: 28323936; PubMed Central PMCID: PMC5460835.
286. Estienne A, Pierre A, di Clemente N, Picard JY, Jarrier P, Mansanet C, Monniaux D, Fabre S. Anti-Mullerian hormone regulation by the bone morphogenetic proteins in the sheep ovary: deciphering a direct regulatory pathway. Endocrinology. 2015;156(1):301-13. Epub 2014/10/17. doi: 10.1210/en.2014-1551. PubMed PMID: 25322464.
287. Monajemi H, Stroes E, Hegele RA, Fliers E. Inherited lipodystrophies and the metabolic syndrome. Clin Endocrinol (Oxf). 2007;67(4):479-84. Epub 2007/06/15. doi: 10.1111/j.1365-2265.2007.02906.x. PubMed PMID: 17561981.
288. Young J, Morbois-Trabut L, Couzinet B, Lascols O, Dion E, Bereziat V, Feve B, Richard I, Capeau J, Chanson P, Vigouroux C. Type A insulin resistance syndrome revealing a novel lamin A mutation. Diabetes. 2005;54(6):1873-8. Epub 2005/05/28. PubMed PMID: 15919811.
289. Laurini E, Martinelli V, Lanzicher T, Puzzi L, Borin D, Chen SN, Long CS, Lee P, Mestroni L, Taylor MRG, Sbaizero O, Pricl S. Biomechanical defects and rescue of cardiomyocytes expressing pathologic nuclear lamins. Cardiovasc Res. 2018. Epub 2018/02/13. doi: 10.1093/cvr/cvy040. PubMed PMID: 29432544.

TABLES

Table 2.1 Clinical features and reproductive hormone levels of study participants.

	PCOS Cases (n = 700)		Controls (n = 165)		P-Value *
	N	Median (1^{st}-3^{rd} quartile)	N	Median (1^{st}-3^{rd} quartile)	
Age (yrs.)	700	28 (24-32)	165	29 (24-34)	0.016
BMI (kg/m^2)	700	35.4 (28.7-41.5)	165	27.6 (22.4-34.1)	<0.0001
T (ng/dL)	669	71 (59-90)	165	26 (19-35)	<0.0001
uT (ng/dL)	497	23 (17-29)	65	4 (3-7)	<0.0001
SHBG (nM)	498	53 (34-78)	65	107 (72-156)	<0.0001
DHEAS (ng/mL)	595	2065 (1446-2886)	90	1349 (1059-1729)	<0.0001
LH (mIU/mL)	518	11 (7-17)	59	3 (3-7)	<0.0001
FSH (mIU/mL)	518	9 (8-11)	59	10 (7-12)	0.74*
AMH (ng/mL)	259	9.3 (5.3-17.5)	126	2.3 (1.2-4.0)	<0.0001*

* All analyses were with Mann-Whitney U test except for those denoted by an asterisk which used ANCOVA adjusted for Age and BMI

To convert values for T from ng/dL to nmol/L, multiply by 0.03467; to convert the values for uT from ng/dL to nmol/L, multiply by 0.03467; to convert the values for DHEAS from ng/mL to μM/L, multiply by 0.00271; to convert values for AMH from ng/mL to pmol/L, multiply by 7.1429.

Table 2.2 Rare *AMH* variants identified in PCOS cases and controls.

Base Change (mRNA) (Nm_000479.3)	AA Change	SNP ID	Population based MAF†	Count Cases	Count Controls	CADD C-score	FATHMM-MKL *P*-value
T254G	V12G	rs149082963	7.40E-04	6	0	10.82	0.867
G289A	A24T	rs775579158	6.60E-05	1	0	4.271	0.133
C355G	P46A	rs148294311	8.30E-05	1	0	12.69	0.777
G491A	R91H	rs534377664	1.70E-05	1	0	7.833	0.110
A514T	T99S	rs200226465	8.50E-05	2	0	15.72	0.867
C647T	T143I	rs139265145	4.10E-03	11	4	8.98	0.257
C670T	P151S	rs370532523	3.30E-05	1	0	15.94	0.933
G685A	A156T	rs374588581	2.30E-04	1	0	6.573	0.309
C772G	Q185E	rs200523942	7.90E-05	1	0	18.95	0.789
GT	splicing (ex2/3)	rs774430982	1.00E-05	1	0	17.46	0.716
G800A	R194H	rs376035065	2.10E-05	1	0	9.266	0.300
C1027T	P270S	rs757506343	1.40E-04	1	0	15.06	0.358
C1069T	P284S	rs769350289	9.00E-06	0	1	14.35	0.806
C1083G	D288E	rs199831511	1.70E-04	3	1	19.64	0.907
G1124A	R302Q	rs536688211	9.9E-04 ‡	1	0	19.25	0.805
A1193G	Q325R	rs140765565	4.40E-03	3	4	16.95	0.843
C1273T	P352S	rs764049634	1.10E-04	3	0	8.455	0.196
C1304T	P362S	rs765380360	6.50E-05	1	0	7.773	0.194
C1317T	P366L	chr19:2251370-2251370*	-	1	0	9.35	0.175
C1334T	A372V	rs541377806	3.50E-04	1	0	10.22	0.276
C1373T	A385V	chr19:2251427-2251427*	-	1	0	12.28	0.564
C1737G	H506Q	rs138571039	4.20E-05	1	0	22.3	0.939
C1775T	A519V	rs200031151	1.40E-03	0	1	13.34	0.228
G1876T	V553L	rs770189890	9.00E-05	1	1	22.2	0.940

*Build GRCh37/hg1

† MAF based on ExAc Aggregated Populations (http://exac.broadinstitute.org)

‡ MAF based on 1000Genomes European ancestry (http://www.1000genomes.org)

Table 2.3 Rare noncoding *AMH* variants identified in PCOS cases and controls.

General AMH Location	Chr	Position*	SNP ID	Population based MAF†	REF	ALT	Count Cases	Count Controls	CADD C-score	FATHMM-MKL *P*-value
Upstream	19	2249171	NA	NA	C	G	1	0	14.45	0.907
Upstream	19	2249215	rs186422293	6.29E-03	G	A	7	2	5.74	0.141
Upstream	19	2249263	rs746807694	2.67E-04	C	G	1	0	14.48	0.750
Upstream	19	2249272	rs777832730	6.68E-05	C	T	1	0	9.69	0.307
5' UTR	19	2249330	rs773283377	2.32E-04	C	T	1	0	6.98	0.128
Intron 1	19	2249774	rs370996450	1.94E-04	C	T	1	0	6.75	0.160
Intron 1	19	2249796	rs149600185	1.47E-03	C	T	2	2	1.95	0.129
Intron 1	19	2250012	rs749466277	2.01E-03	C	T	1	0	1.54	0.147
Intron 1	19	2250061	rs116060400	2.01E-04	C	T	0	1	8.29	0.232
Intron 1	19	2250175	rs546498783	6.62E-03	C	T	10	0	0.00	0.069
Intron 1	19	2250185	rs991519014	3.00E-05 ‡	C	A	1	0	7.57	0.232
Intron 1	19	2250231	rs780396199	3.34E-04	T	C	1	0	6.47	0.209
Intron 1	19	2250302	rs374418184	3.04E-03	A	G	4	0	9.81	0.164
Intron 1	19	2250312	rs183367973	4.17E-04	C	T	2	1	8.69	0.175
Intron 2	19	2250483	NA	NA	C	CA	1	0	13.35	NA
Intron 3	19	2250828	NA	NA	C	T	1	0	8.11	0.231

*Build GRCh37/hg19

† MAF based on Genome Aggregation Database (gnomAD) (http://gnomad.broadinstitute.org/)

‡ TOPMed Program

Table 2.4 Rare *AMHR2* variants identified in PCOS cases and controls.

Base Change (mRNA) (Nm_020547)	AA Change	SNP ID	Population based MAF†	Count Cases	Count Controls	CADD C-score	FATHMM-MKL *P*-value	% Decrease Activity	P-value**
C88T	P30S	chr12:53818110*	NA	1	0	25.80	0.98	87.30	1.76E-03
G1643A	R548Q	rs144262887	2.31E-04	1	1	11.54	0.29	-2.20	8.61E-01

*Build GRCh37/hg19

† MAF based on Genome Aggregation Database (gnomAD) (http://gnomad.broadinstitute.org/)

** Two-tailed t-test

Table 2.5 Rare noncoding *AMHR2* variants in PCOS cases and controls.

General AMHR2 Location	Chr	Position*	SNP ID	Population based MAF†	REF	ALT	Count Cases	Count Controls	CADD C-score	FATHMM-MKL *P*-value
Upstream	12	53814515	NA	NA	A	T	1	0	4.289	0.239
Upstream	12	53815129	NA	NA	A	T	1	0	0.076	0.028
Upstream	12	53815218	rs866630130	6.66E-05	G	C	1	0	9.924	0.135
Upstream	12	53815561	rs181566505	1.90E-03	T	G	5	1	7.775	0.868
Upstream	12	53815671	rs150004525	4.20E-04	T	C	1	0	2.231	0.125
Upstream	12	53815819	NA	NA	C	A	1	0	0.239	0.031
Upstream	12	53816595	NA	NA	C	T	1	0	1.881	0.072
Upstream	12	53816627	NA	NA	TAATA	T	2	0	12.63	NA
Upstream	12	53816766	NA	NA	GTGT	G	1	0	8.159	NA
Upstream	12	53817031	rs547441128	1.26E-03	G	C	1	0	0.853	0.065
Upstream	12	53817053	NA	NA	G	A	1	0	4.957	0.070
Upstream	12	53817187	NA	NA	A	G	1	0	15.57	0.851
Upstream	12	53817402	rs576777893	2.26E-04	T	G	1	0	12.1	0.126
Upstream	12	53817516	rs777964297	9.69E-05	T	G	1	0	18.72	0.947
Upstream	12	53817577	rs148189358	5.49E-03	G	T	7	3	16.53	0.936
Intron 1	12	53817956	rs784894	1.40E-03	C	A	3	0	15.76	0.953
Intron 1	12	53817971	NA	NA	G	A	1	0	1.528	0.143
Intron 1	12	53818016	rs777265708	8.01E-04	T	G	1	0	13.65	0.914
Intron 2	12	53818287	rs784893	4.75E-02	A	G	3	0	6.278	0.206
Intron 2	12	53818404	NA	NA	G	A	1	0	9.413	0.219
Intron 3	12	53818868	NA	NA	A	T	1	0	12.89	0.119
Intron 3	12	53818920	rs2071557	4.73E-02	C	T	26	3	8.65	0.103
Intron 5	12	53819433	rs770641486	1.64E-05	A	G	1	0	1.409	0.160
Intron 6	12	53819825	NA	NA	T	C	1	0	2.77	0.147
Intron 6	12	53819857	NA	NA	G	A	1	0	3.495	0.085
Intron 6	12	53820089	NA	NA	G	A	1	0	4.534	0.086
Intron 6	12	53820101	NA	NA	G	A	1	0	5.393	0.109
Intron 6	12	53820136	rs760484587	2.91E-04	G	A	1	0	6.143	0.117
Intron 6	12	53820139	rs184772202	2.23E-03	G	T	7	1	3.606	0.130
Intron 6	12	53820453	NA	NA	A	C	23	2	7.996	0.142
Intron 6	12	53820620	rs34932524	1.35E-03	C	T	4	0	3.679	0.090
Intron 6	12	53820903	rs555694902	1.29E-04	C	T	1	0	3.548	0.111
Intron 6	12	53821113	rs540050356	1.36E-03	T	C	2	1	3.314	0.143
Intron 6	12	53821177	NA	NA	T	TTTTTA	2	0	1.33	NA
Intron 6	12	53821196	rs551935854	3.23E-05	T	C	2	0	1.508	0.066
Intron 6	12	53821359	NA	NA	G	A	1	0	6.3	0.098
Intron 6	12	53822143	rs142890072	3.23E-05	C	G	1	0	1.502	0.181
Intron 6	12	53822144	rs370723376	1.33E-04	G	A	1	0	2.232	0.134
Intron 6	12	53822176	NA	NA	A	G	1	0	8.916	0.384
Intron 6	12	53822226	rs181813382	3.23E-05	T	C	1	0	10.81	0.212
Intron 6	12	53822277	rs539086433	5.49E-04	T	A	2	1	7.663	0.302
Intron 6	12	53822288	NA	NA	G	A	1	0	7.675	0.236
Intron 6	12	53822505	rs777352969	1.62E-04	C	T	2	1	4.243	0.177

(Continued on following page)

Table 2.5 cont. Rare noncoding *AMHR2* variants in PCOS cases and controls.

General AMHR2 Location	Chr	Position*	SNP ID	Population based MAF†	REF	ALT	Count Cases	Count Controls	CADD C-score	FATHMM -MKL *P*-value
Intron 7	12	53822816	rs775478211	5.51E-05	A	G	1	0	6.516	0.198
Intron 7	12	53822884	rs784892	8.01E-04	G	A	3	0	7.818	0.176
Intron 7	12	53822898	rs558842297	3.24E-05	C	T	1	0	1.959	0.134
Intron 7	12	53822904	NA	NA	C	T	2	0	2.43	0.142
Intron 8	12	53823548	rs527341740	2.26E-04	A	G	1	0	10.84	0.156
Intron 8	12	53823609	rs745713994	4.07E-06	C	T	1	0	7.146	0.232
Intron 9	12	53823773	rs200284824	4.19E-04	G	A	1	0	1.08	0.128
Intron 9	12	53823797	NA	NA	T	TC	1	0	1.035	NA
Intron 9	12	53823828	rs760804136	6.47E-05	C	T	1	0	4.543	0.237
Intron 9	12	53823851	rs577266252	1.62E-04	G	T	2	0	2.173	0.173
Intron 10	12	53824177	rs758971843	NA	A	G	1	0	7.594	0.150
Intron 10	12	53824408	rs784889	1.40E-03	C	T	3	0	5.793	0.145
Intron 10	12	53824508	rs784888	1.13E-03	G	C	3	0	13.44	0.238
Intron 10	12	53824538	rs186948808	4.52E-04	G	A	1	0	11.52	0.112
Intron 10	12	53824543	rs190814349	1.94E-04	A	G	2	0	8.254	0.130
Intron 10	12	53824544	NA	NA	G	T	1	0	7.519	0.132
Intron 10	12	53824871	rs139224064	9.37E-04	A	C	1	0	1.883	0.141

*Build GRCh37/hg19

† MAF based on Genome Aggregation Database (gnomAD) (http://gnomad.broadinstitute.org/)

Table 2.6 Rare nonsynonymous *LMNA* variants in PCOS cases and controls.

Table 2.6 Rare nonsynonymous *LMNA* variants in PCOS cases and controls.

Base Change (mRNA) (Nm_170707)	AA Change	SNP ID	Population based MAF†	Count Cases	Count Controls	CADD C-score	FATHMM-MKL *P*-value
C1201T	R401C	rs61094188	8.70E-05	1	0	18.61	0.959
G1445A	R482Q	rs11575937	8.20E-06	2	0	19.66	0.891
C1453G	P485A	chr1:156106784*	NA	1	0	18.37	0.913
G1634A	R545H	rs142191737	1.40E-04	2	0	19.37	0.960
C1711A	R571S	rs80338938	5.50E-05	1	0	21.90	0.916
C1879T	R627C	rs777841827	1.60E-05	1	0	19.73	0.934
G1931A	R644H	rs368386019	1.20E-04	1	0	18.70	0.796

*Build GRCh37/hg1

† MAF based on Genome Aggregation Database (gnomAD) (http://gnomad.broadinstitute.org/)

Table 2.7 Identified *LMNA* variants in disease.

AA Change	SNP ID	Disease Association†
R401C	rs61094188	
R482Q	rs11575937	Familial partial lipodystrophy 2
P485A	chr1:156106784*	
R545H	rs142191737	Dilated cardiomyopathy 1S
R571S	rs80338938	Dilated cardiomyopathy 1A
R627C	rs777841827	
R644H	rs368386019	

*Build GRCh37/hg1

† Likely pathogenic or pathogenic rating in ClinVar (https://www.ncbi.nlm.nih.gov/clinvar/)

Table 2.8 Rare nonsynonymous *INSR* variants in PCOS cases and controls.

Table 2.8 Rare nonsynonymous *INSR* variants in PCOS cases and controls.

Base Change (mRNA) (Nm_001079817)	AA Change	SNP ID	Population based MAF†	Count Cases	Count Controls	CADD C-score	FATHMM-MKL *P*-value
T41C	L14P	rs745857330	5.30E-04	1	1	15.14	0.816
C356T	A119V	chr19:7267652*	2.70E-05	1	0	29.60	0.987
C959T	T320M	rs138528064	1.60E-05	1	0	25.00	0.758
C2243T ‡	S748L	rs143523271	1.53E-03	1	0	18.63	0.665
C2539T	H847Y	rs149536206	1.58E-05	1	0	14.10	0.777
C2802G	D946E	rs146588336	2.70E-03	4	0	19.30	0.964
G2998A	V1012M	rs1799816	8.10E-03	9	0	32.00	0.906
A3047C	E1028A	rs765562038	0.00	1	0	25.10	0.978
G3122A	R1053H	rs748109926	6.27E-05	1	0	23.30	0.884
C3157G	L1065V	rs56395521	5.80E-04	1	0	21.90	0.959
C3310T	R1116C	rs749951195	0.00	1	0	35.00	0.987

‡ mRNA: NM_000208

*Build GRCh37/hg1

† MAF based on Genome Aggregation Database (gnomAD) (http://gnomad.broadinstitute.org/)

Table 2.9 Frequency of rare nonsynonymous variants in genes of custom targeted next generation sequencing cohort.

	Cases				Controls			
	MAF <0.05		MAF <0.01		MAF <0.05		MAF <0.01	
Gene	Count	Freq	Count	Freq	Count	Freq	Count	Freq
AMH	39	0.0308	31	0.0244	12	0.0392	8	0.0261
AMHR2	2	0.0016	2	0.0016	1	0.0033	1	0.0033
LMNA	10	0.0079	10	0.0079	1	0.0033	1	0.0033
INSR	23	0.0174	22	0.0174	1	0.0033	1	0.0033
LHB	127	0.1002	127	0.1002	39	0.1275	39	0.1275
FSHB	9	0.0071	9	0.0071	1	0.0033	1	0.0033
CPEB2	122	0.0962	92	0.0726	30	0.098	20	0.0654
EIF2AK4	17	0.0134	17	0.0134	3	0.0098	3	0.0098
ENTPD5	5	0.0039	5	0.0039	0	0	0	0
SLC22A1	140	0.1104	42	0.0331	32	0.1046	9	0.0294
AKAP17A	24	0.0189	24	0.0189	7	0.0229	7	0.0229

Note: MAF filters based on 1000Genomes (1000g2014sep_eur)

Table 2.10 Biochemical assays.

Hormone	Assay methodology	Kit Name*	Manufacturer	Units
SHBG	IRMA	DSL-7400	DSL[a]	nM
SHBG	IRMA	DSL-7400**	DSL[a]	nM
SHBG	IRMA	RKSH-1	Siemens[b]	nM
SHBG	Immulite	LKSH-1	DPC[c]	nM
T	RIA	Coat-A-Count® TKTT1, 2, 5	DPC[c]	ng/dL
LH	Double antibody RIA	KLHD1,2	DPC[c]	mIU/mL
LH	IRMA	DSL-4600	DSL[a]	mIU/mL
LH	ELISA	11-LUTHU	ALPCO[d]	mIU/mL
LH	Immulite	LKLH-1	DPC[c]	mIU/mL
FSH	Double antibody RIA	KFSD1,2	DPC[c]	mIU/mL
FSH	IRMA	DSL-4700	DSL[a]	mIU/mL
FSH	ELISA	11-FSHHU-E01	ALPCO[d]	mIU/mL
FSH	Immulite	LKFS-1	DPC[c]	mIU/mL
DHEAS	RIA	Coat-A-Count® DHEA-SO4; TKDS1, 2	DPC[c]	ng/mL
DHEAS	RIA	LKDS-1	DPC[c]	ng/mL

*Kit used as per the manufacturer's instructions.

**The SHBG standard was changed to the WHO 1st International Standard #95/560 and the kit recalibrated in 2005. Accordingly, these SHBG values were coded as a different assay methodology in the analyses.

[a] Diagnostic Systems Laboratories, Inc. (DSL) (Webster, TX, USA) [Note: In October 2005, DSL was acquired by Beckman Coulter (Brea, CA, USA)]

[b] Siemens Medical Solutions USA, Inc. (Malvern, PA, USA)

[c] Diagnostic Products Corporation (DPC) (Los Angeles, CA, USA) [Note: In April 2006, DPC was acquired by Siemens Medical Solutions USA, Inc. (Malvern, PA, USA)]

[d] American Laboratory Products Company (ALPCO) (Salem, NH, USA)

References:

M. G. Hayes *et al.*, Genome-wide association of polycystic ovary syndrome implicates alterations in gonadotropin secretion in European ancestry populations. *Nat Commun* **6**, 7502 (2015).

Table 3.1 Impact of rare *AMH* variants on signaling activity and *Cyp17a1* expression.

AMH AA Change	SNP ID	Count Cases	Count Controls	% Decrease Activity in DLR assay†	DLR P-value**	% Increase in Cyp17a1 expression†	Cyp17a1 P-value**
V12G	rs149082963	6	0	46	3.00E-04	65	1.45E-03
A24T	rs775579158	1	0	65	1.80E-05	57	2.68E-03
P46A	rs148294311	1	0	43	5.70E-05	51	1.08E-02
R91H	rs534377664	1	0	45	6.00E-04	87	3.11E-03
T99S	rs200226465	2	0	56	1.50E-05	88	5.69E-03
T143I	rs139265145	11	4	12	1.00E-01	17	6.75E-02
P151S	rs370532523	1	0	85	5.70E-09	85	9.11E-05
A156T	rs374588581	1	0	76	1.40E-07	82	5.77E-04
Q185E	rs200523942	1	0	86	3.00E-08	82	7.28E-04
splicing (ex2/3)	rs774430982	1	0	83	1.80E-07	97	9.20E-03
R194H	rs376035065	1	0	66	3.60E-06	71	2.00E-03
P270S	rs757506343	1	0	80	3.50E-06	82	3.22E-04
P284S	rs769350289	0	1	-8	8.00E-01	0	9.50E-01
D288E	rs199831511	3	1	15	4.00E-01	18	3.39E-02
R302Q	rs536688211	1	0	46	2.40E-05	70	1.04E-04
Q325R	rs140765565	3	4	14	7.00E-02	2	8.89E-01
P352S	rs764049634	3	0	82	2.00E-06	76	2.99E-04
P362S	rs765380360	1	0	65	3.80E-06	89	4.30E-03
P366L	chr19:2251370-22 51370*	1	0	69	4.60E-06	58	1.15E-03
A372V	rs541377806	1	0	1	8.00E-01	6	6.80E-01
A385V	chr19:2251427-22 51427*	1	0	66	3.60E-06	71	2.00E-03
H506Q	rs138571039	1	0	68	2.10E-06	75	3.18E-03
A519V	rs200031151	0	1	12	1.00E-01	13	2.02E-01
V553L	rs770189890	1	1	8	5.00E-01	14	2.19E-01

*Build GRCh37/hg19

† Percentages relative to reference AMH

** Two-tailed t-test

Table 3.2 Clinical features and reproductive hormone levels of PCOS probands with *AMH* functional variants (n=24) and without *AMH* variants (n=658).

	PCOS with AMH variants		**PCOS without AMH variants**		**P-Value**
	(n = 24)		**(n = 666)**		
	N	**Median (1st-3rd quartile)**	**N**	**Median (1st-3rd quartile)**	*
Age (yrs.)	24	27 (24-33)	658	28 (24-32)	0.627
BMI (kg/m^2)	24	39.7 (29.2-43.5)	658	35.3 (28.7-41.2)	0.188
T (ng/dL)	23	75 (68-84)	629	71 (59-90)	0.292
uT (ng/dL)	19	22 (18-27)	467	22 (17-29)	0.957
SHBG (nM)	19	54 (33-88)	468	54 (35-78)	0.882
DHEAS (ng/ mL)	21	2277 (1927-2739)	559	2074 (1444-2902)	0.398
LH (mIU/mL)	16	12 (10-22)	487	11 (7-17)	0.129
FSH (mIU/mL)	16	9 (8-10)	487	9 (7-11)	0.679*
AMH (ng/mL)	12	7.1 (4.8-7.7)	243	9.9 (5.4-17.6)	0.116*

* Mann-Whitney U test except for those denoted by an asterisk which used ANCOVA adjusted for Age and BMI

To convert values for T from ng/dL to nmol/L, multiply by 0.03467. To convert the values for uT from ng/dL to nmol/L, multiply by 0.03467. To convert the values for SHBG to nmol/L, multiply by 1. To convert the values for DHEAS from ng/mL to micromole/L, multiply by 0.00271. To convert the values for LH and FSH from mIU/mL to IU/L, multiply by 1. To convert values for AMH from ng/mL to pmol/L, multiply by 7.1429.

Table 4.1 Deleteriousness ranking of rare *AMH* noncoding variants.

General AMH Location	Chr	Position*	SNP ID	Population based MAF†	REF	ALT	Count Cases	Count Controls	CADD C-score	FATHMM-MKL *P*-value
Upstream	**19**	**2249171**	**NA**	**NA**	**C**	**G**	**1**	**0**	**14.45**	**0.907**
Upstream	**19**	**2249263**	**rs746807694**	**2.67E-04**	**C**	**G**	**1**	**0**	**14.48**	**0.750**
Upstream	**19**	**2249272**	**rs777832730**	**6.68E-05**	**C**	**T**	**1**	**0**	**9.69**	**0.307**
Intron 1	19	2250185	rs991519014	3.00E-05 ‡	C	A	1	0	7.57	0.232
Intron 1	19	2250061	rs116060400	2.01E-04	C	T	0	1	8.29	0.232
Intron 3	19	2250828	NA	NA	C	T	1	0	8.11	0.231
Intron 1	19	2250231	rs780396199	3.34E-04	T	C	1	0	6.47	0.209
Intron 1	19	2250312	rs183367973	4.17E-04	C	T	2	1	8.69	0.175
Intron 1	19	2250302	rs374418184	3.04E-03	A	G	4	0	9.81	0.164
Intron 1	19	2249774	rs370996450	1.94E-04	C	T	1	0	6.75	0.160
Intron 1	19	2250012	rs749466277	2.01E-03	C	T	1	0	1.54	0.147
Upstream	**19**	**2249215**	**rs186422293**	**6.29E-03**	**G**	**A**	**7**	**2**	**5.74**	**0.141**
Intron 1	19	2249796	rs149600185	1.47E-03	C	T	2	2	1.95	0.129
5' UTR	19	2249330	rs773283377	2.32E-04	C	T	1	0	6.98	0.128
Intron 1	19	2250175	rs546498783	6.62E-03	C	T	10	0	0.00	0.069
Intron 2	19	2250483	NA	NA	C	CA	1	0	13.35	NA

Note: Variants chosen for functional follow-up are in bold type

*Build GRCh37/hg19

† MAF based on Genome Aggregation Database (gnomAD) (http://gnomad.broadinstitute.org/)

‡ TOPMed Program

Table 4.2 Deleteriousness ranking of rare *AMHR2* noncoding variants.

General AMHR2 Location	Chr	Position*	SNP ID	Population based MAF†	REF	ALT	Count Cases	Count Controls	CADD C-score	FATHMM-MKL *P*-value
Intron 1	**12**	**53817956**	**rs784894**	**1.40E-03**	**C**	**A**	**3**	**0**	**15.76**	**0.953**
Upstream	**12**	**53817516**	**rs777964297**	**9.69E-05**	**T**	**G**	**1**	**0**	**18.72**	**0.947**
Upstream	**12**	**53817577**	**rs148189358**	**5.49E-03**	**G**	**T**	**7**	**3**	**16.53**	**0.936**
Intron 1	**12**	**53818016**	**rs777265708**	**8.01E-04**	**T**	**G**	**1**	**0**	**13.65**	**0.914**
Upstream	**12**	**53815561**	**rs181566505**	**1.90E-03**	**T**	**G**	**5**	**1**	**7.775**	**0.868**
Upstream	**12**	**53817187**	**NA**	**NA**	**A**	**G**	**1**	**0**	**15.57**	**0.851**
Intron 6	12	53822176	NA	NA	A	G	1	0	8.916	0.384
Intron 6	12	53822277	rs539086433	5.49E-04	T	A	2	1	7.663	0.302
Upstream	**12**	**53814515**	**NA**	**NA**	**A**	**T**	**1**	**0**	**4.289**	**0.239**
Intron 10	12	53824508	rs784888	1.13E-03	G	C	3	0	13.44	0.238
Intron 9	12	53823828	rs760804136	6.47E-05	C	T	1	0	4.543	0.237
Intron 6	12	53822288	NA	NA	G	A	1	0	7.675	0.236
Intron 8	12	53823609	rs745713994	4.07E-06	C	T	1	0	7.146	0.232
Intron 2	12	53818404	NA	NA	G	A	1	0	9.413	0.219
Intron 6	12	53822226	rs181813382	3.23E-05	T	C	1	0	10.81	0.212
Intron 2	12	53818287	rs784893	4.75E-02	A	G	3	0	6.278	0.206
Intron 7	12	53822816	rs775478211	5.51E-05	A	G	1	0	6.516	0.198
Intron 6	12	53822143	rs142890072	3.23E-05	C	G	1	0	1.502	0.181
Intron 6	12	53822505	rs777352969	1.62E-04	C	T	2	1	4.243	0.177
Intron 7	12	53822884	rs784892	8.01E-04	G	A	3	0	7.818	0.176
Intron 9	12	53823851	rs577266252	1.62E-04	G	T	2	0	2.173	0.173
Intron 5	12	53819433	rs770641486	1.64E-05	A	G	1	0	1.409	0.160
Intron 8	12	53823548	rs527341740	2.26E-04	A	G	1	0	10.84	0.156
Intron 10	12	53824177	rs758971843	NA	A	G	1	0	7.594	0.150
Intron 6	12	53819825	NA	NA	T	C	1	0	2.77	0.147
Intron 10	12	53824408	rs784889	1.40E-03	C	T	3	0	5.793	0.145
Intron 6	12	53821113	rs540050356	1.36E-03	T	C	2	1	3.314	0.143
Intron 1	**12**	**53817971**	**NA**	**NA**	**G**	**A**	**1**	**0**	**1.528**	**0.143**
Intron 6	12	53820453	NA	NA	A	C	23	2	7.996	0.142
Intron 7	12	53822904	NA	NA	C	T	2	0	2.43	0.142
Intron 10	12	53824871	rs139224064	9.37E-04	A	C	1	0	1.883	0.141
Upstream	**12**	**53815218**	**rs866630130**	**6.66E-05**	**G**	**C**	**1**	**0**	**9.924**	**0.135**

(Continued on following page)

Table 4.2 cont. Deleteriousness ranking of rare *AMHR2* noncoding variants.

General AMHR2 Location	Chr	Position*	SNP ID	Population based MAF†	REF	ALT	Count Cases	Count Controls	CADD C-score	FATHMM-MKL *P*-value
Intron 6	12	53822144	rs370723376	1.33E-04	G	A	1	0	2.232	0.134
Intron 7	12	53822898	rs558842297	3.24E-05	C	T	1	0	1.959	0.134
Intron 10	12	53824544	NA	NA	G	T	1	0	7.519	0.132
Intron 6	12	53820139	rs184772202	2.23E-03	G	T	7	1	3.606	0.130
Intron 10	12	53824543	rs190814349	1.94E-04	A	G	2	0	8.254	0.130
Intron 9	12	53823773	rs200284824	4.19E-04	G	A	1	0	1.08	0.128
Upstream	12	53817402	rs576777893	2.26E-04	T	G	1	0	12.1	0.126
Upstream	12	53815671	rs150004525	4.20E-04	T	C	1	0	2.231	0.125
Intron 3	12	53818868	NA	NA	A	T	1	0	12.89	0.119
Intron 6	12	53820136	rs760484587	2.91E-04	G	A	1	0	6.143	0.117
Intron 10	12	53824538	rs186948808	4.52E-04	G	A	1	0	11.52	0.112
Intron 6	12	53820903	rs555694902	1.29E-04	C	T	1	0	3.548	0.111
Intron 6	12	53820101	NA	NA	G	A	1	0	5.393	0.109
Intron 3	12	53818920	rs2071557	4.73E-02	C	T	26	3	8.65	0.103
Intron 6	12	53821359	NA	NA	G	A	1	0	6.3	0.098
Intron 6	12	53820620	rs34932524	1.35E-03	C	T	4	0	3.679	0.090
Intron 6	12	53820089	NA	NA	G	A	1	0	4.534	0.086
Intron 6	12	53819857	NA	NA	G	A	1	0	3.495	0.085
Upstream	12	53816595	NA	NA	C	T	1	0	1.881	0.072
Upstream	12	53817053	NA	NA	G	A	1	0	4.957	0.070
Intron 6	12	53821196	rs551935854	3.23E-05	T	C	2	0	1.508	0.066
Upstream	12	53817031	rs547441128	1.26E-03	G	C	1	0	0.853	0.065
Upstream	12	53815819	NA	NA	C	A	1	0	0.239	0.031
Upstream	**12**	**53815129**	**NA**	**NA**	**A**	**T**	**1**	**0**	**0.076**	**0.028**
Upstream	12	53816627	NA	NA	TAATA	T	2	0	12.63	NA
Upstream	12	53816766	NA	NA	GTGT	G	1	0	8.159	NA
Intron 6	12	53821177	NA	NA	T	TTTTTA	2	0	1.33	NA
Intron 9	12	53823797	NA	NA	T	TC	1	0	1.035	NA

Note: Variants chosen for functional follow-up are in bold type

*Build GRCh37/hg19

† MAF based on Genome Aggregation Database (gnomAD) (http://gnomad.broadinstitute.org/)

Table 4.3 *AMHR2* intronic PCOS-specific variants and impact on signaling activity.

General AMHR2 Location	Chr	Position*	SNP ID	Population based MAF†	REF	ALT	Count Cases	CADD C-score	FATHMM-MKL *P*-value	% Decrease Activity‡	P-value**
Intron 8	12	53823548	rs527341740	2.26E-04	A	G	1	10.84	0.156	-10	3.39E-01
Intron 8	12	53823609	rs745713994	9.01E-06	C	T	1	7.146	0.232	70	1.45E-08
Intron 9	12	53823773	rs200284824	4.19E-04	G	A	1	1.08	0.128	74	1.97E-09
Intron 9	12	53823828	rs760804136	6.68E-05	C	T	1	4.543	0.237	-13	8.29E-02
Intron 9	12	53823851	rs577266252	3.34E-04	G	T	2	2.173	0.173	20	6.34E-03
Intron 10	12	53824177	rs758971843	NA	A	G	1	7.594	0.150	32	4.34E-04
Intron 10	12	53824408	rs784889	1.40E-03	C	T	3	5.793	0.145	26	3.85E-03
Intron 10	12	53824508	rs784888	1.13E-03	G	C	3	13.44	0.238	9	2.25E-01
Intron 10	12	53824538	rs186948808	4.00E-04	G	A	1	11.52	0.112	65	8.68E-08
Intron 10	12	53824543	rs190814349	2.00E-04	A	G	2	8.254	0.130	69	2.69E-08
Intron 10	12	53824544	NA	NA	G	T	1	7.519	0.132	75	1.17E-08
Intron 10	12	53824871	rs139224064	1.67E-03	A	C	1	1.883	0.141	26	1.43E-03

Note: None of the listed variants were found in control subjects.

*Build GRCh37/hg19

† MAF based on Genome Aggregation Database (gnomAD) (http://gnomad.broadinstitute.org/)

‡ Percentages relative to reference AMHR2

** Two-tailed t-test

Table 4.4 Functionally validated variants identified in *AMH* and *AMHR2*.

Gene	AA Change	Chr	Position*	SNP ID	Population based MAF†	REF	ALT	Count Cases	Count Controls
AMHR2	NA	12	53814515	NA	NA	A	T	1	0
AMHR2	NA	12	53815129	NA	NA	A	T	1	0
AMHR2	NA	12	53815218	rs866630130	6.66E-05	G	C	1	0
AMHR2	NA	12	53817187	NA	NA	A	G	1	0
AMHR2	NA	12	53817956	rs784894	1.40E-03	C	A	3	0
AMHR2	NA	12	53817971	NA	NA	G	A	1	0
AMHR2	NA	12	53818016	rs777265708	8.01E-04	T	G	1	0
AMHR2	P30S	12	53818110	NA	NA	C	T	1	0
AMHR2	NA	12	53823609	rs745713994	9.01E-06	C	T	1	0
AMHR2	NA	12	53823773	rs200284824	4.19E-04	G	A	1	0
AMHR2	NA	12	53823851	rs577266252	3.34E-04	G	T	2	0
AMHR2	NA	12	53824177	rs758971843	NA	A	G	1	0
AMHR2	NA	12	53824408	rs784889	1.40E-03	C	T	3	0
AMHR2	NA	12	53824538	rs186948808	4.00E-04	G	A	1	0
AMHR2	NA	12	53824543	rs190814349	2.00E-04	A	G	2	0
AMHR2	NA	12	53824544	NA	NA	G	T	1	0
AMHR2	NA	12	53824871	rs139224064	1.67E-03	A	C	1	0
AMH	NA	19	2249171	NA	NA	C	G	1	0
AMH	NA	19	2249263	rs746807694	2.67E-04	C	G	1	0
AMH	NA	19	2249272	rs777832730	6.68E-05	C	T	1	0
AMH	V12G	19	2249366	rs149082963	2.69E-03	T	G	6	0
AMH	A24T	19	2249401	rs775579158	1.02E-04	G	A	1	0
AMH	P46A	19	2249467	rs148294311	2.25E-04	C	G	1	0
AMH	R91H	19	2249603	rs534377664	1.70E-05	G	A	1	0
AMH	T99S	19	2249626	rs200226465	4.44E-04	A	T	2	0
AMH	P151S	19	2250374	rs370532523	8.36E-05	C	T	1	0
AMH	A156T	19	2250389	rs374588581	8.96E-05	G	A	1	0
AMH	Q185E	19	2250476	rs200523942	1.69E-04	C	G	1	0
AMH	splicing (ex2/3)	19	2250480	rs774430982	3.95E-05	G	T	1	0
AMH	R194H	19	2250676	rs376035065	2.10E-05	G	A	1	0
AMH	P270S	19	2250991	rs757506343	5.42E-05	C	T	1	0
AMH	R302Q	19	2251178	rs536688211	1.46E-04	G	A	1	0
AMH	P352S	19	2251327	rs764049634	9.91E-04	C	T	3	0
AMH	P362S	19	2251357	rs765380360	6.94E-05	C	T	1	0
AMH	P366L	19	2251370	NA	6.77E-05	C	T	1	0
AMH	A385V	19	2251427	NA	NA	C	T	1	0
AMH	H506Q	19	2251791	rs138571039	7.84E-05	C	G	1	0

*Build GRCh37/hg19

† MAF based on Genome Aggregation Database (gnomAD) (http://gnomad.broadinstitute.org/)

CURRICULUM VITAE

LIDIJA K. GORSIC

29W204 103rd Street
Naperville, IL 60564
Lkg17@u.northwestern.edu
(630) 207-4205

EDUCATION

Northwestern University Chicago, IL
Ph.D. Life Sciences, Genetics and Genomics 9/2013 – 6/2018
Thesis Research: Characterization of rare genetic variation in polycystic ovary syndrome

Elmhurst College Elmhurst, IL
Bachelor of Science *Cum Laude* 9/2005 – 6/2009
Majors: Biology, German, Philosophy *Minors*: Chemistry, Psychology

RESEARCH AND CLINICAL EXPERIENCE

Northwestern University, Department of Endocrinology, Chicago, IL
Doctoral Student, Driskill Graduate Program 9/2013 – 6/2018
Thesis Advisor: Margrit Urbanek, Ph.D.

- Application of next-generation sequencing technologies to identify rare genetic variants associated with polycystic ovary syndrome (PCOS) in a large case/control cohort
- Awarded NRSA training grant in the Northwestern University Program in Diabetes, Endocrinology and Hormone Action (NUPEDHA)

Main Research Findings:

- Identified functional PCOS-specific rare coding and noncoding variants in members of the anti-Müllerian hormone (AMH) pathway. Variants resulted in reduced AMH signaling. Loss of AMH inhibition on steroidogenesis is predicted to increase androgen synthesis in these women, a cardinal feature of PCOS.

Skills and Techniques:

- Implemented software tools for read alignment, variant calling, annotation and analyses: BWA, PICARD, ANNOVAR, GATK, VCFtools, CADD, FATHMM-MKL.
- Knowledge of databases/tools: UCSC Genome Browser, ExAc/gnomAD, ClinVar.
- Optimized and performed molecular assays to determine functional impact of identified variants. Laboratory expertise in cell culture, cloning, mutagenesis, transfections, dual luciferase reporter assays, PCR, qRT-PCR, Sanger sequencing.

Relevant Continued Education:

- Weekly clinical case presentations by Northwestern physicians/fellows (2017-2018).
- ACMG Genetics and Genomics Review Course (May 2017).
- Skills & Careers in Science Writing course at Northwestern University (2016).
- NHGRI-funded Short Course on NGS: Technology & Statistical Methods at University of Alabama at Birmingham (2014).

University of Chicago, Department of Medicine, Chicago, IL
Senior Research Technologist 1/2012 – 8/2013
Research Technologist 1/2010 – 1/2012

- Research under principal investigator, Dr. M. Eileen Dolan, in the section of Hematology/Oncology focusing research on pharmacogenomics of anticancer agents.
- Laboratory procedures and techniques: tissue culture using suspension and adherent cells, high-throughput measurements of apoptosis and cell growth, drug preparation, cell transfection, RNA isolation, RNA reverse transcription, qRT-PCR, protein processing, mycoplasma detection, and processing clinical trial samples.
- Skills acquired: experiment optimization, developing protocols, data analysis, graphing, and publication writing.
- Trained 3 postdoctoral scholars, 1 clinical fellow, 4 graduate students and 3 employees.

St. Josefskrankenhaus, Freiburg, Germany 10/2008 – 11/2008
Patient Care Intern

- Became more familiar with health care systems and research in a foreign country. Observed the importance of local and international collaborations for medical innovation.

Alexian Brothers Medical Center, Elk Grove Village, Illinois 3/2006 – 6/2008
Patient Care Technician

- Direct patient care responsibilities included phlebotomy, 12-Lead EKG, wound/ostomy care, post-surgical drain management, patient ambulation/hygiene assistance, surgical site asepsis, vital signs, and remote telemetry.
- *Spirit of Excellence Award* (2007), institution-wide recognition for outstanding presence on patient satisfaction reviews and in reference to a patient's letter written to administration.

TEACHING EXPERIENCE

Elmhurst College, Department of Biology, Elmhurst, IL 6/2017 – 12/2017
Adjunct Professor

- Human Genetics & Society: upper level undergraduate course with lecture and laboratory (fall semester 2017).
- Principles of Biology: introductory level undergraduate course with lecture and laboratory (summer term 2017).

Northwestern University, Searle Center, Evanston, IL Completed 6/2017
Teaching Certificate Program

- Teaching assistant undergraduate Genetics and Molecular Processes Laboratory (fall quarter 2015).

Sheldon College, Brisbane, Australia 1/2008
Teaching Assistant

- Assisted in several science classes ranging from freshman to senior levels of high school.

PUBLICATIONS

Peer-Reviewed Publications:

1. **Gorsic LK**, Legro RS, Hayes MG, Urbanek M. Rare genetic variation in members of the anti-Müllerian hormone pathway in women with PCOS. (in preparation)

2. **Gorsic LK***, Navarro A*, Stevens JV, Legro RS, Hayes MG, Urbanek M. Rare genetic variation in genes for Mendelian forms of insulin resistance identified in women with PCOS. (in preparation)

3. **Gorsic LK**, Kosova G, Werstein B, Sisk R, Legro RS, Hayes MG, Teixeira JM, Dunaif A, Urbanek M. (2017). Pathogenic Anti-Müllerian Hormone Variants in Polycystic Ovary Syndrome. *J Clin Endocrinol Metab,* 102(8):2862-2872.

4. Stark AL, Madian AG, Williams SW, Chen V, Wing C, Hause RJ, To LA, Gill AL, Myers JL, **Gorsic LK**, Ciaccio MF, White KP, Jones RB, Dolan ME. (2017). Identification of novel protein expression changes following cisplatin treatment and application to combination therapy. *J Proteome Res*, 3;16(11):4227-4236.

5. Yang R, Kerschner JL, Gosalia N, Neems D, **Gorsic LK**, Safi A, Crawford GE, Kosak ST, Leir SH, Harris A. (2016). Differential contribution of cis-regulatory elements to higher order chromatin structure and expression of the CFTR locus. *Nucleic Acids Research*, 44(7):3082-94.

6. Komatsu M, Wheeler HE, Chung S, Low SK, Wing C, Delaney SM, **Gorsic LK**, Takahashi A, Kubo M, Kroetz D, Zhang W, Nakamura Y, Dolan ME. Pharmacoethnicity in Paclitaxel-Induced Sensory Peripheral Neuropathy. *Clinical Caner Research*, 21(19):4337-46, 2015.

7. Hause RJ, Stark AL, Antao NN, **Gorsic LK**, Chung SH, Brown CD, Gill DF, Myers JL, White KP, Dolan ME, Jones RB. (2014). Identification and validation of genetic variants that influence transcription factor and cell signaling protein levels. *American Journal of Human Genetics*, 95(2):194-208.

8. Stark AL, Hause RJ, **Gorsic LK**, Antao NN, Wong SS, Gill DF, Chung SF, Im HK, White KP, Jones RB, Dolan ME. (2014). Protein quantitative trait loci identify novel candidates modulating cellular response to chemotherapy. *PLoS Genetics*, 10(4):e1004192.

9. **Gorsic LK**, Stark AL, Wheeler HE, Wong SS, Im HK, Dolan ME. (2013). *EPS8* inhibition increases cisplatin sensitivity in lung cancer cells. *PLoS One*, 8(12):e82220.

10. Gamazon ER, Lamba J, Pounds S, Stark AL, Wheeler HE, Cao X, Im HK, Mitra AK, Rubnitz JE, Ribeiro RC, Raimondi S, Campana D, Crews KR, Wong SS, Welsh M, Hulur I, **Gorsic L,** Hartford CM, Cox NJ, Dolan ME. (2013). Comprehensive genetic analysis of cytarabine sensitivity in a cell-based model identifies polymorphisms associated with outcome in AML patients. *Blood*, 121(21):4366-76.

11. O'Donnell PH, Stark AL, Gamazon ER, Wheeler HE, McIlwee BM, **Gorsic LK**, Im HK, Huang RS, Cox NJ, Dolan ME. (2012). Identification of novel germline polymorphisms governing capecitabine sensitivity. *Cancer*, 118(16):4063-73, 2012.

12. Njiaju UO, Gamazon ER, **Gorsic LK**, Delaney SM, Wheeler HE, Im HK, Dolan ME. (2012). Whole genome studies identify solute carrier transporters in cellular susceptibility to paclitaxel. *Pharmacogenetics and Genomics*, 22(7):498-507.

13. Wheeler HE, Gamazon ER, Stark AL**,** O'Donnell PH, **Gorsic LK**, Huang RS, Cox NJ, Dolan ME. (2011). Genome-wide meta-analysis identifies variants associated with platinating agent susceptibility across populations. *The Pharmacogenomics Journal*, 13(1):35-43.

14. Wen Y*, **Gorsic LK***, Wheeler HE, Ziliak DM, Huang RS, and Dolan ME. (2011). Chemotherapeutic-induced apoptosis – A phenotype for pharmacogenomics studies. *Pharmacogenetics and Genomics*, 21(8):476-88.

15. Wheeler HE, **Gorsic LK**, Welsh M, Stark AL**,** Gamazon ER, Cox NJ, Dolan ME. (2011). Genome-wide local ancestry approach identifies genes and variants associated with chemotherapeutic susceptibility in African-Americans. *PLoS One*, 6(7):e21920.

* designates equal contribution

First-Author Abstracts:

1. **Gorsic LK**, Legro RS, Hayes MG, Urbanek M. Polycystic ovary syndrome (PCOS) associated functional rare variants identified in the anti-Müllerian hormone pathway. *Endocrine Society*, Chicago, IL, April 2018.

2. **Gorsic LK**, Kosova G, Werstein B, Sisk R, Legro RS, Hayes MG, Teixeira JM, Dunaif A, Urbanek M. Rare anti-Müllerian hormone (*AMH*) variants with functional impact *in vitro* identified in women with polycystic ovary syndrome. *Sex Inclusion in Biomedical Research*, Chicago, IL, January 2017.

3. **Gorsic LK**, Kosova G, Werstein B, Sisk R, Legro RS, Hayes MG, Teixeira JM, Dunaif A, Urbanek M. Rare anti-Müllerian hormone (*AMH*) variants with functional impact *in vitro* identified in women with polycystic ovary syndrome. *American Society of Human Genetics*, Vancouver, Canada, October 2016.

4. **Gorsic L**, Navarro A, Sisk R, Vellanki P, Hayes MG, Torchen L, Urbanek M, Dunaif A. Exome sequencing in a familial partial lipodystrophy (FPL) family identifies functional variant in GPRC6A. *Endocrine Society*, Boston, MA, April 2016.

5. **Gorsic L**, Sisk R, Vellanki P, Hayes M.G, Urbanek M, Dunaif A. The complexity of familial partial lipodystrophy: efforts in identifying causal variants through exome sequencing in a family study. *Medicine Research Day*, Chicago, IL, June 2015.

6. **Gorsic L**, Sisk R, Vellanki P, Hayes MG, Urbanek M, Dunaif A. The complexity of familial partial lipodystrophy: efforts in identifying causal variants through exome sequencing in a family study. *Lipodystrophy Symposium*, Ann Arbor, MI, October 2014.

7. **Gorsic L**, Sisk R, Vellanki P, Hayes MG, Urbanek M, Dunaif A. The complexity of familial partial lipodystrophy: efforts in identifying causal variants through exome sequencing in a family study. *Illinois Symposium on Reproductive Sciences*, Chicago, IL, October 2014.

8. **Gorsic LK**, Stark AL, Wheeler HE, Im HK, Dolan ME. Identification of common genetic variants contributing to cisplatin-induced apoptosis and cytotoxicity in lymphoblastoid cell lines. *American Association of Cancer Research*, Chicago, IL, March-April 2012.

REVIEWER

Fertility and Sterility